



**POLITECNICO
DI TORINO**

Master of Science in Mechanical Engineering

Master Thesis

Development through numerical simulation
of an innovative energy management strategy
for a 48V Mild-Hybrid vehicle

Tutor

Prof. Federico Millo

Candidate

Francesco Accurso

Confidentiality agreement

This report contains some information which are not intended for publication. All the rights on the thesis, including the distribution through electronic media, are held by Politecnico di Torino. The content of this work cannot be published or transmitted to third parties without an explicit written authorization from Politecnico di Torino.

Clausola di riservatezza

Questo lavoro contiene informazioni non destinate alla pubblicazione. Tutti i diritti sul lavoro di tesi, inclusa la diffusione attraverso mezzi multimediali, sono detenuti dal Politecnico di Torino. Il contenuto di questo lavoro non può essere pubblicato o trasmesso a terzi senza un'approvazione esplicita e scritta da parte del Politecnico di Torino.

Abstract

The need to reduce the emissions of greenhouse gases and pollutants substances has led all car manufacturers in the last years to develop innovative technologies to comply with the limits imposed by the regulatory framework. In this context the electrification of the powertrains is a very effective solution. Considering the complexity of such systems, in addition to the manufacturers' profitability needs, the electrification process is developing gradually, and Mild-Hybrid 48 Volt vehicles are certainly a valid solution and a good compromise between costs and benefits. The study that will be carried out concerns precisely 48 V hybrid electric propulsion systems.

Firstly, a deep steady-state analysis on different engines scenarios was performed, to highlight both benefits and the criticalities of the electrified propulsion systems chosen as case study. Starting from a current market engine, after the update to current emissions regulation compliance (stoichiometric combustion in the overall engine map), several investigation activities were performed aimed to achieve both performance and consumption improvements.

As second step, a transient analysis was carried out. Three different powertrain concepts were developed and simulated: a fully Real Driving Emission (RDE) compliant engine, a Mild-Hybrid powertrain equipped with a fully compliant RDE engine and a 48V Belt Starter Generator (BSG), a Mild-Hybrid powertrain equipped with a fully RDE compliant high efficiency engine and a 48V BSG.

As far as the Energy Management Strategy is concerned, the activity was focused on the implementation and update of an Equivalent Consumption Minimization Strategy (ECMS) technique. The ECMS is based on the minimization of an equivalent fuel flow rate that considers also the energy coming from the battery and intended to propulsion. In this activity the capability of manage electric power was extended to electric power to be used for electrical auxiliaries, and therefore not directly exploited for the vehicle propulsion (eSupercharger, eCatalyst ...).

Fuel consumption and performance of the above-mentioned propulsion system concepts were evaluated according to homologation and RDE driving cycles and several transient maneuvers.

Sommario

La necessità di ridurre le emissioni di gas serra e sostanze inquinanti ha portato tutti i produttori di automobili negli ultimi anni a sviluppare tecnologie innovative per rispettare i limiti imposti dal quadro normativo. L'elettrificazione dei propulsori in questo contesto è sicuramente una soluzione molto efficace. Considerando la complessità di tali sistemi, oltre alle esigenze di redditività dei produttori, il processo di elettrificazione si sta sviluppando gradualmente e i veicoli Mild-Hybrid 48 Volt rappresentano sicuramente una soluzione valida e un buon compromesso tra costi e benefici. Lo studio che verrà condotto riguarda precisamente i sistemi di propulsione ibrida 48 V.

In primo luogo, è stata eseguita un'approfondita analisi in stazionario su diversi scenari di motori, per evidenziare sia i vantaggi che le criticità dei sistemi di propulsione elettrificati scelti come case study. Partendo da un motore attualmente in produzione, dopo un aggiornamento mirato a renderlo conforme all'attuale normativa sulla regolazione delle emissioni (combustione stechiometrica nella mappa generale del motore), sono state condotte diverse attività di indagine volte a conseguire miglioramenti delle prestazioni e del consumo.

Come seconda fase, è stata effettuata un'analisi in transitorio. Tre diverse configurazioni di powertrain sono stati sviluppati e simulati: un motore conforme alle normative RDE (Real Driving Emission), un powertrain Mild-Hybrid equipaggiato con un motore conforme alle normative RDE e con un Belt Stater Generator 48 V (BSG), un powertrain Mild-Hybrid equipaggiato con un motore ad alta efficienza pienamente conforme a RDE e un BSG a 48 V.

Per quanto riguarda la strategia di gestione dell'energia, l'attività si concentra sull'implementazione e l'aggiornamento della strategia Equivalent Consumption Minimization Strategy (ECMS). L'ECMS si basa sulla minimizzazione di una portata di combustibile equivalente che tiene in conto anche l'energia proveniente dalla batteria e destinata alla propulsione. In questa attività la capacità di gestire l'energia elettrica è stata estesa alla quota parte da utilizzare per gli ausiliari elettrici, e quindi non direttamente sfruttata per la propulsione del veicolo (eSupercharger, eCatalyst ...).

Il consumo di combustibile e le prestazioni dei suddetti configurazioni di powertrain sono stati valutati su cicli guida omologativi e su cicli guida RDE, oltre che per diverse manovre transitorie.

Acknowledgments

Vorrei ringraziare alcune persone per avermi aiutato a raggiungere questo traguardo.

Per primo il mio pensiero va alla mia famiglia, che sempre mi ha supportato da lontano in questi anni, mi ha insegnato ad affrontare le difficoltà e ad avere rispetto per il lavoro.

Vorrei ringraziare il professor Millo, Alessandro e tutti i ragazzi del team, che in questo di lavoro sono stati accanto, sempre pronti ad aiutarmi e da cui ho appreso tantissimo.

Vorrei ringraziare Marzia, per mille ragioni, per essere stata al mio fianco, sempre, per aver creduto in me, per avermi sopportato e supportato nei momenti di difficoltà.

Infine, un grazie di cuore va a tutti gli amici con cui ho trascorso gli ultimi cinque anni qui a Torino, tra i banchi al Poli, nelle camere in residenza, e anche i ragazzi “d giù”, con cui ancora una volta condivido la mia felicità, e ormai rappresentano una certezza per me.

La mia più grande gioia è quella di avere tante persone accanto con cui poter festeggiare un traguardo così importante.

Acronyms

| Item | Description | Unit |
|-------------|--|-------------|
| AT | After Treatment | - |
| BMEP | Brake Mean Effective Pressure | Bar |
| BSFC | Brake Specific Fuel Consumption | g/kWh |
| BSG | Belt Starter Generator | - |
| CAD | Crank Angle Degree | - |
| CFD | Computational Fluid-Dynamics | - |
| CR | Compression Ratio | - |
| ECMS | Equivalent Coumption Minimazation Strategy | - |
| EIVC | Early Intake Valve Closure | - |
| EM | Electric Machine | - |
| EMS | Energy Management Strategy | - |
| eSC | eSupercharger | - |
| EV | Electric Vehicle | - |
| FMEP | Friction Mean Effective Pressure | Bar |
| ICE | Internal Combustion Engine | - |
| IMEP | Indicated Mean Effective Pressure | Bar |
| HEV | Hybrid Electric Vehicle | - |
| LIVC | Late Intake Valve Closure | CAD |
| MFB50 | 50 % Mass Fraction Burned Angle | CAD |
| MFB10-90 | 10 % - 90% Mass Fraction Burned Angle | CAD |
| MHEV | Mild-Hybrid Electric Vehicle | - |
| NEDC | New European Driving Cycle | - |
| OEM | Original Equipment Manufacturer | - |
| OOL | Optimum Operating Line | - |
| PI | Performance Index | - |

| | | |
|------|--|-----|
| PMEP | Pumping Mean Effective Pressure | Bar |
| RDE | Real Driving Emissions | - |
| SoC | State of Charge | % |
| TC | TurboCharger | - |
| VVA | Variable Valve Actuation | - |
| WG | Waste-Gate | - |
| WPTC | Worldwide Harmonized Light-Duty Test Cycle | - |
| WLTP | Worldwide Harmonized Light-Duty Test Procedure | - |
| ZEV | Zero Emission Vehicle | - |

Contents

| | |
|--|-----|
| Abstract..... | v |
| Sommario | vii |
| Acknowledgments | ix |
| Acronyms | xi |
| 1 Introduction..... | 1 |
| 1.1 Regulatory Framework | 2 |
| 2 Hybrid Electric Vehicles | 7 |
| 2.1 Classification | 7 |
| 2.2 48V Mild-Hybrid Vehicles | 9 |
| 2.2.1 Architecture Overview | 10 |
| 2.2.2 eSupercharger | 12 |
| 2.3 Hybrid Control Strategy..... | 13 |
| 2.3.1 Equivalent Consumption Minimization Strategy | 15 |
| 3 Case Study..... | 19 |
| 3.1 Engine Characteristics | 19 |
| 3.2 Engine Modelling Approach..... | 20 |
| 3.3 Full Load Engine Model Validation | 21 |
| 3.4 Part Load Engine Model Validation | 23 |
| 4 Steady-State Analysis..... | 29 |
| 4.1 Toward RDE Standards | 29 |
| 4.2 Engine Concepts Development..... | 33 |
| 4.2.1 Conventional Engine Concept..... | 34 |
| 4.2.2 Electrified Engine Concept..... | 35 |
| 4.3 Results..... | 42 |
| 4.3.1 Full Load | 42 |
| 4.3.2 Part Load | 45 |
| 5 Vehicle Transient Analysis | 49 |
| 5.1 P0 48V Architecture | 51 |
| 5.2 Electrified Vehicle Model Assessment..... | 52 |

| | | |
|-------|--|----|
| 5.2.1 | Hybrid Control Modelling..... | 55 |
| 5.3 | eSupercharger Control Strategy..... | 58 |
| 6 | Results..... | 64 |
| 6.1 | Hybrid Control Strategy Results..... | 65 |
| 6.1.1 | CO ₂ Emissions..... | 66 |
| 6.1.2 | Transient Maneuvers..... | 70 |
| 6.2 | Sensitivity Analysis Transmission Ratio..... | 72 |
| 6.3 | Sensitivity Analysis EM Size..... | 75 |
| 7 | Conclusions..... | 83 |
| | Bibliography..... | 85 |

1 Introduction

The actual propulsion system scenario is deeply developing toward more efficient and more environmentally aware solutions. Fuel consumption and pollutants emission regulations are driving car manufacturers toward an electrification process. Electrification is absolutely a very effective solution, and considering a sufficiently long-time frame, it will lead to a broad diffusion of Zero Emission Vehicles (ZEV) [1]. Electric vehicles do not produce any pollutant substance during driving operation and they could rely to energy provided by a selection of renewable sources.

It must however be stressed that the above-mentioned solutions with the current market needs and the actual state of art concerning materials and technologies, show some critical issues: battery cost and energy storage capability, strong and intrusive modification of the current production process, inadequate infrastructures for reasonable time charging operation.

Hence, the actual powertrain scenario is evolving towards pure electric vehicles through a gradual process that provides the adoption of a simultaneous utilization of fuel energy and electric energy for propulsion purpose. In Figure 1.1 a comprehensive overview of next year's vehicles' market is proposed.

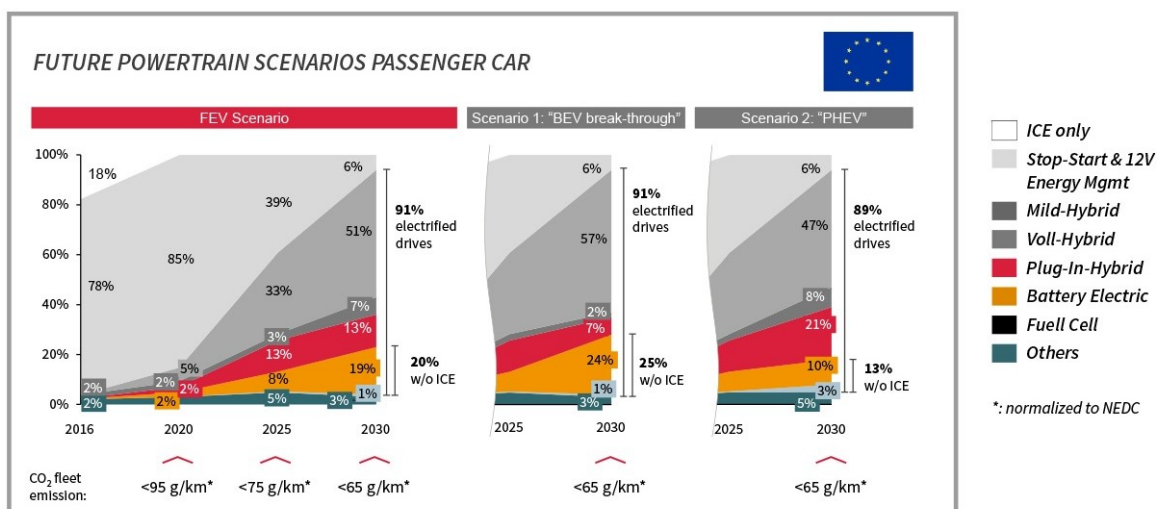


Figure 1.1 - Future Powertrain Scenarios in Europe [2]

Hybrid Electric Vehicles (HEVs) represent the rational connection between the conventional Internal Combustion Engine (ICE) based powertrain and Electric Vehicle (EV). The adoption of HEVs allows us to maintain a central role in the ICE and to exploit

the advantages of this type of propulsion system, combining it with new electrical technologies that will become increasingly predominant.

On a Hybrid Electric Vehicle there is the possibility to fully exploit in a flexible way the two energy sources, managing the simultaneous propulsion power availability. The energy management system decides the power split between ICE and Electric Machine, thus leading to a more efficient utilization of the energy. The possibility of storing energy in the battery allows a more efficient utilization of the ICE that is no more constrained by the output power demand. The drawbacks of such a flexible system is the increased complexity with respect to a conventional vehicle, as well as the production cost and also the price of these new technologies. Cost over benefits is the usual way in which a new technology is evaluated ([3]). Dealing with fuel consumption, the benefits can be measured as the reduction of CO₂; however, nowadays also other aspects are becoming even more important, for example drivability, safety and comfort.

The increased power availability in a 48V mild hybrid system allows the introduction of electric auxiliaries that disruptly expand the capabilities of conventional vehicle. In this context an electric supercharger can be adopted. It is able to reduce the time response of the vehicle in tip-in maneuvers increasing very rapidly the Boost Pressure of the engine and filling the lack of response that is typical of a traditional TurboCharged (TC) engine due to the mechanical and the fluid dynamical inertia of the system (the so called *turbolag* effect).

In the following chapter a brief overview about the regulatory framework will be presented; it represents the “boundary conditions” that the product development projects have to comply.

1.1 Regulatory Framework

The technological development of powertrains for transport purpose is actually guided by pollutant emission target and CO₂ regulation compliance. Each vehicle can be introduced on the market only if it has fully complied a homologation procedure.

The current legislation (Regulation 443/2009/EC, adopted on 23 April 2009) defines a limit value curve of permitted emissions of CO₂ for new vehicles according to the mass of the vehicle. The curve is set in such a way that a fleet average for all new cars of 130 grams of CO₂ per kilometer is achieved ([4]).

According to the EU REGULATION (EC) 2017/1151 ([5]) by the 1st September 2017 the official Test Procedure for homologation is the WLTP (Worldwide harmonised Light-duty vehicles Test Procedure), and the related driving cycle is the WLTC (Worldwide harmonised Light-duty vehicles Test Cycle). It substitutes the NEDC (New European Driving Cycle), used up to that date.

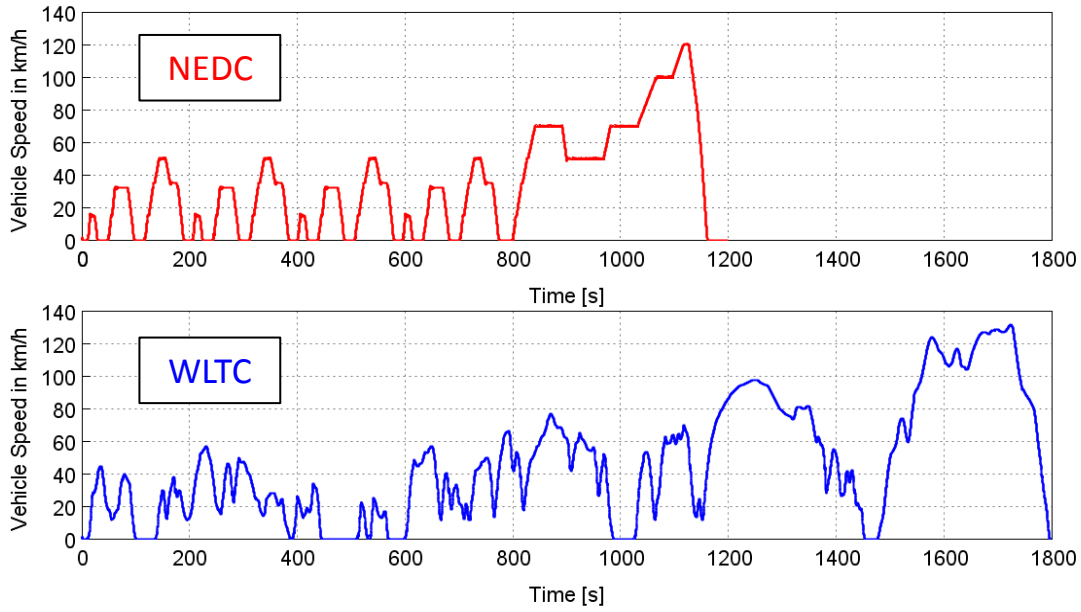


Figure 1.1 - NEDC and WLTC homologation driving cycles

During the homologation procedure, the vehicle reproduces the driving cycle on a chassis dyno. The procedure aims to closely reproduce the real driving activity in terms of vehicle velocity and acceleration. For this reason, the target speed profile is defined with a statistic approach; the WLTC is considered more representative of everyday driving with respect to the NEDC and the homologation procedure closely reproduce the real driving condition (additional weight, electric loads etc.).

According to the EU REGULATION (EC) 2017/1151 ([5]) Sub-Annex 8 Appendix 2, for NOCV-HEV (Non Off-Vehicle Chargeable HEV) the values of CO₂ in terms of g/km can be compared if the charge sustaining condition is respected; it is formulated as:

$$C_{criterion} = \frac{E_{battery_depleted}}{E_{fuel}} < 0,005 \quad i.e. < 0,5\% \quad (1.1)$$

It implies that the difference between the energy in the battery at the initial state and the energy at the final state of the driving cycle ($E_{battery_depleted}$) is lower than the 0.5 % of the fuel chemical energy used in the cycle E_{fuel} .

The legislation EC 333/2014 sets from the 2020 the long-term target as 95 grams of CO₂ per kilometer for the reference mass vehicle ([6]). This target, at least for gasoline engines, is far beyond current system capabilities.

1 Introduction

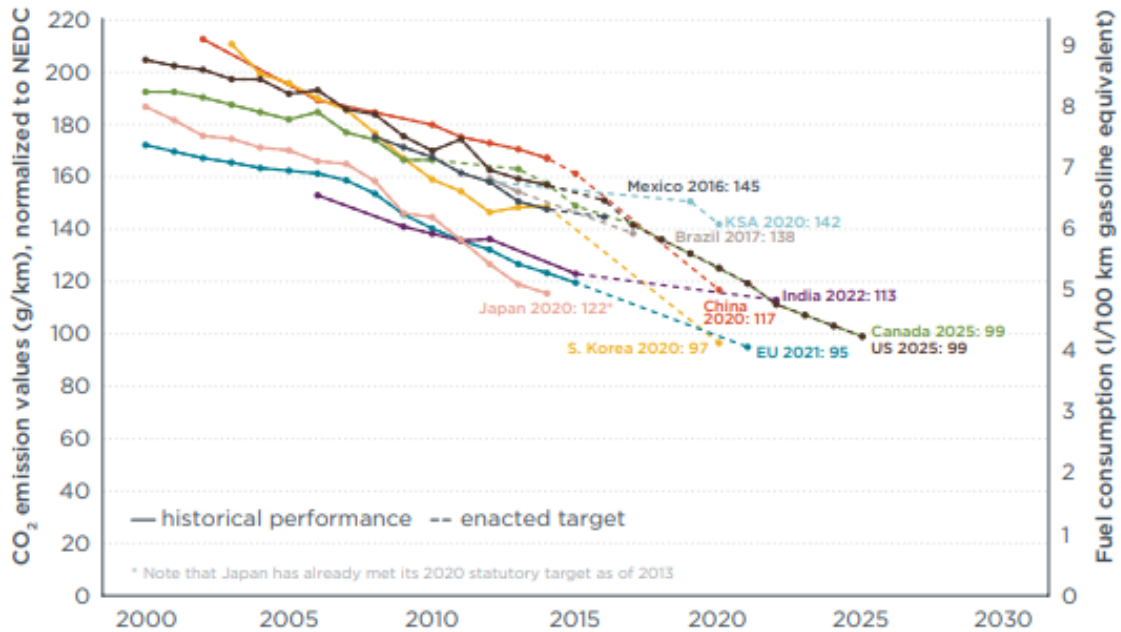


Figure 1.2 - Historical fleet CO₂ emissions performance and current standards (gCO₂/km normalized to NEDC) for passenger cars [7]

In addition, the path taken by the Regulatory Agencies, in the Europe and worldwide, is the want to introduce a procedure that really measure emissions of pollutants and greenhouse gasses during real driving. Real Driving Emission (RDE) procedures will be intensively adopted in the following years and it entails further improvements in engine development. Differently from a driving cycle, in which the operating points of the engine can be easily detected if vehicle and engine data are known, during a real driving the operating point cannot be defined a priori. The consequence is that the overall engine map should be optimized for pollutants and fuel consumption reduction.

2 Hybrid Electric Vehicles

Hybrid Electric Vehicles (HEVs) combine two sources of power that can provide propulsion; the primary energy source is generally the chemical energy stored in the fuel feeding the internal combustion engine, the second is the electrical energy stored in a on board battery. The advantage of electrified powertrains is the possibility to split the total power request among the fuel and the energy buffered in the battery, exploiting the optimum combination for fuel consumption minimization ([8-10]).

2.1 Classification

Several classifications for HEVs have been proposed and can be found in literature, however the most used among car manufacturers concerned the path followed by the power flow from the energy sources to the wheels ([9]):

- Series Hybrid Vehicles: the Electric Machine (EM) is the only propulsion system that is able to deliver power to the road. The ICE is connected to an electric generator and is used to charge the battery. The main idea beyond the Series HEV concept is the aim to operate in a very high efficiency region of the ICE and to provide the fluctuating power required at the wheels with an electrical machine, taking advantages of its quite high efficiency in the overall operating map.

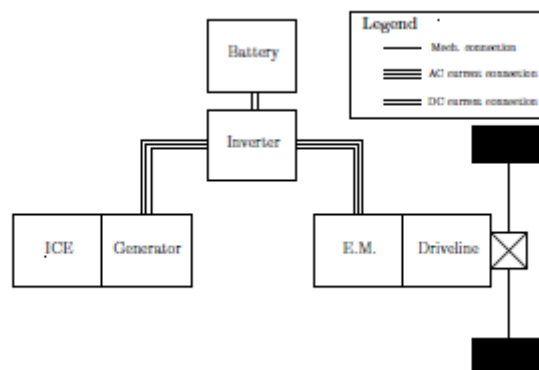


Figure 2.1 - Scheme of a Series Hybrid Layout [10]

- Parallel Hybrid Vehicles: both ICE and EM simultaneously fulfil the driver power demand; the power supplied by the two propulsion systems sum together at different level of the transmission line: Single Shaft HEV, Double Shaft or Double

2 Hybrid Electric Vehicles

Drive Parallel HEVs are parallel architectures in which the power provided by the two propulsors join together respectively at ICE crankshaft, transmission or road level. The control of such a system is generally more complex which respect to a series HEV, because they evidence a larger number of degrees of freedom for the power split operation.

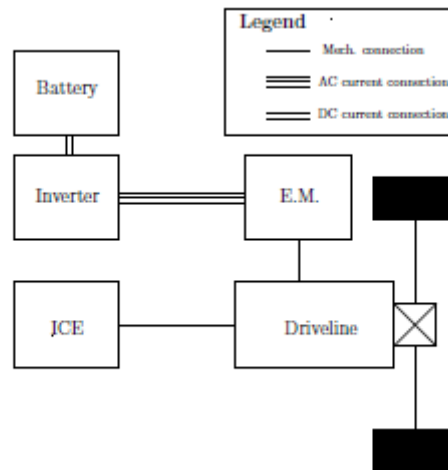


Figure 2.2 - Scheme of Parallel Hybrid Layout [10]

- Complex Hybrid Vehicles: they can be obtained by increasing the number of traction motors/ICEs, by increasing the number of energy and power sources; or by coupling parallel and series concepts on the same powertrain architecture. Complex HEVs are able to combine in a very efficient way the ICEs and EMs operation; unfortunately, the level of control strategy complexity consequently increases.

Another widely used classification regarding HEVs is based on the location of the EM which respect to the ICE, namely P0, P1, P2, P3 and P4. Different Hybrid architectures allow the exploiting of different functionalities as shown in Figure 2.3.

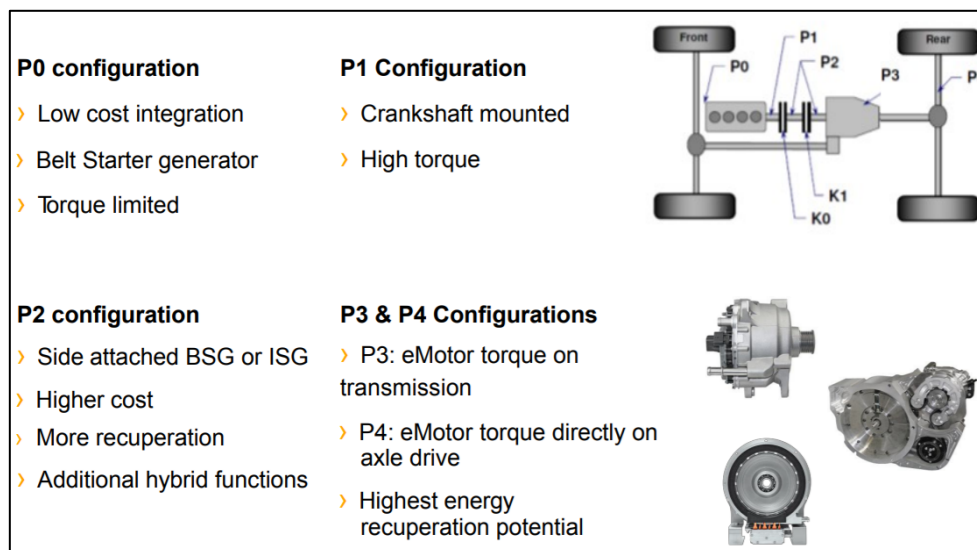


Figure 2.3 - Classification of hybrid architecture and main functionalities [11]

A last general classification for HEVs should be mentioned, formulated on the base of the Electric Power available on board, as reported in Table 2.1.

| | Voltage Range [V] | Electric Power Range [kW] | Battery Charge |
|---------------------|-------------------|---------------------------|-------------------|
| Micro-Hybrid | 12-48 | 1-6 | Charge Sustaining |
| Mild-Hybrid | < 48 - > 200 | 5 - 20 | Charge Sustaining |
| Full-Hybrid | Hundreds | >20 | Charge Depleting |

Table 2.1 - Hybrid Classification based on electric power and voltage

Actually, increasing the electric power, the benefits in terms of fuel consumption and CO2 Tank To Wheel (TTW) increase to, as well as the cost of the products.

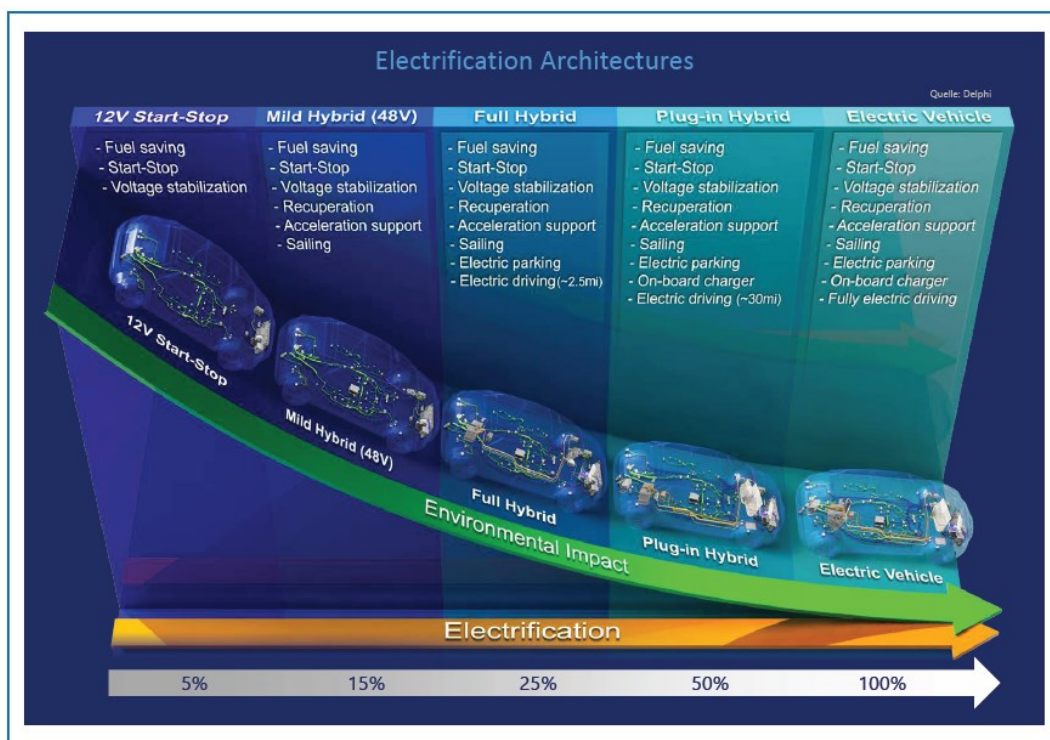


Figure 2.4 - Electrification architecture overview [12]

2.2 48V Mild-Hybrid Vehicles

Low level hybridization is one of the most convenient powertrain concepts that car manufacturers are prompt to introduce on the market because a quite limited change in

production process and in the product design is needed. Definitely, 48V Mild-Hybrid Electric Vehicles (48V MHEVs) are for sure a good compromise between fuel consumption reduction effectiveness and manufacturers' needs.

2.2.1 Architecture Overview

On Mild-Hybrid 48V vehicles are present two voltage electric network, respectively 12V and 48V. The two electric system are connected with a DC/DC converter. While the 12V boardnet, as in a conventional vehicle, supplies electric power buffered in a battery to all the 12V loads present on board, the 48V network feed the 12V network through the converter and it can provide energy to all 48V loads. A 48V EM is present, leading to a P0 or a P2 hybrid architecture. The functionality that the EM usually accomplish are:

- *Regenerative Braking*: a partial recovery of the energy during deceleration phases, that otherwise has to be completely dissipated by brakes. It represents usually the most efficient method for charging the battery in a hybrid control strategy. The amount of energy recoverable depends on the actuated strategy of regenerative braking as well as the size of the electric machine and the hybrid architecture.

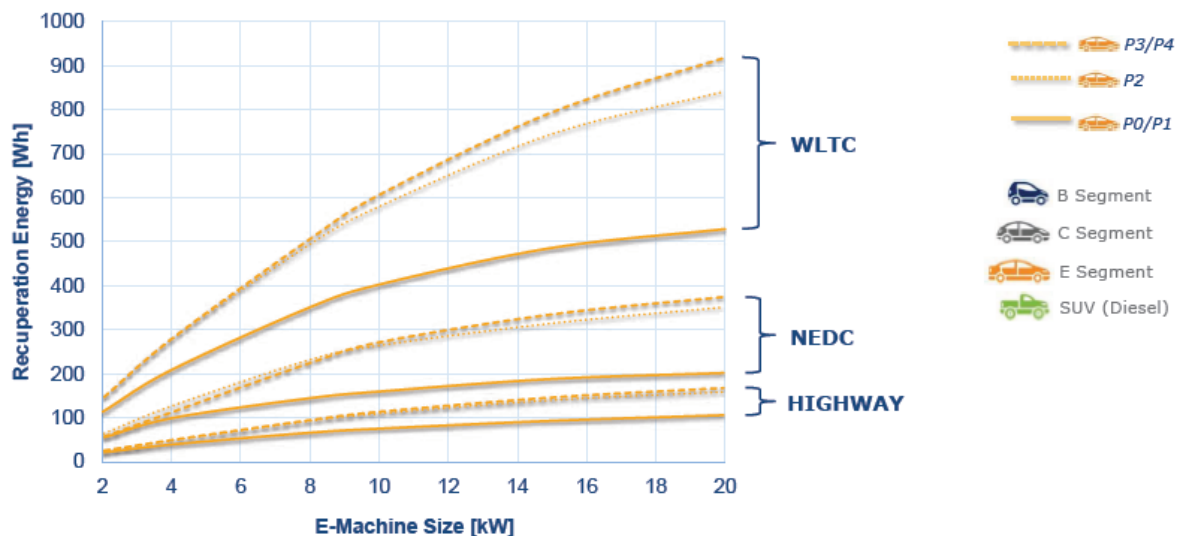


Figure 2.5 - Recoverable Energy with different hybrid architectures for different hybrid architectures on WLTC, NEDC and highway driving cycle [13]

- *Load Point Moving*: shift of the engine operating point toward the Optimum Operating Line (OOL) of the engine. If the engine should operate at high load a boosting operating from the EM could be convenient, on the other side, mainly for gasoline propulsion system that shows a quite low efficiency at low load, a increase of the load together with a braking operation from the EM (charging the battery) could be an effective solution.

- *Electric Drive*: possibility to keep the engine off during the starting phases and provide the overall driver power demand with the electric motor. In this way the low engine load starting phases in which the engine operates with a very poor efficiency are avoided. Of course, this functionality can be exploited only with an appropriate Battery and EM size. With a P0 architecture exploiting the Electric Drive features, also pumping and friction power have to be taken into account, representing a surplus of power need for traction; for this reason, usually P2 and other architectures are preferred for Electric Drive potentiality.
- *Coasting*: functionality which provides the idling state of the engine and filling the power driver demand only with the Electric Machine. It is usually performed in high speed and at low load engine conditions that means very poor efficiency.

A MHEV architecture allow also to investigate a limited level of *downsizing*. The boost effect of the EM recovers the eventual lack of peak power and torque; on the other side the ICE operates on average at higher load and consequently at higher efficiency region.

Another interesting opportunity for a dual voltage vehicle as a 48V MHEV is the utilization of high power electrical auxiliaries (eSupercharger, eCatalyst, eWater Pump, active suspension,...). They can lead to fuel consumption reduction, to after treatment (AT) warm-up but also to drivability and comfort improvements. It is worth to be highlighted that further hybrid control strategy modifications are usually required in order to manage in an optimum way the overall electric power consumption, aimed for propulsion purpose or not.

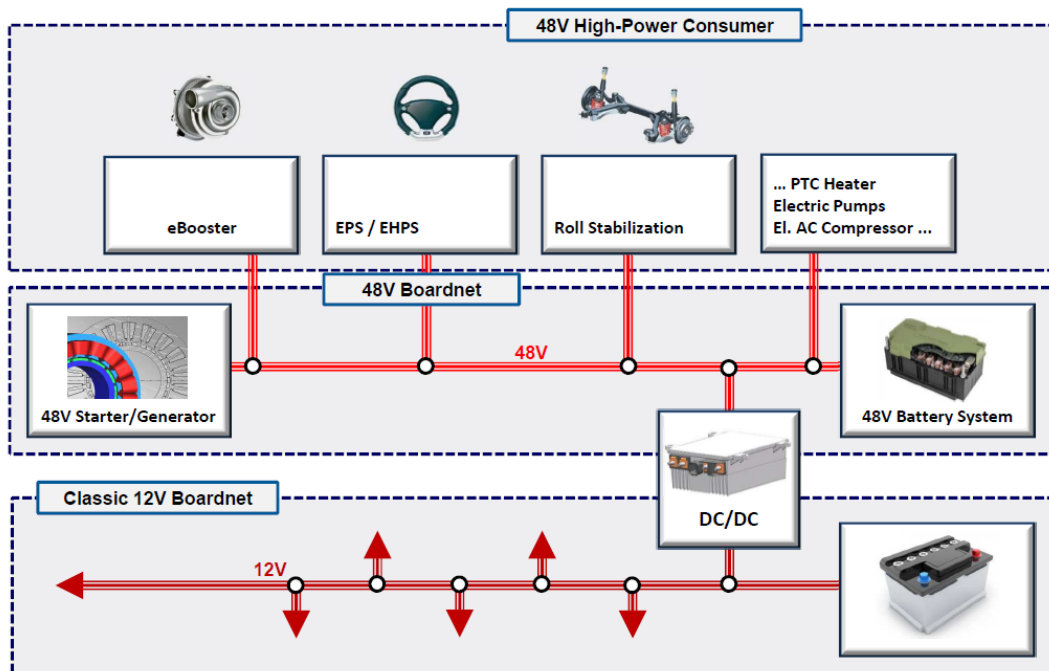


Figure 2.6 - Scheme of electric network for a 48V MHEV: dual voltage network and scheme of electrical ancillaries [14]

In the following chapter a detailed presentation of the above-mentioned eSupercharger will be reported.

2.2.2 eSupercharger

The eSupercharger, alternatively called also eBooster or eCompressor, is spreading in the market because of its relevant benefits in terms of fuel consumption reduction and transient response improvements for a gasoline ICE equipped vehicle and also for a better EGR control in Diesel powertrains ([15]).

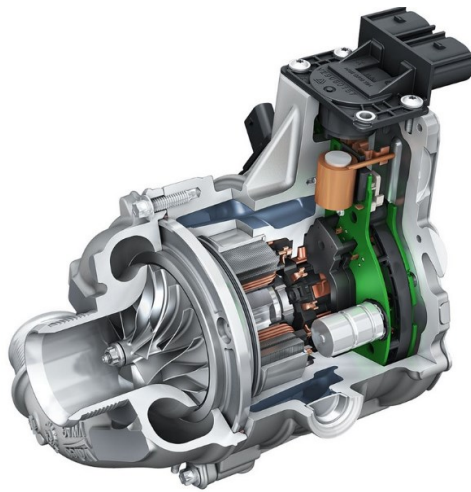


Figure 2.7 – eSupercharger picture: compressor and integrated electric motor

Consisting of a compact unit (low inertia and low mechanical and electrical losses), reliable and able to withstand high temperatures, usually water cooled, the eSupercharger is designed to increase supercharging pressure and improve transient behavior without increasing exhaust gases back-pressure. The eSupercharger boosts the engine in situations where the classic turbocharger shows too long response times to reach the nominal working pressure (the typical turbo-lag) [16]. In this situation the electric compressor intervenes instantaneously allowing a rapid growth of the effects of the supercharging and reducing the response delay of the motor to the driver actuation very to zero. Both upstream and downstream layout of the eSupercharger with respect to the Turbocharger are possible: upstream is preferred for packaging needs; downstream instead shows benefits for transient response.

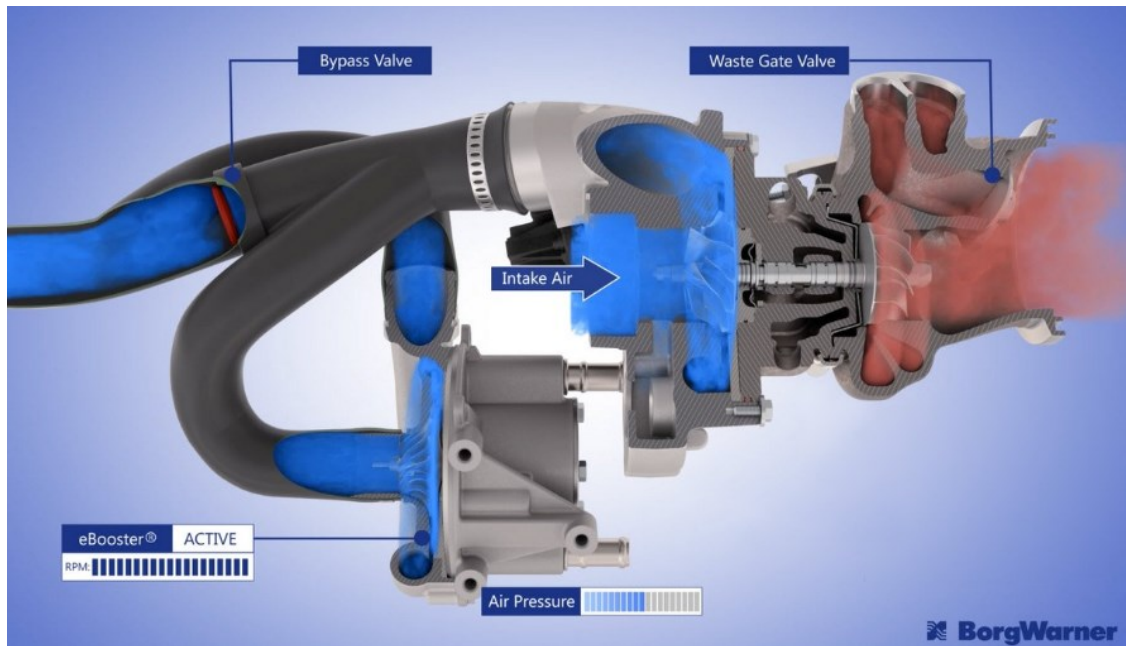


Figure 2.8 - Dual stage supercharging layout with eSupercharger [17]

This study is aimed to exploit not only transient performance benefits of the eSupercharger, but also the potentialities of this device for a fuel consumption reduction. It is worth to be anticipated that a higher level of management complexity will be the consequence of that choice. Based on that, in the next chapter a general overview of the current Hybrid Control Strategy will be presented, trying to briefly underline strengths and weakness of each one.

2.3 Hybrid Control Strategy

As reported in [18], “*Energy management in hybrid vehicles consists in deciding the amount of power delivered at each instant by the energy sources present in the vehicle while meeting several constraints*”.

In a conventional vehicle a low-level controller is present (i.e. Engine Control Unit ECU), that translates information coming from the actuators (accelerator pedal, brake pedal,..) to a several number of input in the engine (spark-advance, energizing time for the injectors,..). In a HEV an additional control level has to be considered, namely energy management system. It is composed of two parts:

- *Supervisory Controller*: defines the engine status and determine the optimum HEV functionality (load point moving, Electric Drive,..) taking into account all the state variable for a given time instant (driver power demand, vehicle speed, clutch status,..).
- *Energy Management System*: defines the power split between ICE and EM when the Supervisory Controller outputs provides a power split operation.

2 Hybrid Electric Vehicles

The Figure 2.9 reports a schematic representation of how the HEV control system works.

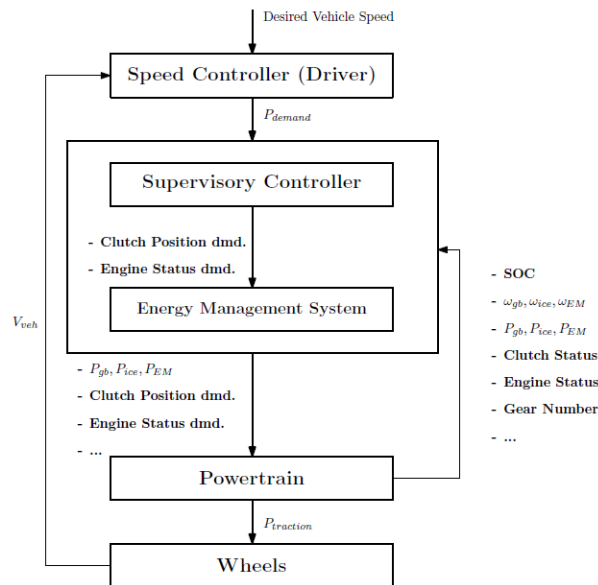


Figure 2.9 - Schematic representation of HEV control system: work flow of supervisory controller and energy management strategy [10]

This task is performed with a particular purpose: in most cases, the strategies tend to minimize the fuel consumption, but the objective could also include the minimization of pollutant emissions, the maximization of power delivery, or – more often – a compromise among all these goals.

According to [11], even if several families of energy management strategies are proposed in literature, two main subdivision will be proposed: *rule based optimization* and *model based optimization* method.

- *Rule Based* energy management strategies are based on heuristics, on the experience or on the result of some more detailed optimization algorithm; the main strengths of such a tool is the feasibility to be implement in a control unit also because do not require any a priori knowledge of the mission profile.
- *Model Based* energy management strategies the goal is the minimization of a given cost function over a fixed and know driving cycle. They cannot be directly used for a real-time implementation in a control unit, because of the too large complexity level and the a priori knowledge of the mission profile. They can be used for rules extraction for on-line implementation and as benchmark solution to evaluate the performance of other control strategies.

It is possible to sub-divide model-based techniques into *analytical* and *numerical* approaches.

In numerical optimization methods, like dynamic programming [10], the entire driving cycle is taken into consideration and the global optimum is found numerically.

Analytical optimization methods, on the other hand, use an analytical problem formulation to find the solution in closed, analytical form, or at least provide an analytical formulation that makes the numerical solution faster than the purely numerical methods. Among these methods, Pontryagin's minimum principle [18] is the most important. Equivalent Consumption Minimization strategy also belongs to this category in that it consists in the minimization, at each time step of the optimization horizon, of an appropriately defined instantaneous cost function. This leads (ideally) to the minimization of the global cost function, if the instantaneous cost function (similar to an instantaneous equivalent fuel consumption) is suitably defined. On the last years, several research projects [19-21] aimed to develop a suitable ECMS tool capable to be implemented on an on-line control unit. They are called Adaptive ECMS. A more detailed presentation about ECMS is reported in the following chapter.

2.3.1 Equivalent Consumption Minimization Strategy

The ECMS is based on the idea that the battery can be considered an energy buffer, and, under the hypothesis of charge-sustaining HEV such that there will be no difference, or at least negligible, between the State of Charge (SOC) at the initial and at the final state of the mission profile, there will be a perfect balance of the energy delivered and stored into the battery. This means that chemical energy of the fuel and electrical energy are definitely equivalent and there could be a conversion from one form to the other.

At a given operating point two cases are possible:

1. the battery power is positive (discharge phase) at the present time; this implies that at some future time the battery will need to be recharged, resulting in some additional fuel consumption in the future. How much fuel will be required to replenish the battery to its desired energy state depends on two factors: (1) the operating condition of the engine at the time the battery is recharged; and (2) the amount of energy that can be recovered by regenerative braking. Both factors are in turn dependent on the vehicle load, and therefore on the driving cycle.
2. the battery power is negative (charge phase): the stored electrical energy will be used to alleviate the engine load required to meet the vehicle road load, implying an instantaneous fuel saving. Again, the use of electrical energy as a substitute for fuel energy depends on the load imposed by the driving cycle.

The principle underlying the ECMS approach is that a cost is assigned to the electrical energy, so that the use of electrical stored energy is made equivalent to using (or saving) a certain quantity of fuel. This cost is obviously unknown, as it depends on future vehicle behavior, but it has been shown that the cost can be related to driving conditions in a broad sense (for example, urban versus highway driving).

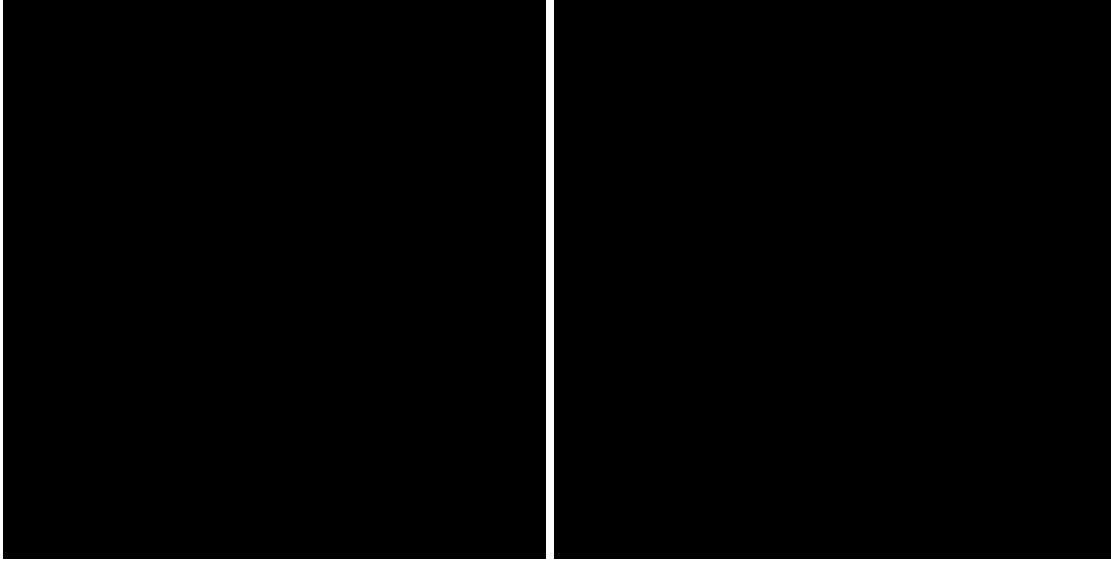


Figure 2.10 - Equivalent fuel flow representation during battery charge (right) and discharge (left) [10]

The idea of the ECMS is to define an equivalent fuel consumption associated to the electrical power flow of the battery. It corresponds to the future fuel flow required to recharge the battery or to the future fuel flow result of an increase of the SOC. The equivalent future fuel flow rate, $\dot{m}_{ress}(t)$ can be summed to the present real flow rate $\dot{m}_f(t)$ to obtain the instantaneous equivalent fuel consumption, $\dot{m}_{f,eq}(t)$:

$$\dot{m}_{f,eq}(t) = \dot{m}_f(t) + \dot{m}_{ress}(t) \quad (2.1)$$

$\dot{m}_{ress}(t)$ can be computed from the battery power considering all the power losses in the flow between the engine and the battery in case of discharge (2.2) or charge (2.3) ([22]):

$$\dot{m}_{ress}(t) = \frac{1}{LHV} \frac{1}{\eta_{ICE} \eta_{batt,chg} \eta_{EM,chg} \eta_{trasm}} P_{batt}(t) \quad (2.2)$$

$$\dot{m}_{ress}(t) = \frac{1}{LHV} \frac{\eta_{batt,dis} \eta_{EM,dis} \eta_{trasm}}{\eta_{ice}} P_{batt}(t) \quad (2.3)$$

The chain of efficiencies through which fuel is transformed into electrical power and vice-versa represents the cost of the use of electricity; it is generally defined as *equivalence factor* it changes for each operating condition of the powertrain.

$$\dot{m}_{ress}(t) = \frac{s(t)}{LHV} P_{batt}(t) \quad (2.4)$$

The equivalence factor $s(t)$ is a set of values, one for charge and one for discharge, and converts electrical power into equivalent fuel consumption. It changes for each operating condition of the powertrain.

The equivalence factor is often set as a constant value, equal for charge and discharge case for the overall driving cycle: despite this simplification could have a great influence on the quality of the control strategy, it simplifies the complexity of the EMS. The selected value has to comply with charge-sustaining condition, and usually depend on the driving cycle itself, on the Driver Power Demand, on the strategy of regenerative braking.

As reported in [18], the following steps must be executed to implement ECMS:

1. Given the state of the system in terms of P_{req} , ω_{eng} , ω_{em} , SoC , . . . , identify the acceptable range of control $[P_{batt,min}(t), \dots, P_{batt,max}(t)]$ which satisfies the instantaneous constraints (power, torque, current limits);
2. Discretize the interval $[P_{batt,min}(t), \dots, P_{batt,max}(t)]$ into a finite number of control candidates;
3. Calculate the equivalent fuel consumption $\dot{m}_{f,eq}(t)$ corresponding to each control candidate;
4. Select the control value P_{batt} that minimizes $\dot{m}_{f,eq}(t)$.

3 Case Study

The main subject of this thesis work is the development of a suitable EMS that is able to take into account the electric power not directly used for propulsion. This represents an update with respect to the current state of art about energy management technique; in response to the increasing demand of electric ancillaries in modern Hybrid architectures, a global management of the energy on board is necessary in order to effectively optimize the use of such a device from an energetic point of view. The adopted EMS is a modified version of the ECMS.

The case study is a B-SUV segment vehicle equipped with a gasoline current market engine. The hybrid architecture adopted is a P0 including an eSupercharger. The modelling approach for the powertrain is a fully dynamics implemented in the 1-D CFD commercial software *GT-SUITE*, whilst the ECMS was implemented with a *Matlab-Simulink* tool.

In the next chapter, the main characteristics of the powertrain will be presented.

3.1 Engine Characteristics

The selected reference engine is a current production gasoline engine whose characteristics are reported in the Table 3.1:

| | |
|------------------------------|---|
| Type | 4 cylinders in line, s.i., turbocharged (wastegate) |
| Bore/Stroke | 72/84 mm |
| Displacement | 1368 cm ³ |
| Compression Ratio | 9.8:1 |
| Maximum Power | 121 kW at 5500 rpm |
| Maximum Torque | 250Nm at 2250 rpm |
| Fuel Metering System | Port Fuel Injection |
| Air Management System | VVA - MultiAir |

Table 3.1 - Engine Technical Data

3.2 Engine Modelling Approach

The engine has been modeled in GT-SUITE 1D-CFD Software. As CFD software GT-SUITE solves the Navier-Stokes system of equations in a discretized domain composed by a certain number of *volumes*. All the thermal and fluid-dynamics properties are function of 1 coordinate only, thus reducing the computational time with respect to a 3D CFD software but with a lower level of accuracy.

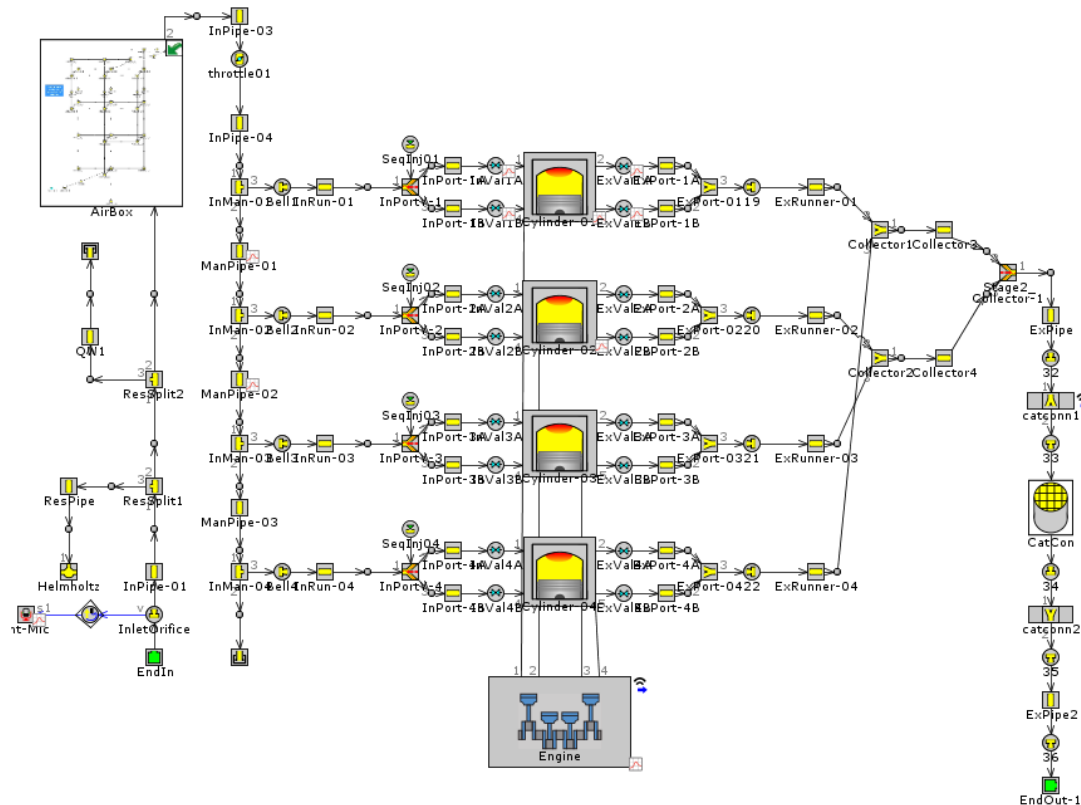


Figure 3.1 - GT-SUITE Engine Modelling example [23]

Recently, the simulation of engine and vehicle on driving cycles are becoming very important and appreciated in the product development phase. Even if 1D-CFD numerical simulation requires relatively low computational time with respect to a 3D-CFD simulation, they could result not suitable for that purpose, and a new type of 1-D model was developed, i.e. *Fast Running Model* (FRM). They are obtained through a model reduction process of the detailed model: lumping volumes together, reducing the number of flow volumes and, consequently, increasing the time step size. An example of FRM assessment used for real time application is reported in Figure 3.2.

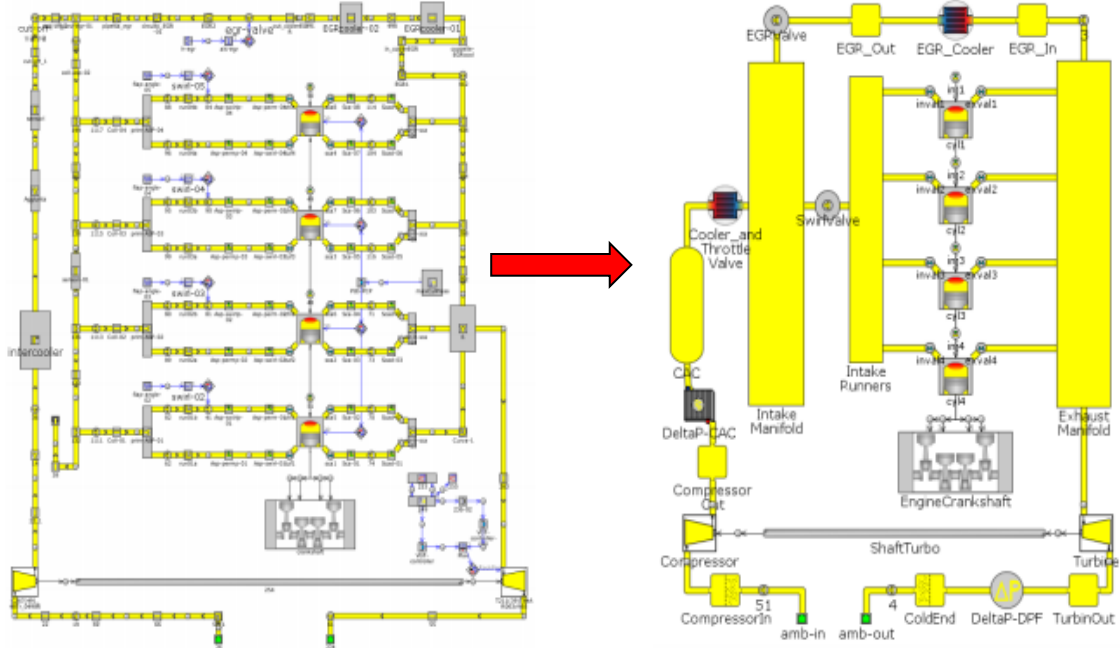


Figure 3.2 - Example of FRM assessment [24]

As reported in [25], for the test case engine the number of flow volumes was reduced from 216 subvolumes to 41 only in the FRM. Even if with the drastic reduction of flow fidelity high frequency dynamics effect such as wave propagation cannot be correctly simulated, the main fluid-dynamics phenomena are still well predicted.

The FRM of the test case engine has been validated at both full load and a part load; a broad set of experimental data was available for full load operation, while at part load. since actuators and combustion timing data were not available, a control-based model was built and validated with respect to the experimental results available. In the following two sections, the validation activity will be explained more in detail.

3.3 Full Load Engine Model Validation

Full load engine model has been performed setting the experimental boost pressure as target and imposing the experimental combustion parameter (MFB50 and MFB10-90) and the equivalence ratio lambda. A simple PI controller acts on the waste-gate opening to achieve the target boost pressure.

In the next graphs is possible to check the accuracy of the FRM, comparing experimental value of mass flows, pressure and temperature with the predicted ones.

3 Case Study

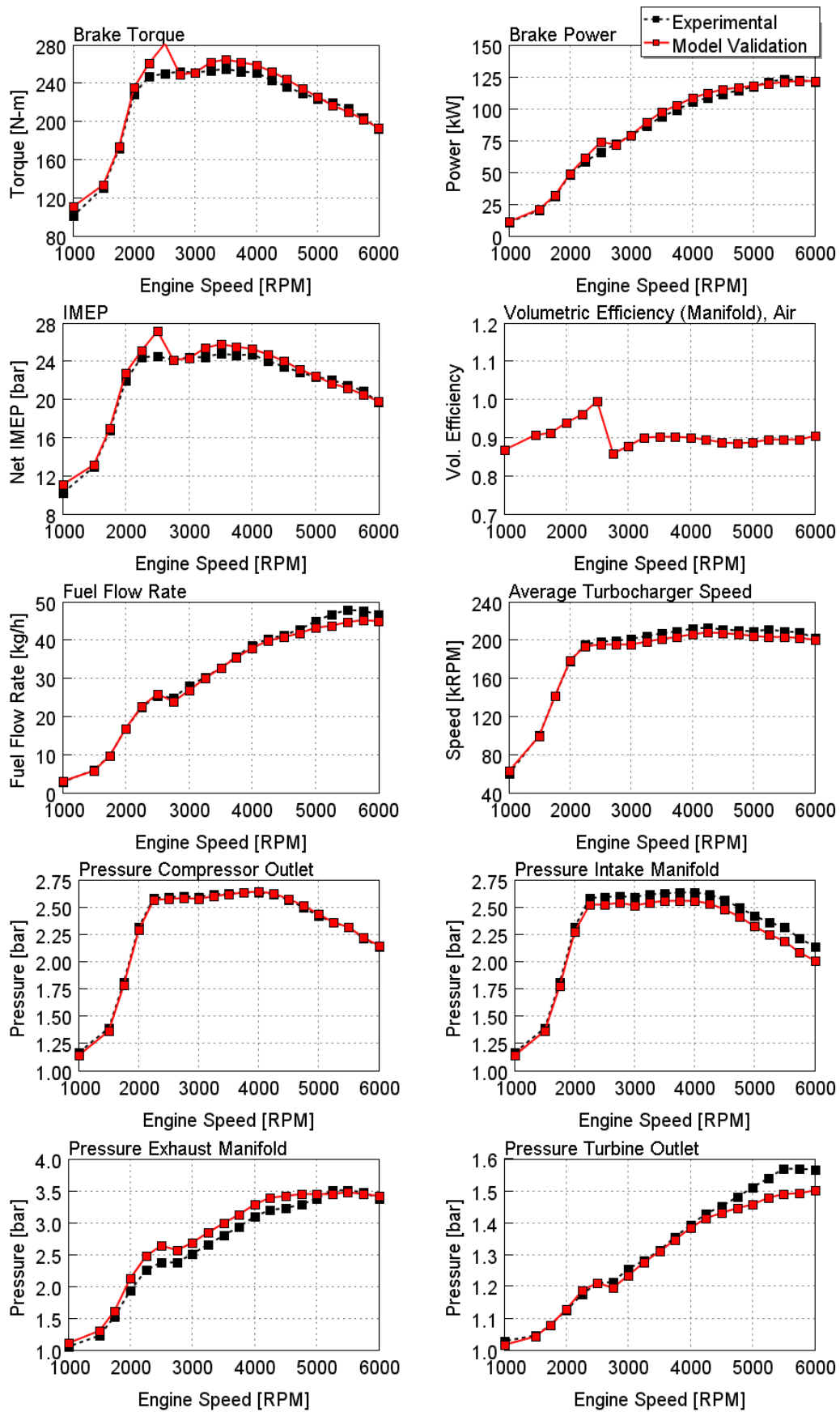


Figure 3.3 - Full Load Engine Model Validation – 1

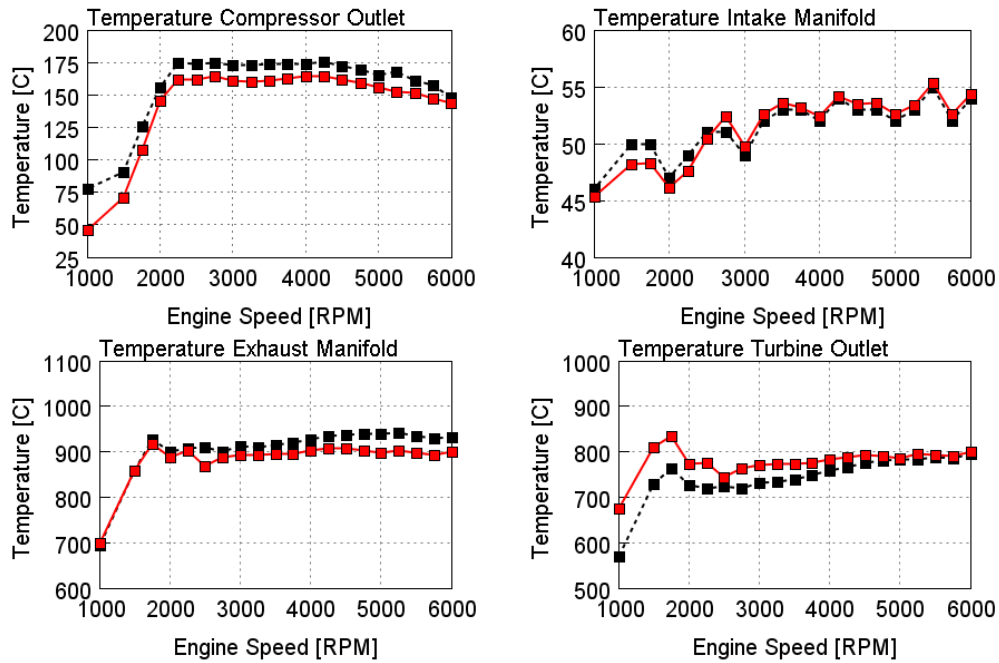


Figure 3.4 - Full Load Engine Model Validation - 2

The full load validation has been considered satisfactory. Although deviations between simulated and experimental values are present, for the purpose of this study, the errors are not relevant.

3.4 Part Load Engine Model Validation

For what concerns part load engine validation, a control-based model was implemented, aiming to replicate the engine operation. The idea of this model is that, following a target boost pressure or brake torque, a certain number of controllers are implemented that act on Waste-Gate (WG) diameter of the turbocharging system and on throttle angle and simultaneously satisfy constraints of TC, Temperature etc.

| Target | Constraint |
|--------------------------------|---------------------------------------|
| Boost Pressure (for full load) | T2 Max = 180°C |
| | T3 Max (experimental @ FL) |
| | Surge line Compressor |
| | TC Max Speed = 240 kRPM |
| Brake Torque (for part load) | Knock Limit (experimental @ FL) |
| | Min Lambda (experimental @ FL) |
| | Max MFB-50 (experimental @ FL) |
| | Min Pressure Int. Manifold = 0,25 bar |

Table 3.2 - Engine Model Controllers targets and constrains

3 Case Study

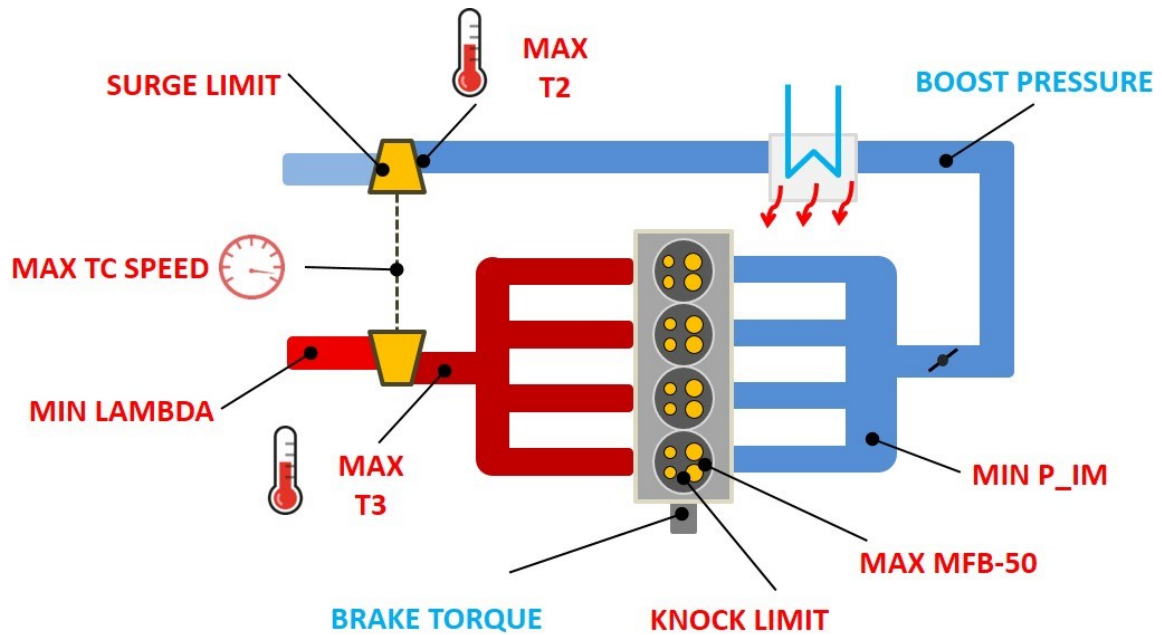


Figure 3.5 - Control-Based Model Engine Scheme

The model was validated at full load (Experimental Boost Pressure targeting). It is able to reproduce almost perfectly both Relative Air-Fuel Ratio and MFB-50.

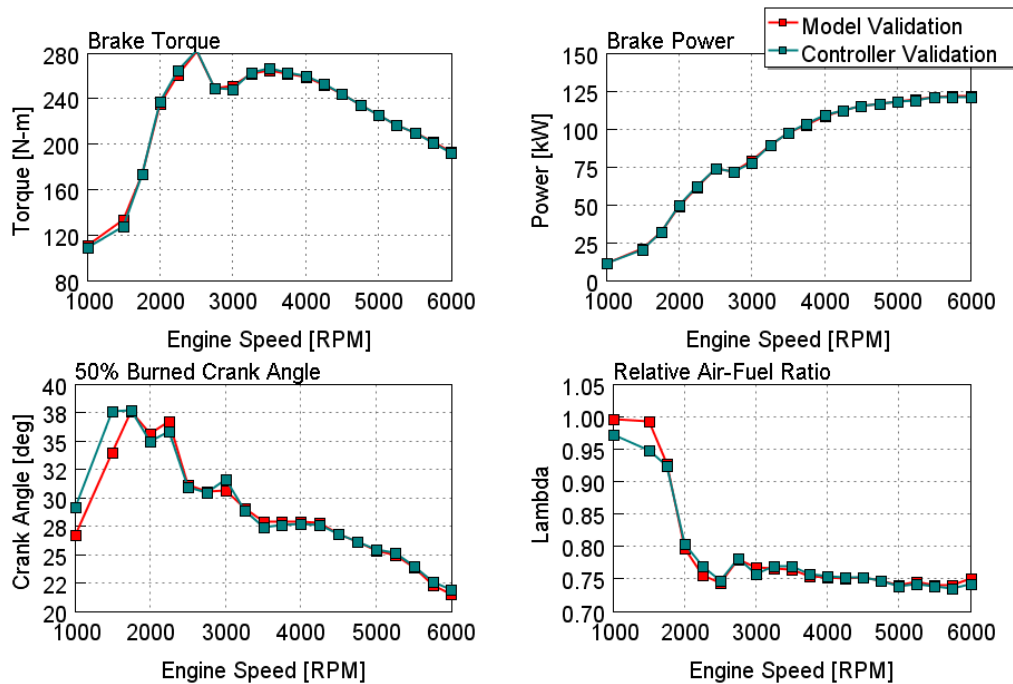


Figure 3.6 - Control-Based Engine Model Validation

This model can be used for Part Load validation. In this case, the aim is to reproduce the available experimental values: IMEP (Indicated Mean Effective Pressure), FMEP (Friction Mean Effective Pressure), Volumetric Efficiency and BSFC (Brake Specific Fuel Consumption).

At part load the engine model is Brake Torque (or BMEP) targeting. A related Intake Manifold Pressure correspond to each engine point. Based on that two regions can be defined on the intake manifold pressure engine map:

1. Throttle regulation: the target brake torque can be achieved without turbocharging.
2. Wastegate regulation: a turbocharging is needed, and the engine will operate at wide-open throttle (WOT) and regulating the wastegate in order to reach the boost pressure required for that operating points.

In the Figure 3.7 these two regions are presented. The WOT curve, represented in Figure with the light blue points, is obtained maintaining the Wastegate as the maximum equivalent diameter and imposing as target a very high values torque curve.

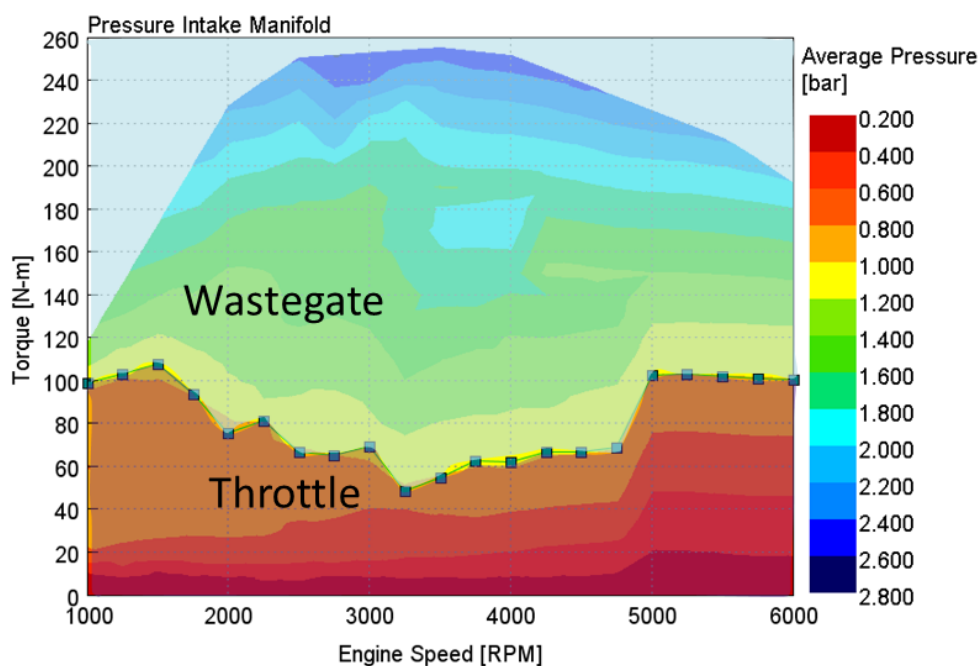


Figure 3.7 - Part Load Engine Control - Throttle and WG controlling regions

The bar plots in the Figure 3.8 show the relative error between experimental and simulated results of IMEP, FMEP, Volumetric Efficiency and BSFC for the WLTC highest frequency operating points (expressed as [RPM] x [Torque]). The deviation from the experimental values do not exceed the 10%, and the average error is much lower for all the parameters. Considering the lack of a broad experimental dataset required for the calibration of the engine model leading to a satisfactory validation, the result has been considered valid for the purpose of this project.

3 Case Study

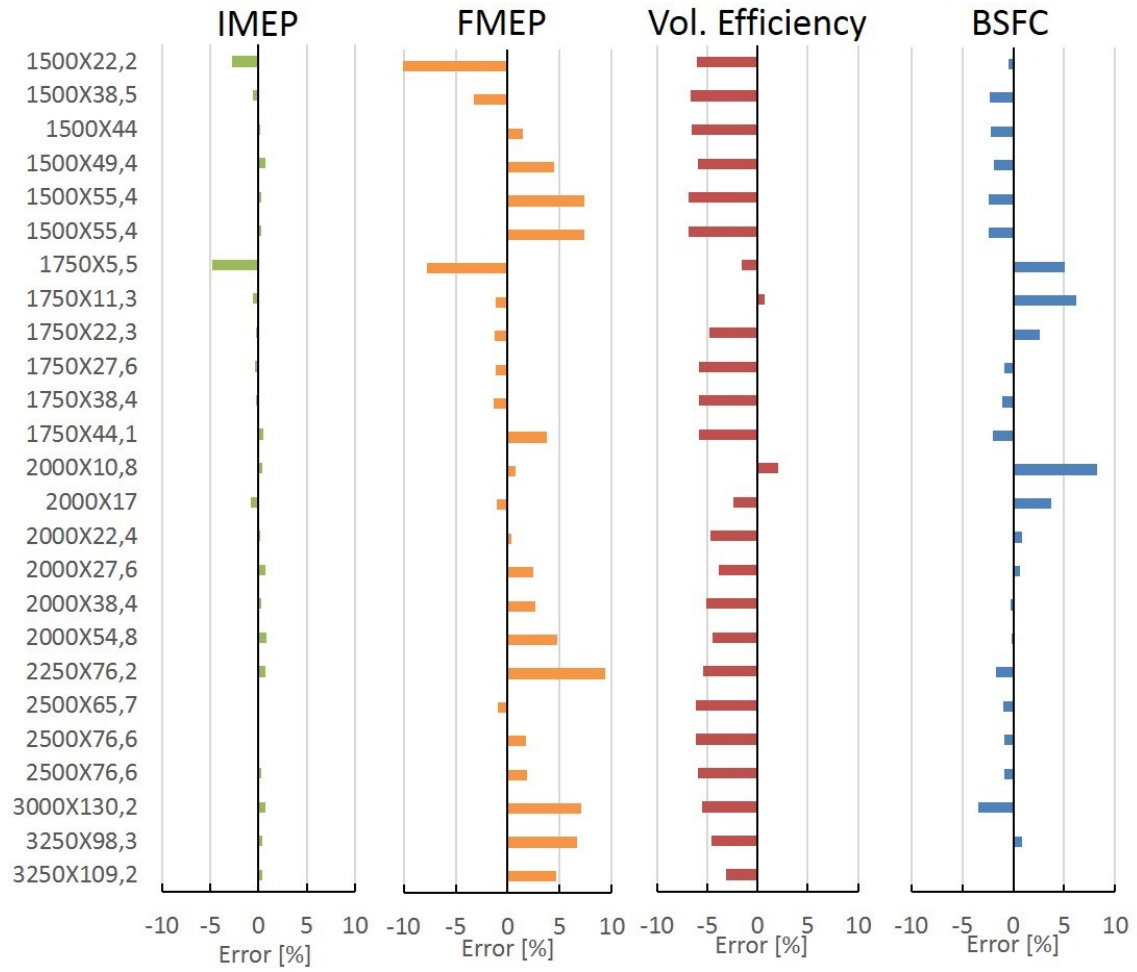


Figure 3.8 - Part Load Engine Model Validation – Relative error of IMEP (green), FMEP (orange), volumetric efficiency (red) and BSFC (blue)

4 Steady-State Analysis

Even though the main subject of the proposed study is to update the energy management strategy of a 48V MHEV, a steady-state analysis of the engine was needed in order to develop an actual engine scenario, both in terms of new regulation compliance and in adoption of new technologies concerning the current state of art for engine development.

4.1 Toward RDE Standards

The first requirement for the engine development was to adopt a fully stoichiometric combustion in the engine model. The reason of this constraint is the future RDE regulation. The test case engine adopts a mixture enrichment at full load. The mixture enrichment was up to now a common practice for gasoline turbocharged engine. For these applications the exhaust gases temperature (usually indicated as T_3) must be lower than the maximum temperature suitable for turbine material; it is often a limit for engine performance. The exceeding fuel present in a rich mixture (Relative Air-Fuel Ratio <1), not completely oxidized during combustion process, acts as diluent reducing the exhaust gases temperature. The result is a reduction of the combustion efficiency, in addition to the not proper working condition for the After Treatment (AT) system of the exhaust gasses. Although mixture enrichment is usually adopted in a limited region of the engine map, usually not reached during type approval driving cycle, like NEDC. The introduction of RDE test procedures does not allow effective but not efficient solution like mixture enrichment for performance.

The validated engine model, as reported in Figure 4.1, confirms for the test case engine a quite broad region of mixture enrichment. The requirement was to avoid this practice, investigating a stoichiometric combustion engine.

4 Steady-State Analysis

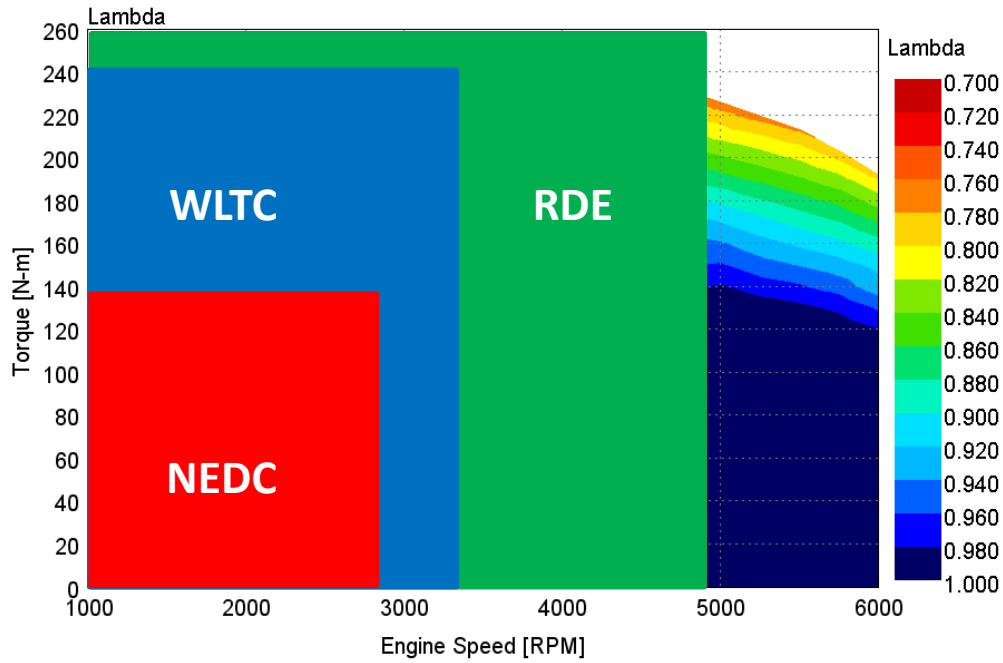


Figure 4.1 - Relative Air-Fuel Ratio Engine Map and driving cycles operating regions

Two different alternatives have been investigated:

- A. Stoichiometric combustion engine, $T_3 \text{ max} = \text{experimental } T_3 @FL (\leq 940^\circ\text{C})$;
- B. Stoichiometric combustion engine, $T_3 \text{ max} = 980^\circ\text{C}$.

The results are reported in the Figures.

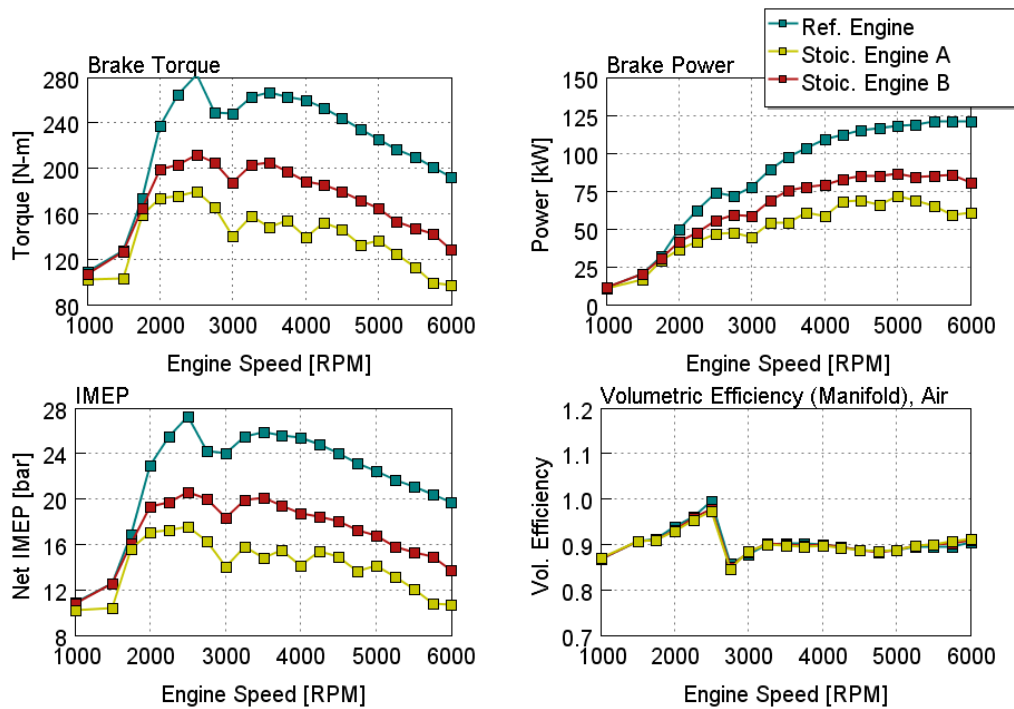


Figure 4.2 – Full Load Stoichiometric Engine Results – 1

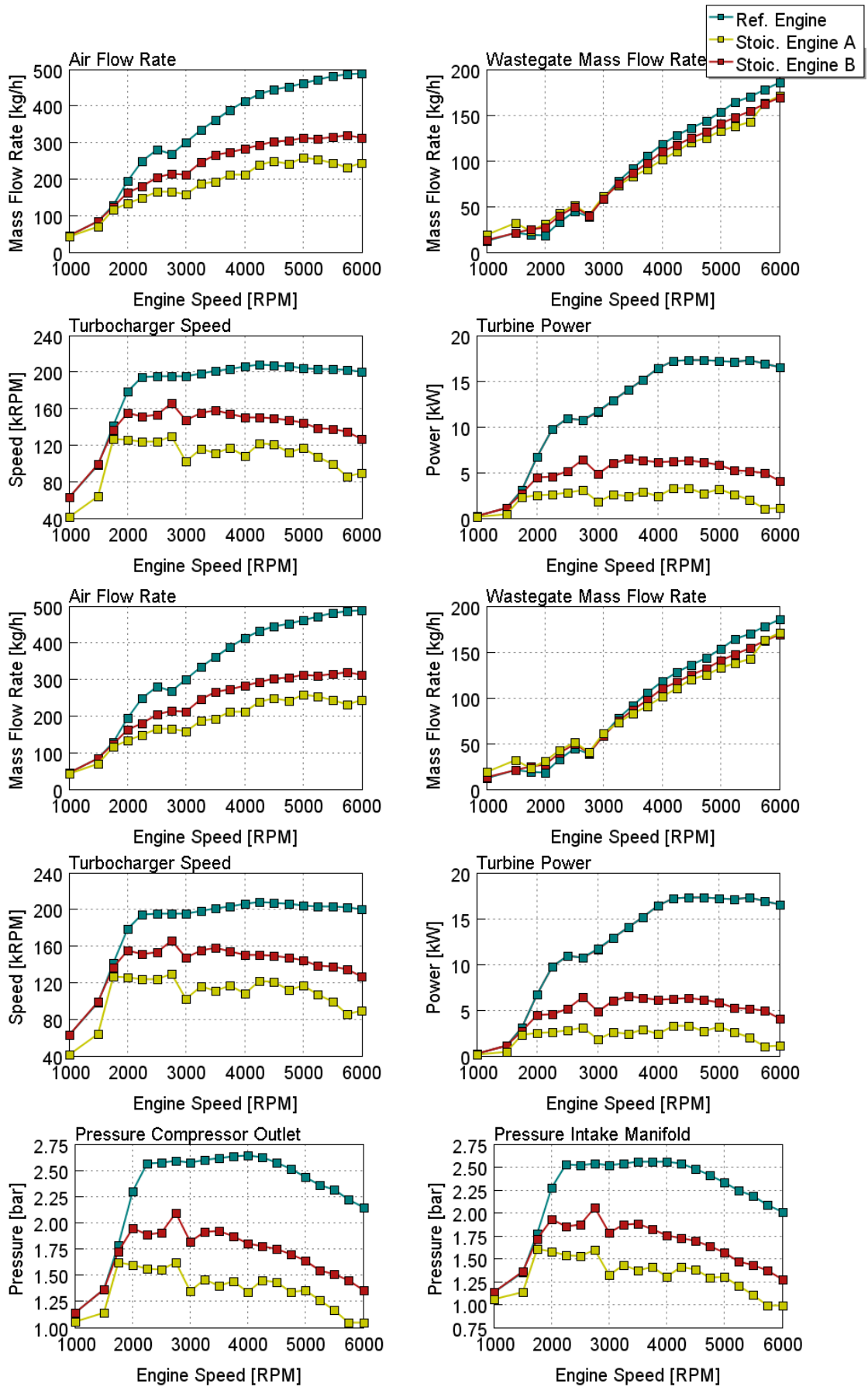


Figure 4.3 – Full Load Stoichiometric Engine Results – 2

4 Steady-State Analysis

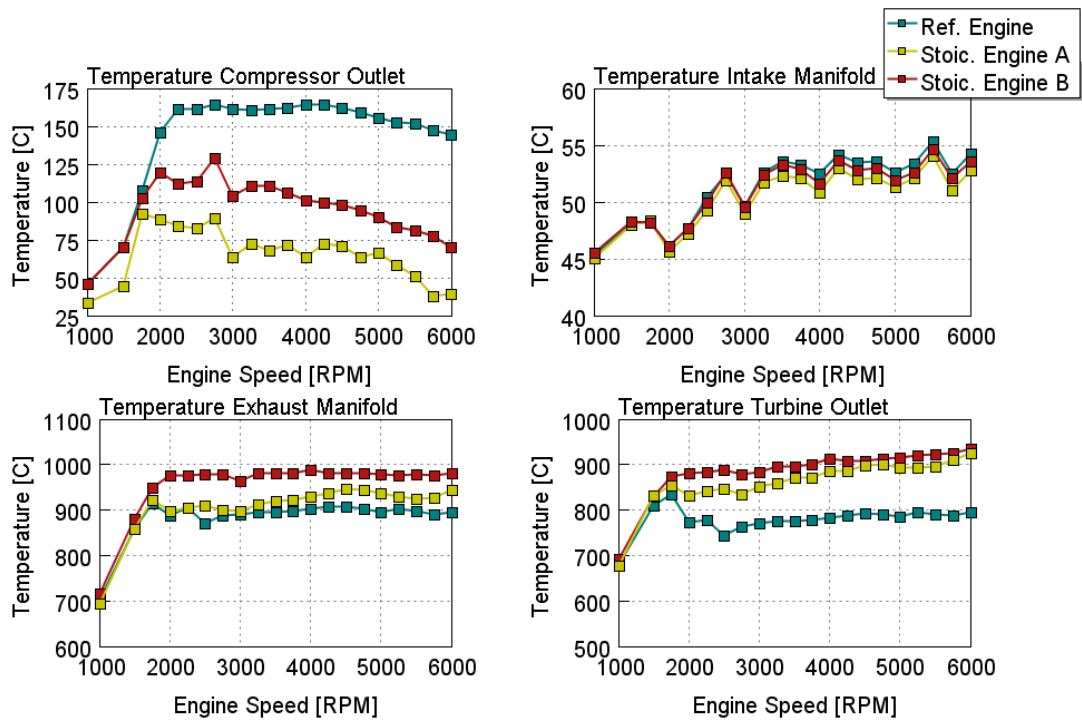


Figure 4.4 - Full Load Stoichiometric Engine Results - 3

Moving to a stoichiometric engine there is a severe deterioration of engine performance. Boost pressure must be reduced in order to keep the temperature at the turbine inlet lower than the material limit one. Wastegate valve is maintained open, in particular at high engine speed region, thus increasing the turbine outlet temperature up to the catalyst limit temperature ($\approx 940\text{ }^{\circ}\text{C}$).

| | Lambda < 1 | Lambda = 1 | |
|--------------------------|---------------------------------------|---------------------------------------|-------------------------------|
| Max. T3 | $\approx 940\text{ }^{\circ}\text{C}$ | $\approx 940\text{ }^{\circ}\text{C}$ | $980\text{ }^{\circ}\text{C}$ |
| Max. T4 | $800\text{ }^{\circ}\text{C}$ | $925\text{ }^{\circ}\text{C}$ | $935\text{ }^{\circ}\text{C}$ |
| Max. Brake Torque | 250 Nm @ 2500 – 4000 RPM | 180 Nm @ 2500 RPM | 210 Nm @ 2500 RPM |
| Max. Brake Power | 123 kW @ 5500 RPM | 72 kW @ 5000 RPM | 86 kW @ 5000 RPM |

Table 4.1 - Full Load Engine Comparison -

Considering the severe derating with a limit turbine inlet temperature of $940\text{ }^{\circ}\text{C}$, the second alternative was selected. However, a reduction of the peak power of 30% and a lowering of the brake torque curve in the overall engine speed region, (reduction of maximum brake torque of 40 Nm) are considered not acceptable. In the next two chapters two different innovative engine concepts will be presented, which performance recovery and efficiency increase have been investigated on.

4.2 Engine Concepts Development

The RDE compliant engine, even with the adoption of a higher inlet turbine temperature, do not satisfy need and requirement of a current state of art gasoline engine. In [26] and [27] an analysis of turbocharged, downsized gasoline engine technology developments and trends is proposed. Gasoline Direct Injection (GDI), a flexible variable valve timing (VVT) are for sure solutions that OEMs are gradually introducing on their products.

Focusing on full load, in Figure 4.5 the main limitations for a downsized turbocharged gasoline engine are shown.

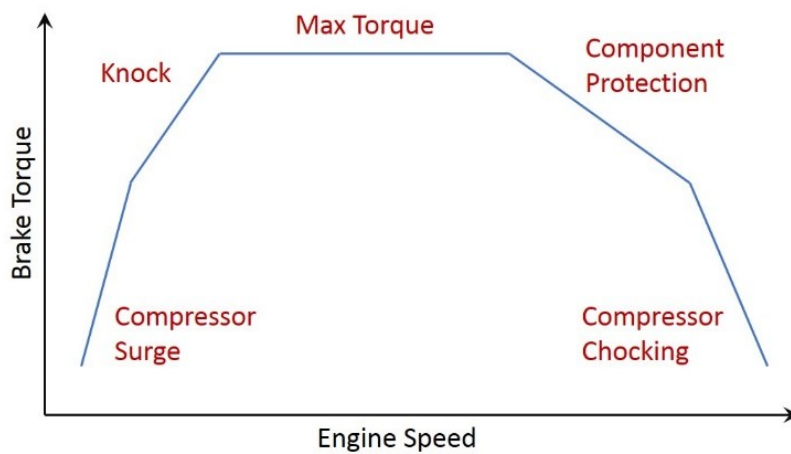


Figure 4.5 - SI Engine Limitations

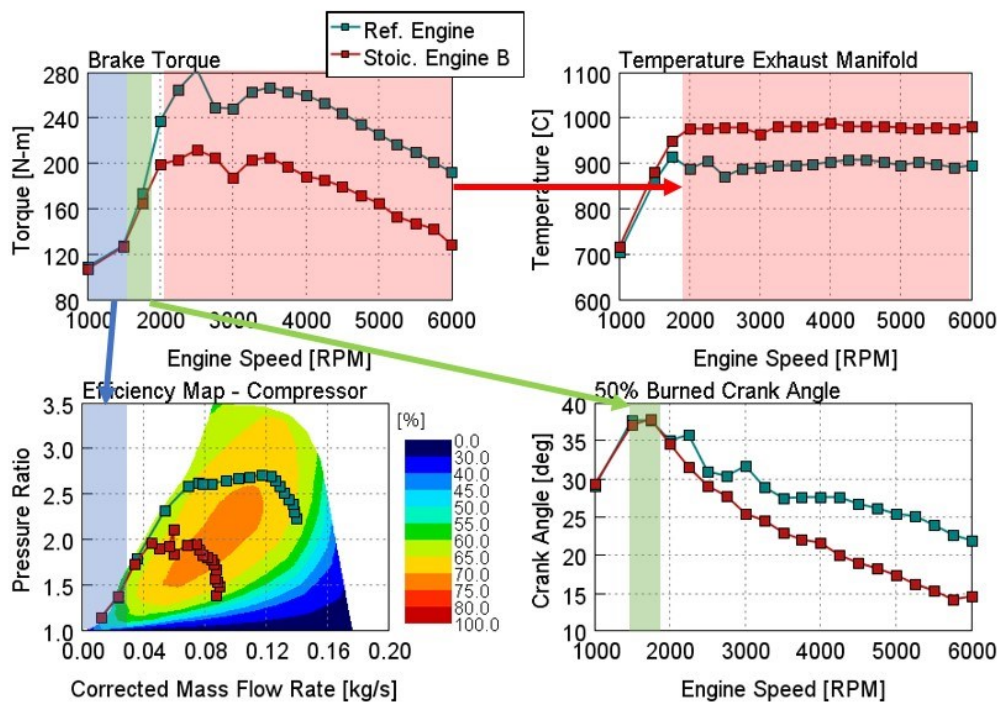


Figure 4.6 - Stoichiometric Engine Limitations

As it is possible to note from Figure 4.6, the turbine inlet temperature limits the brake torque at engine speed higher than 2000 RPM. In the low speed region, the compressor operating points stay on the surge line and the combustion is extremely delayed. Further investigations will be proposed, in order to recover engine performance.

4.2.1 Conventional Engine Concept

A detailed knock model, developed in [28], has been introduced in the model in order to assess the real knock behavior of the engine. More in detail, the knock model used is a Douaud & Eyzat model [29]; the main features are reported in the Table 4.2.

| Knock Model | Douaud & Eyzat |
|---|----------------|
| End Gas Zones | Single Zone |
| Fuel Octane Number (AKI¹) | 90 |
| Knock Induction Time Multiplier | 2.2 |
| Activation Energy Multiplier | 1 |
| Knock Index Multiplier | 1 |

Table 4.2 - Knock Model Data

The model was calibrated on experimental test cases done on the same engine.

Knock for downsized turbocharged gasoline engines is a limitation for the low-end torque performance. Engines usually works in a knock-limit condition: spark advance is calibrated as large as knock likelihood is kept negligible. The spark-advance is set as trade-off between performance and durability of the material, because of thermomechanical fatigue effect due to pressure waves propagating for knock phenomenon ([30]).

The knock model applied on the stoichiometric engine provide completely knock-free operation at full load, according to the Douaud & Eyzat model. Up to now the knock was controlled imposing as limit the knock index from experimental results; the stoichiometric engine is coherent from a knock point of view with the experimental calibration. A reason for a margin from the knock limit operation could be the need to preserve durability of a passenger car engine.

¹ The AKI (Anti Knock Index) octane number express the anti-knock property of the fuel. It is the average of the RON (Research Octane Number) and the MON (Motoring Octane Number).

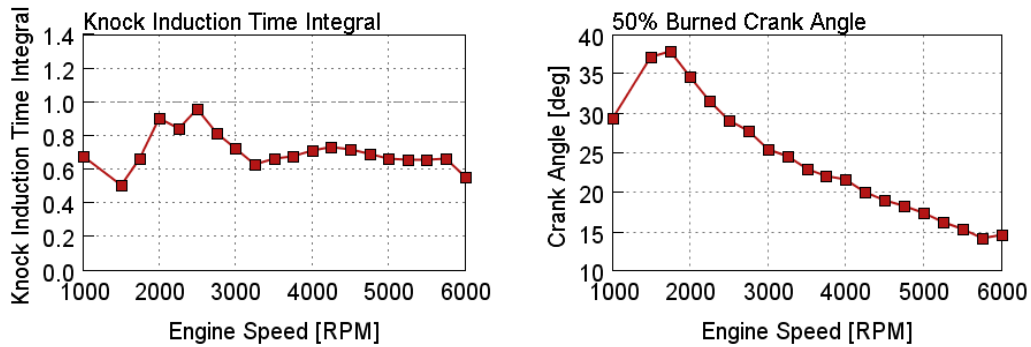


Figure 4.7 - Knock detection results

As Figure 4.7 shows, MFB-50 can be advanced in the overall engine speed region, thus leading to an increasing of full load brake torque curve and improving engine efficiency at high load region of the engine map.

The knock limit operation has been imposed targeting a **2% of unburned gas fraction at knock onset**.

4.2.2 Electrified Engine Concept

Further improvements can be reached focusing on air management. As it is possible to be noticed from Figure 4.6, the turbocharger works at limit condition (Surge line of the compressor map) at very low engine speed, while it presents a quite broad margin at medium-high engine speed. The idea is to couple the conventional turbocharging system with an electric Supercharger and to change intake valves closure (ICV) adopting a *Millerization* of the engine cycle.

The advantage of a Miller cycle for a turbocharged gasoline engine are explained in a detailed way in [31]: advancing (or delaying) the IVC the effective compression ratio decreases, leading to a lower charge temperature at the spark timing. If the supercharging is able to increase the amount of air in cylinder, the result will be a reduced likelihood of knock and a growth of engine performance. Because of the great effectiveness of this technique for knock mitigation, a Miller cycle is often coupled with the adoption of a larger compression ratio that improves engine efficiency at part load.

eSupercharger

The eSupercharger adopted for the study is a 48V eSupercharger. The main technical data are reported in the Table 4.3.

| | |
|---|-----------|
| Compressor Max Speed | 75000 rpm |
| Compressor Max Pressure Ratio | 1,5 |
| Compressor Max Corrected Mass Flow | 0,10 kg/s |
| Compressor Peak Efficiency | 0,82 |
| Compressor Max Speed | 75000 rpm |
| Motor Nominal Torque | 0,6 Nm |
| Motor Electrical Power | 5,3 kW |
| Motor Peak Efficiency | 0,85 |

Table 4.3 - eSupercharger Technical Data

The layout chosen is eSupercharger upstream of the TurboCharger; however, in GT-SUITE a flexible airpath layout has been modelled, allowing to switch from base layout (no eSC) to eSC upstream or downstream.

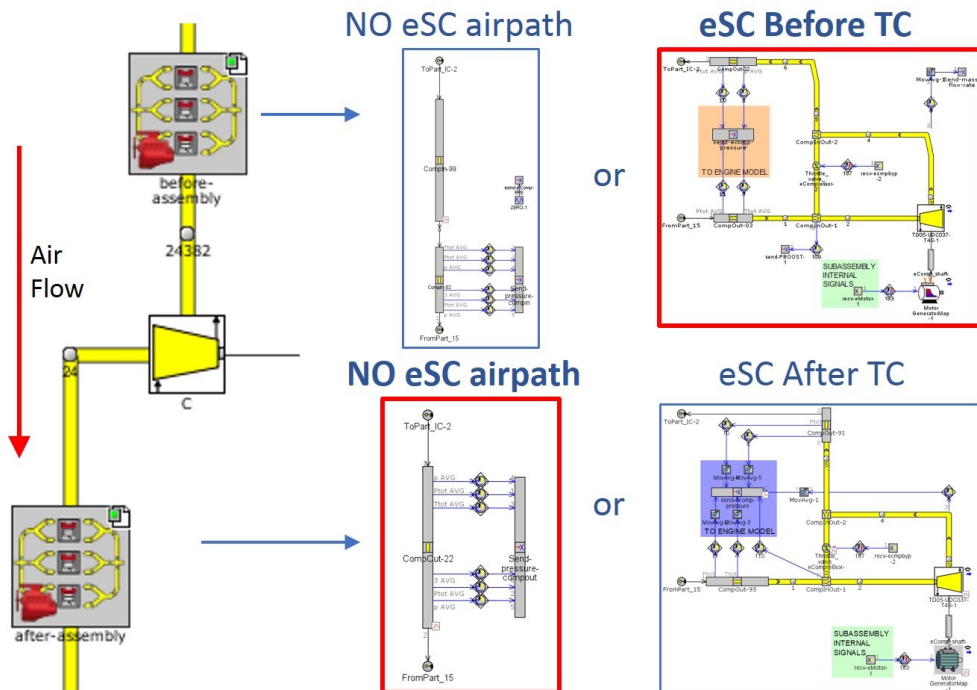


Figure 4.8 - Airpath layout - eSupercharger upstream TC

The adoption of the eSupercharger entails an update of the controller used in the engine model. While at full load without the eSupercharger the wastegate is usually controlled

in order to comply with knock, surge line and the other constraints, in this case boost pressure can be controlled both with wastegate and eSupercharger electric power. The difference is that supercharging the engine with the electric device does not require any backpressure increase, as it happens closing the wastegate valve in a conventional TC system. Lower backpressure means lower residual fraction trapped in cylinder and consequently lower temperature at the start of compression, as well as lower pumping work. For these reasons at full load operation the electric supercharging rather than the turbocharging is preferred, and consequently the waste-gate is kept open if necessary. The influence of the Supercharger layout should be pointed out too: the eSC upstream of the TC is not able to charge larger amount of fresh air, it can be used only for engine speed lower than 3000 RPM. At higher engine speed a by-pass valve will be opened, avoiding the eSupercharging operation.

Miller Cycle

Miller cycle is nowadays one of the most effective solution for knock mitigation in downsized turbocharged gasoline engine ([31]). Two strategy are possible for Miller cycle actuation: Early Intake Valve Closure (EIVC), and Late Intake Valve Closure (LIVC); both strategies can be performed with a VVA system, such as MultiAir technology. A variable effective compression ratio can be achieved with such a system, decreasing the likelihood of knock and decreasing exhaust gas temperature. Because of volumetric efficiency decreases, the boost pressure needs to be enhanced in order to maintain the same amount of trapped air. The strategy used for the Miller cycle in this case is LIVC.

In Figure 4.9 is reported the comparison between the full load engine cycle of the reference valve actuation and the engine cycle with a LIVC (delay of 30 CAD). Both cases are at knock limit and at T3 limit conditions. The Miller cycle is coupled with a Compression Ratio equal to 12 (increased from the base compression ratio of 9.8). In the diagram reported in Figure 4.9, the increase of the work cycle area is evident, as well as the decrease of the pumping loop area and the different levels of intake and exhaust pressures.

4 Steady-State Analysis

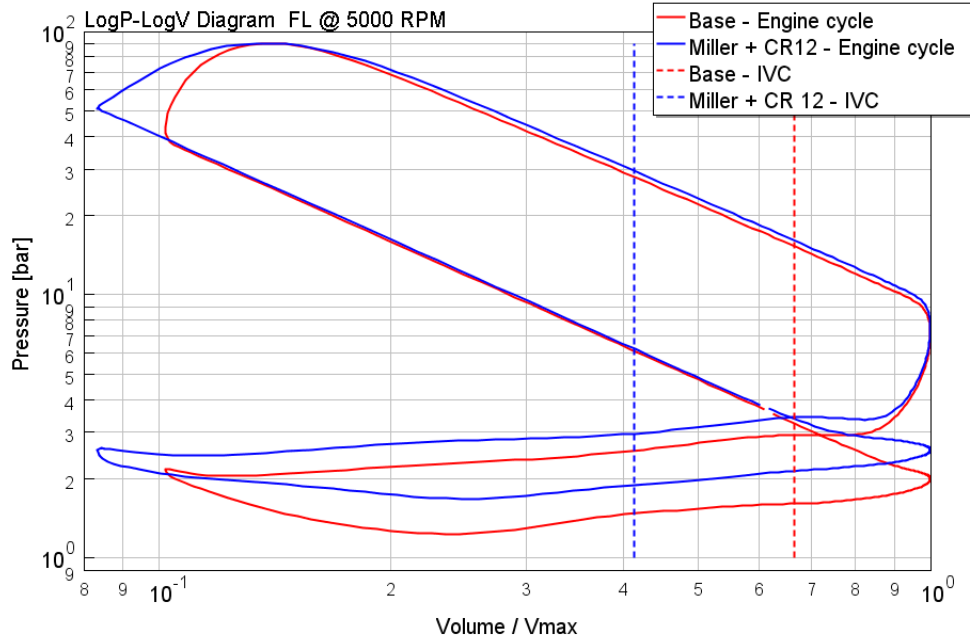


Figure 4.9 - Comparison of conventional and millerized cycle in LogP-LogV diagram

The strategy used is LIVC and it is implemented by keeping the valve at maximum lift for a certain crank angular interval. The reference valve lift profiles are the ones defined by MultiAir strategy.

The strategy of LIVC adopted at full load has been defined aiming to increase the brake torque curve, taking advantage of the available boost pressure and of the flexibility of the MultiAir technology. As example, the investigation of the LIVC of two different engine speed points will be presented, including eSupercharger operation and not.

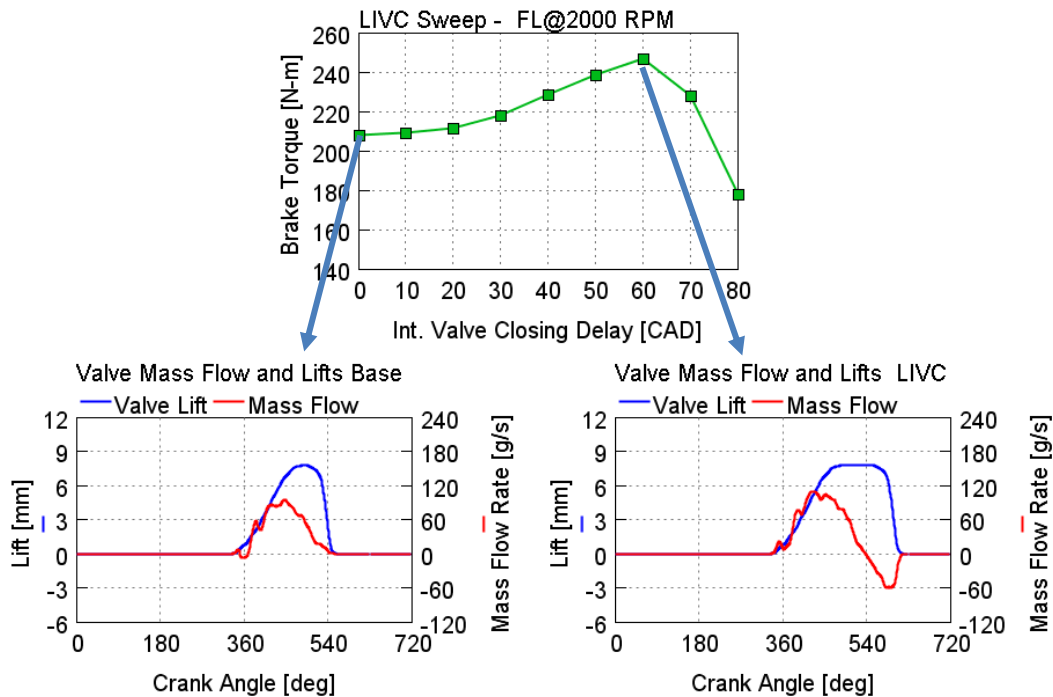


Figure 4.10 - LIVC sweep at 2000 RPM

At 2000 RPM knock phenomenon (more sensible to CR12 adoption) limits Brake Torque. Delaying the Intake Valve the charge Temperature decreases and spark-advance can be increased. The optimum value of delay is 60 CAD. For larger values of delay, both compressors will be limited.

| Engine Concept | Stoic. C | + CR12 | +Miller & eSC |
|---------------------|----------|--------|---------------|
| Brake Torque | 237 Nm | 208 Nm | 247 Nm |

Table 4.4 - Brake Torque Comparison for different engine concepts at 2000 RPM

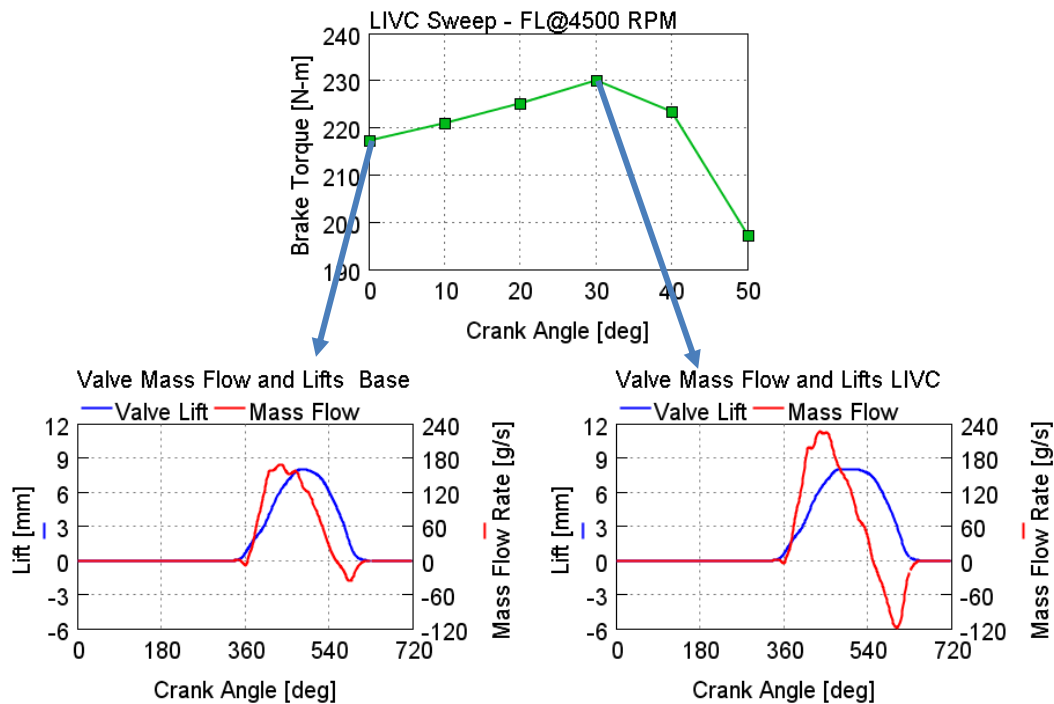


Figure 4.11 - LICV sweep at 4500 RPM

At 4500 RPM the main limitation is T3 temperature. Increasing the Intake Valve closing delay (with CR 12) and consequently Boost Pressure, the exhaust gases temperature reduces. The optimum value of delay is 30 CAD. For larger values of delay, limitation of T2 temperature (and also TC speed) is reached.

| Engine Concept | Stoic. C | + CR12 | +Miller |
|---------------------|----------|--------|---------|
| Brake Torque | 217 Nm | 230 Nm | 230 Nm |

Table 4.5 - Brake Torque Comparidon for different engine concepts at 4500 RPM

The LIVC computed in order to maximize performances is not constant in the overall speed range. The IVC timing angle decrease in low speed range, up to the base IVC value at 1000 RPM. With the closing delay values reported in Figure 4.12, the potential of the Miller cycle is maximized, as the supercharging system (Turbocompressor and eSupercharger) works up to limitation:

- Low engine speed: Surge of Compressor and eSC max speed;
- Middle-high speed range: T2 limit temperature and max TC speed.

4 Steady-State Analysis

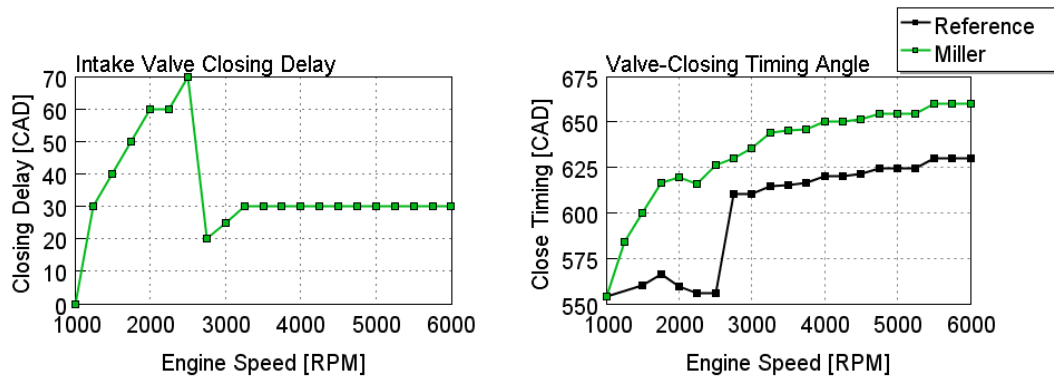


Figure 4.12 - LIVC vs reference valve closing timing comparison

For what concerns Partial Load, LIVC strategy has defined in order to minimize the power demand from fuel. At high speed range (>3000 RPM) the Fuel Flow Rate is the meaningful parameter, and for a certain value of Brake Torque, the target is to minimize it. At lower engine speed instead, the eSC electric power demand must be taken into account. For this purpose, an Equivalent Fuel Flow rate has been defined, as reported in the Equation 4.1.

$$\dot{m}_{f,tot} = \dot{m}_f + \frac{BSFC_{ICE} P_{el,eSC}}{\eta_{el}} \quad (4.1)$$

The LIVC defined for each engine speed correspond to the angle that minimizes the Equivalent Fuel Flow. The assumption is that the engine working at that operating condition produces the power electric power required to the eSupercharger in order to reach a certain operating ICE condition. η_{el} is the overall electrical board net efficiency (alternator, battery charge and discharge), assumed constant and equal to 0,6. For sake of simplicity one engine speed optimization will be reported only.

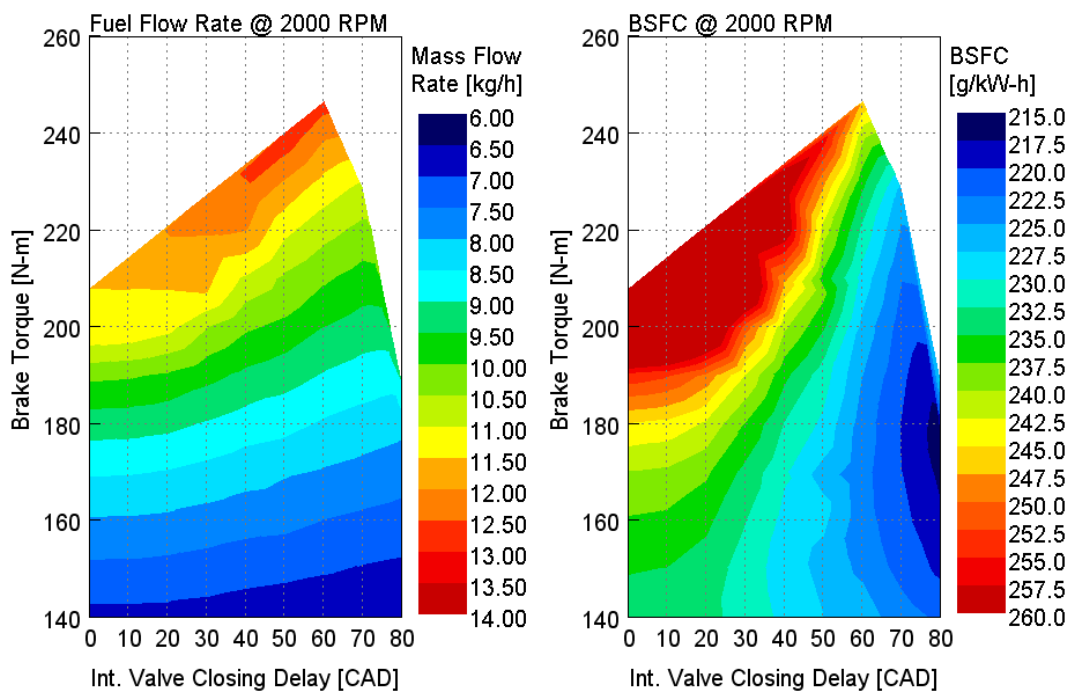


Figure 4.13 - Part Load results for LIVC sweep - 1

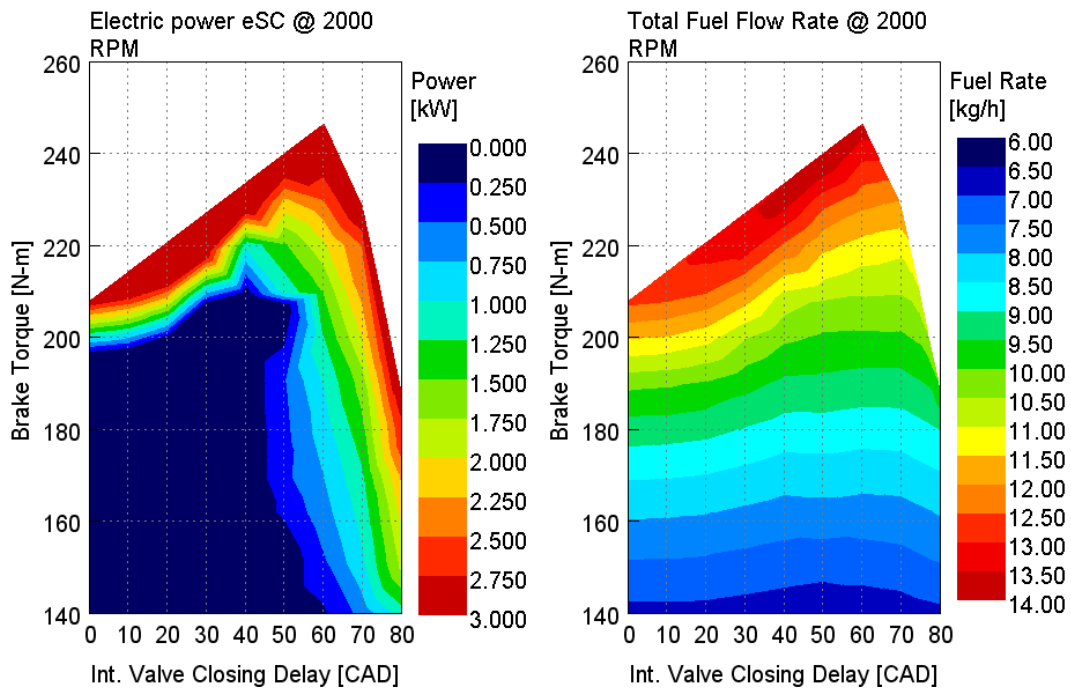


Figure 4.14 - Part Load results for LIVC sweep - 2

The Total Fuel Flow rate function is minimum at the value of LIVC result of the definition at full load in the high load region, while it is almost flat for brake torque values lower than 140 Nm. The most effective strategy is for each engine speed a constant LIVC angle is adopted, able to maximise performances at full load but also to reduce the fuel energy demand.

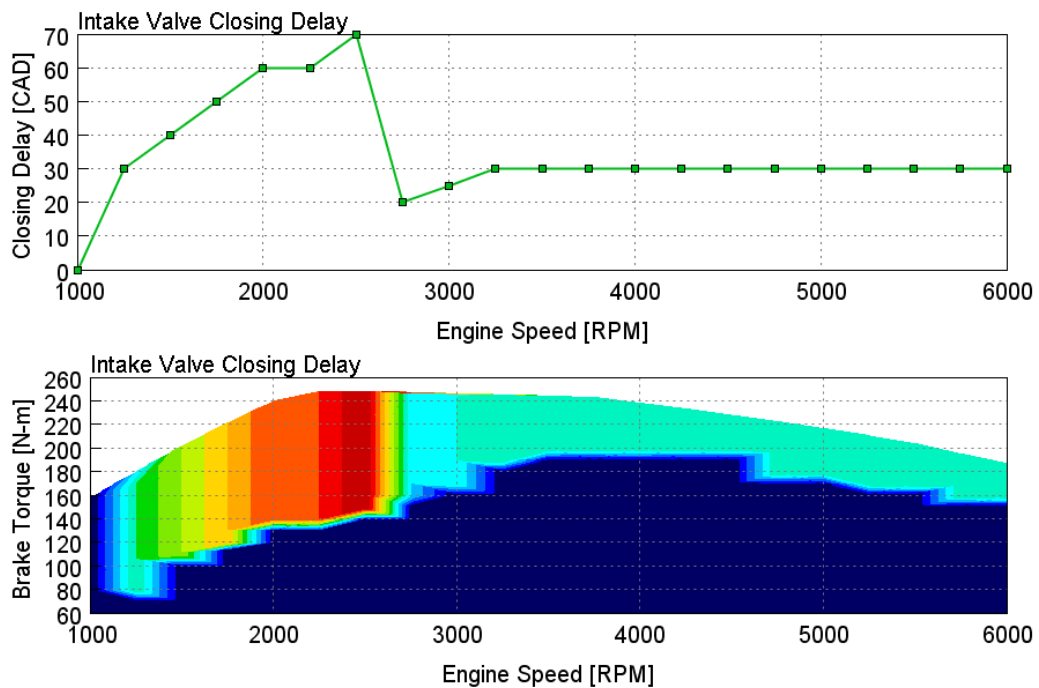


Figure 4.15 - LICV Strategy

4.3 Results

In this section, a detailed comparison between the proposed engine concepts will be presented, both at full load and at part load.

4.3.1 Full Load

| Legend | Lambda Min | T3 Max [°C] | Knock Limit | CR | eSupercharger | Valve Strategy |
|------------------|------------|-------------|-------------|-----|---------------|-------------------|
| Reference Engine | 0,7 | 940 | Base | 9,8 | ✗ | MultiAir |
| Stoic. Engine B | 1 | 980 | Base | 9,8 | ✗ | MultiAir |
| Stoic. Engine C | 1 | 980 | Updated | 9,8 | ✗ | MultiAir |
| Stoic. Engine D | 1 | 980 | Updated | 12 | ✓ | MultiAir & Miller |

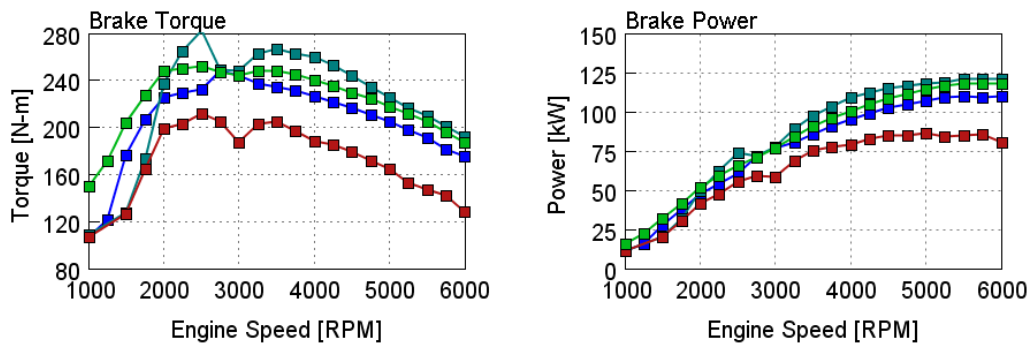


Figure 4.16 - Full Load Engine Concepts Results - 1

As far as performance concerns, the recalibration of the combustion timing at knock limited operation is able to increase brake torque curve, up to 240 Nm at 3000 RPM and to reach a peak power of 110 kW at 5000 RPM. The high efficiency engine concept increases to 250 Nm the maximum brake torque and it is capable, taking advantage of the Miller cycle, of recovering almost completely the engine peak power (117 kW).

| Engine Concept | Ref. Engine | Stoic. Engine B | Stoic. Engine C | Stoic. Engine D |
|-------------------|---------------------------|------------------|-------------------|-------------------|
| Brake Torque [Nm] | 280 @ 2500 RPM (exp. 250) | 210 @ 2500 RPM | 243 @ 2750 RPM | 255 @ 2250 RPM |
| Brake Power [kW] | 123 kW @ 5500 RPM | 86 kW @ 5000 RPM | 110 kW @ 5500 RPM | 117 kW @ 5500 RPM |

Table 4.6 - Performance comparison for different engine concepts

| Legend | Lambda Min | T3 Max [°C] | Knock Limit | CR | eSupercharger | Valve Strategy |
|------------------|------------|-------------|-------------|-----|---------------|-------------------|
| Reference Engine | 0,7 | 940 | Base | 9,8 | ✗ | MultiAir |
| Stoic. Engine B | 1 | 980 | Base | 9,8 | ✗ | MultiAir |
| Stoic. Engine C | 1 | 980 | Updated | 9,8 | ✗ | MultiAir |
| Stoic. Engine D | 1 | 980 | Updated | 12 | ✓ | MultiAir & Miller |

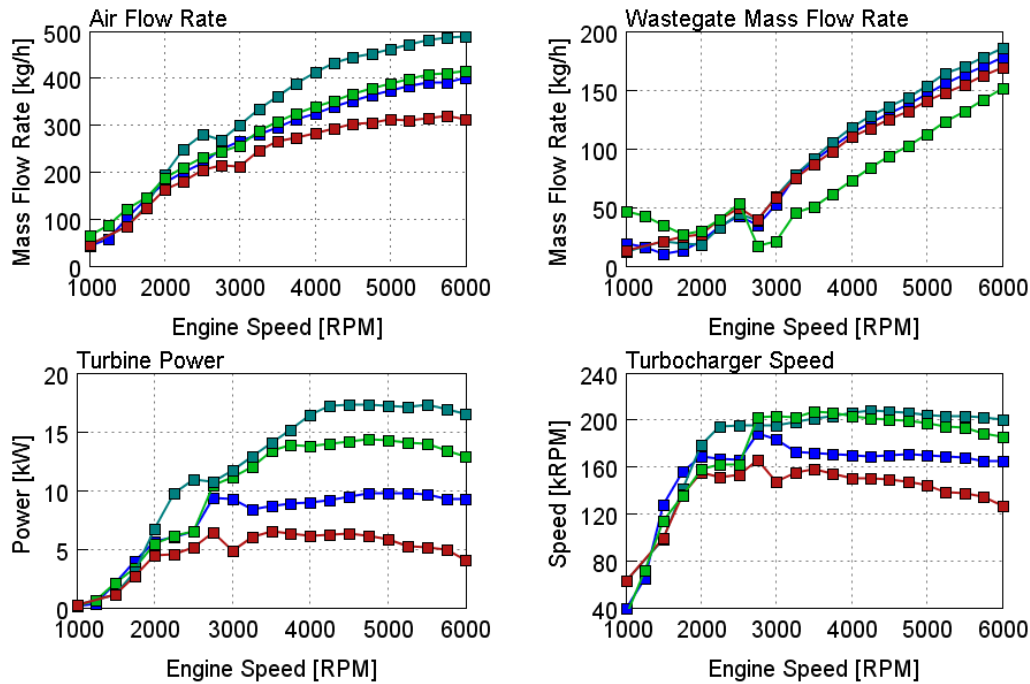


Figure 4.17 - Full Load Engine Concepts Results - 2

It is worth to be pointed out that even if the peak power is almost recovered with the electrified and millerized engine concept, the air mass flow rate is reduced, and consequently also the fuel flow rate. In the low engine speed region, the wastegate valve is maintained opened in the electrified engine, because eSC operation is preferred.

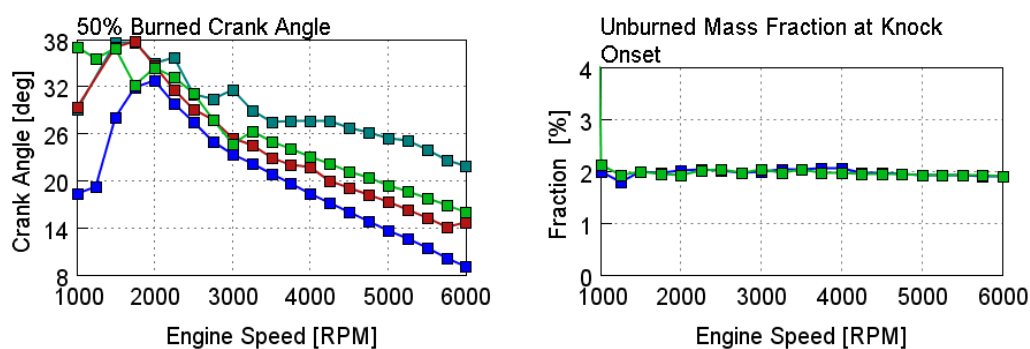


Figure 4.18 - Full Load Engine Concepts Results - 3

The update of the knock model leads to a reduction of the MFB-50 combustion angle. With the Miller cycle, because of the increased boost pressure, the combustion must be delayed in order to fill the limit of unburned mass fraction at knock onset equal to 2%. Further results concerning performance, pressure and temperature will be provided.

4 Steady-State Analysis

| Legend | Lambda Min | T3 Max [°C] | Knock Limit | CR | eSupercharger | Valve Strategy |
|------------------|------------|-------------|-------------|-----|---------------|-------------------|
| Reference Engine | 0,7 | 940 | Base | 9,8 | ✗ | MultiAir |
| Stoic. Engine B | 1 | 980 | Base | 9,8 | ✗ | MultiAir |
| Stoic. Engine C | 1 | 980 | Updated | 9,8 | ✗ | MultiAir |
| Stoic. Engine D | 1 | 980 | Updated | 12 | ✓ | MultiAir & Miller |

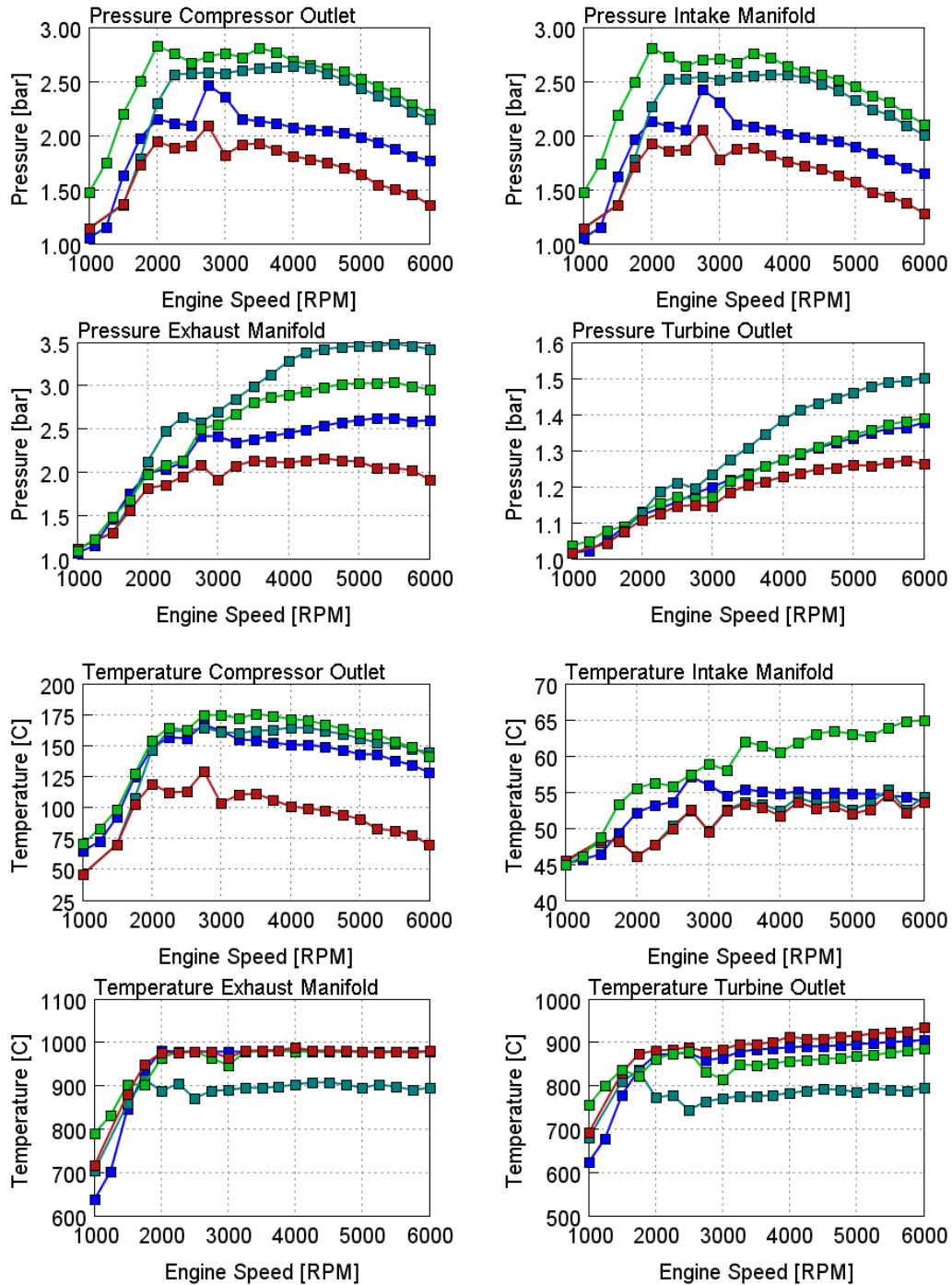


Figure 4.19 - Full Load Engine Concepts Results - 4

4.3.2 Part Load

For what concerns part load comparison, the discussion will be focused on the engine stoichiometric C and D. This choice is mainly due to the unacceptable full load performance of the other engine concept. It is worth to be pointed out that fuel consumption of the electrified engine concept is affected by the electric power required from the eSupercharger.

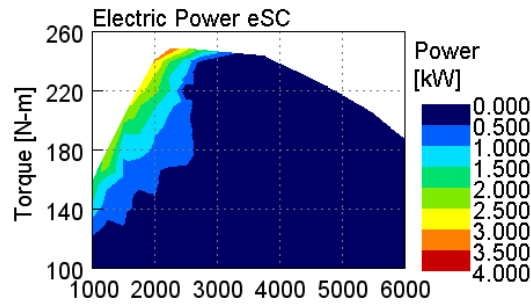


Figure 4.20 - eSC requested electric power

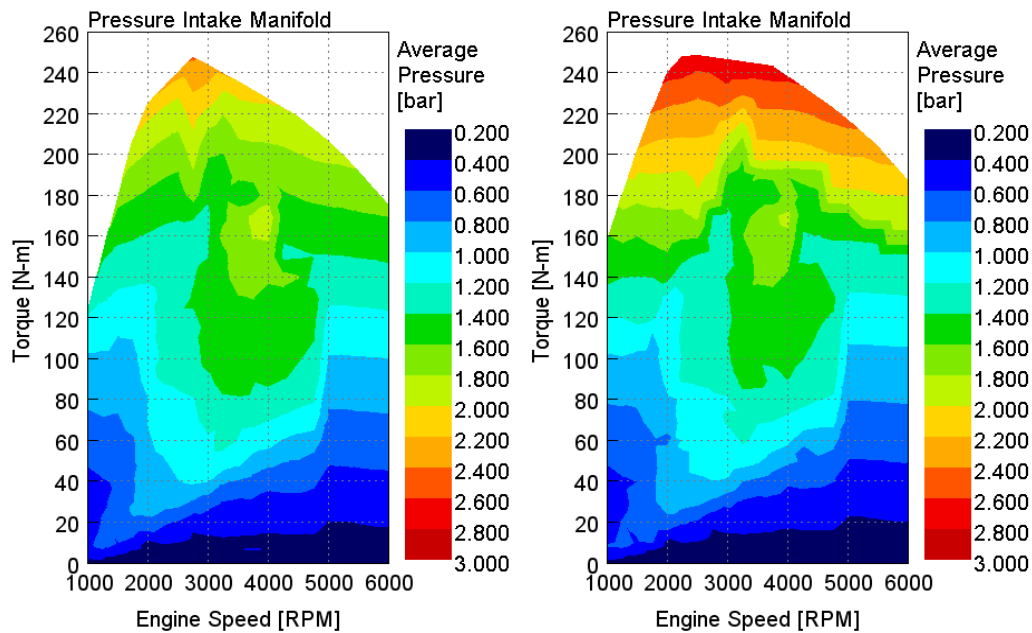
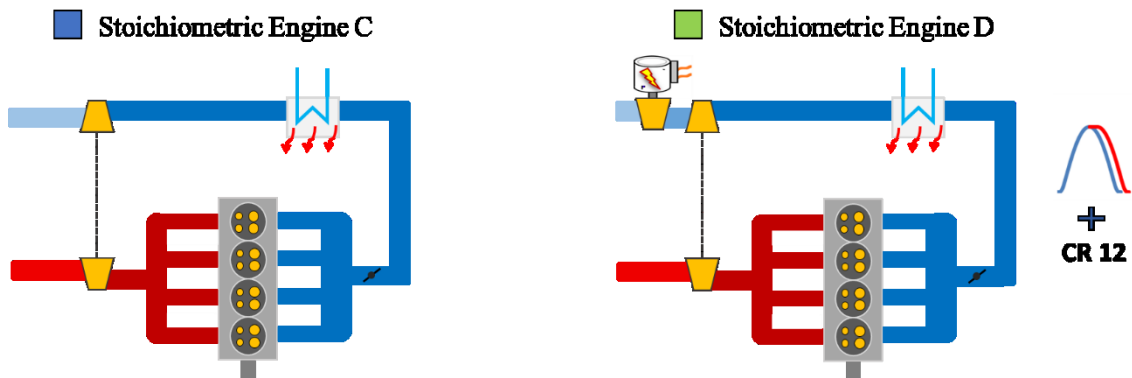


Figure 4.21 - Part Load Engine Concepts Comparison - 1

4 Steady-State Analysis

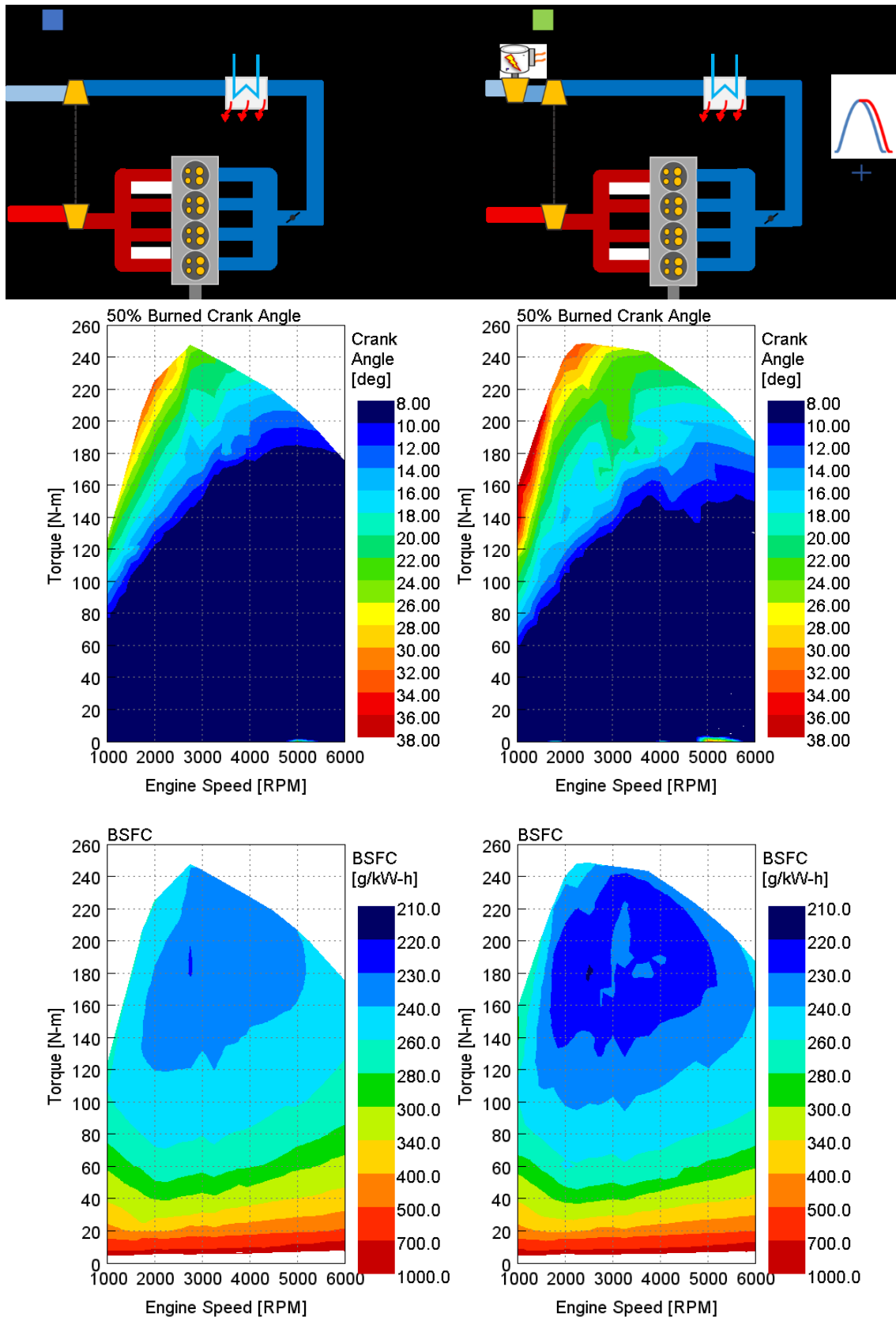


Figure 4.22 - Part Load Engine Concepts Comparison - 2

The stoichiometric engine D is characterized by a globally higher efficiency with respect to the C configuration. The minimum BSFC is 220 g/kWh (229.5 g/kWh for the C

concept). However, the increment of efficiency with the adoption of a CR12 is partially jeopardize from the knock mitigation need at high load: the MFB-50 is delayed thus deteriorating the efficiency of the combustion. In addition, an increase of boost pressure is required in order to balance the combustion delay and the result is an increase of backpressure. At low load and in particular in the low speed region the improvement of brake efficiency is quite reduced. In Figure 4.23 a detailed analysis is presented for six operating points. The fuel energy split is proposed, both for stoichiometric engine C and D. In the low load region, the difference of the two engine concepts is the CR only, so the difference of the results is attributable to that feature. With the higher CR the exhaust gasses enthalpy percentage decreases but an increase of the friction aliquot and the heat transfer in cylinder can be appreciated. The result is an increase of the brake efficiency adopting the CR 12 depending on the engine speed and the load, as reported in Table 4.23. The assumption was that combustion parameters(timing and duration) do not depend on the value of CR, and it could jeopardize the increase of brake efficiency of the engine.

| BSFC Comparison | | | |
|-----------------|----------|----------|----------|
| | 1000 RPM | 2000 RPM | 3000 RPM |
| 20 Nm | - 0,1 % | - 1,77 % | - 2,05 % |
| 50 Nm | - 0,6 % | - 2,22 % | - 2,73 % |

Figure 4.23 - BSFC comparison for six operating points at part load

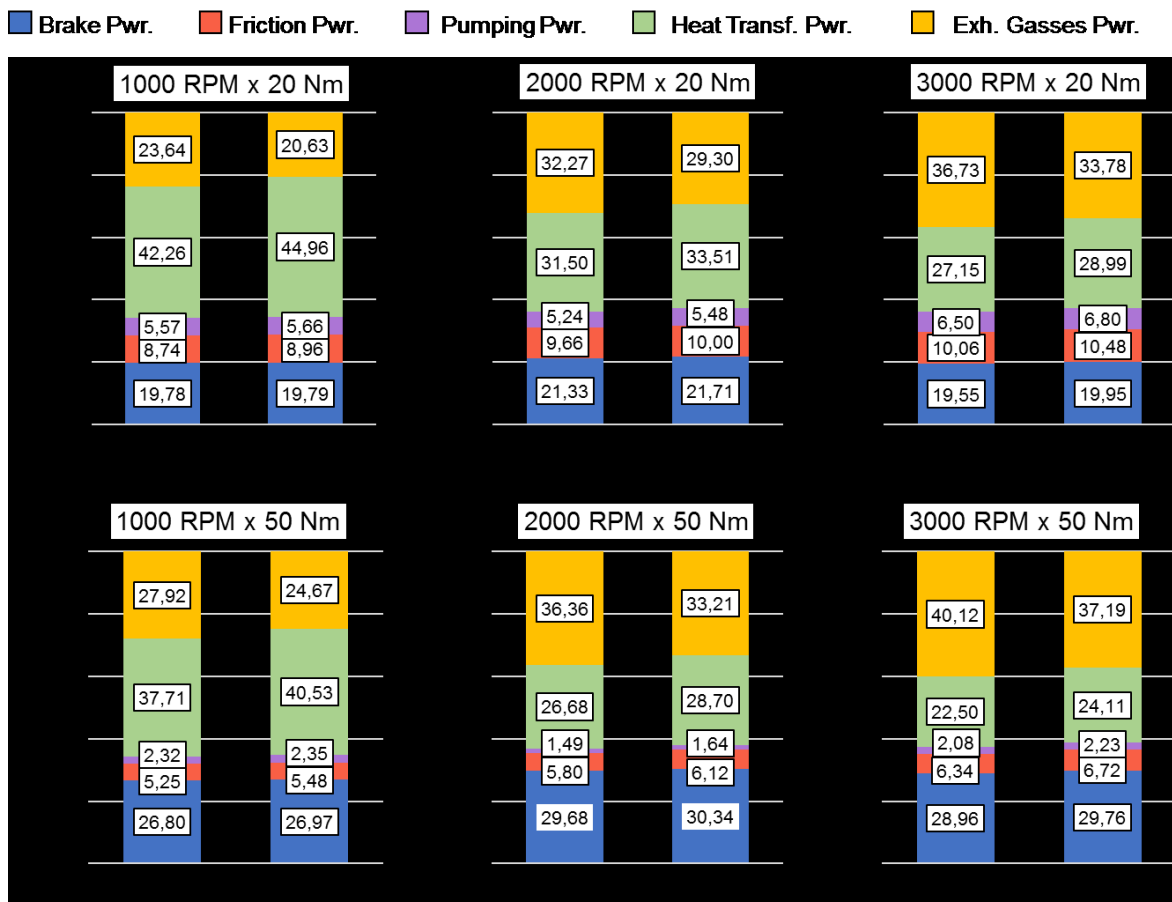


Figure 4.24 - Energy balance for six operating points at part load

5 Vehicle Transient Analysis

In this chapter the energy management strategy investigation will be investigated by means of vehicle transient simulation. The engine concepts developed and commented in the previous chapter are the ones used for the vehicle analysis. Different powertrain concepts will be presented and investigated.

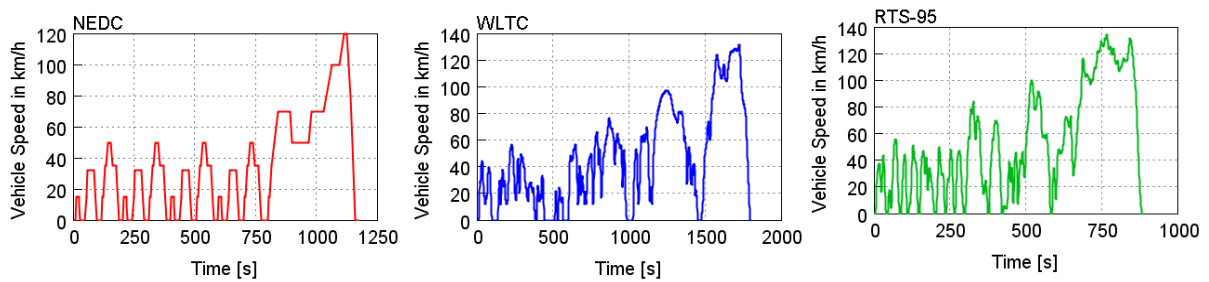


Figure 5.1 - Driving cycles used for fuel consumption evaluation

| | NEDC | WLTC | RTS-95 |
|---|-------|-------|--------|
| Total time [s] | 1180 | 1800 | 886 |
| Distance [km] | 10.93 | 23.27 | 12.93 |
| Maximum speed [km/h] | 120 | 131.3 | 134.45 |
| Average speed [km/h] | 33.35 | 46.5 | 52.52 |
| Average speed excluding stops [km/h] | 43.10 | 53.5 | 56.68 |
| Maximum acceleration [m/s²] | 1.04 | 1.67 | 2.62 |

Table 5.1 - Driving cycle statistics

In addition to fuel consumption evaluation on driving cycles the attention will be focused also on transient performance evaluation on several commonly used maneuvers:

- 0-100 km/h
- 60 → 100 km/h in V gear
- 80 → 120 km/h in VI gear
- 40 → 80 km/h in IV gear
- 60 → 80 km/h in VI gear

5 Vehicle Transient Analysis

The vehicle chosen as test case is a B-SUV Segment vehicle. On the Figure 5.2 a scheme of the powertrain configurations is reported:

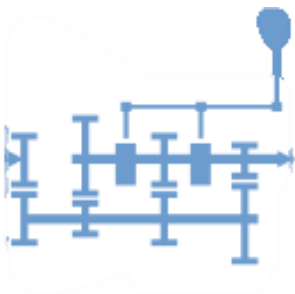
Segment B-SUV



| B-SUV | NEDC | WLTP | RTS-95 |
|----------------------------|--------|--------|--------|
| Mass [kg] | 1470 | 1630 | 1630 |
| Length [m] | 4.250 | 4.250 | 4.250 |
| Rolling Radius [m] | 0.333 | 0.333 | 0.333 |
| F0 [N] | 143 | 170 | 170 |
| F1 [N/kph] | 0.2 | 0.2 | 0.2 |
| F2 [N/(kph ²)] | 0.0424 | 0.0443 | 0.0443 |
| El. Load [W] | 220 | 400 | 220 |

Table 5.2 - B-SUV Technical Data

Manual Transmission



| Gear | Transmission Ratio |
|-------------|--------------------|
| I | 4.154 |
| II | 2.118 |
| III | 1.486 |
| IV | 1.116 |
| V | 0.897 |
| VI | 0.767 |
| Final Drive | 4.118 |

Table 5.3 - Manual Transmission Data

Gasoline Engine

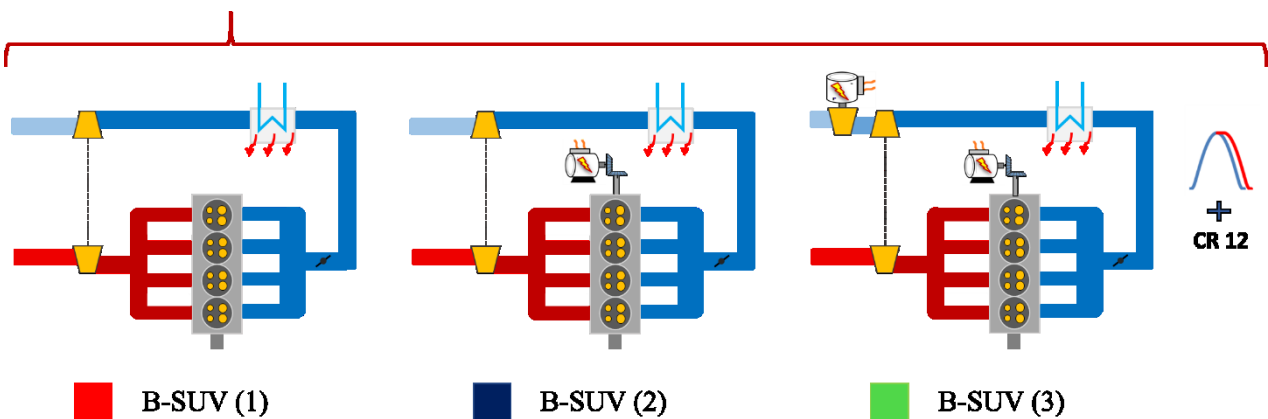


Figure 5.2 - Vehicle Configurations Set

In the Table 5.4 the main characteristics of the powertrains chosen for the vehicle analysis are reported.

| Legend | Engine | Hybrid Architecture | Electric Network | eSupercharger | EMS |
|-----------|-----------------|---------------------|------------------|---------------|------|
| B-SUV (1) | Stoic. Engine C | ✗ | 12 V | ✗ | ✗ |
| B-SUV (2) | Stoic. Engine C | P0 48 V | 12+48 V | ✗ | ECMS |
| B-SUV (3) | Stoic. Engine D | P0 48 V | 12+48 V | ✓ | ECMS |

Table 5.4 - Vehicle Configurations Features

5.1 P0 48V Architecture

The P0 layout has been chosen as hybrid architecture for the study. The reason of this choice is that it represents the optimum compromise between cost and benefits for a small-medium vehicle, and in addition it does not require further analysis on the energy management control strategy that are out of the scope of this project. In Figure 5.3 a schematic representation of a P0 48 V Hybrid Architecture is reported.

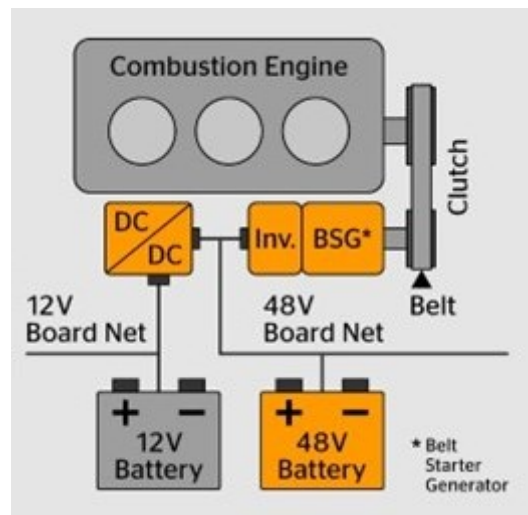


Figure 5.3 - Electric Network P0 48V system [32]

In a P0 architecture the typical mechanical coupling of the Electric Motor and the ICE is a belt system: the conventional belt system, used for mechanical ancillaries as oil pump and A/C compressor, is substituted with an innovative system, whose advantage is the capability to transmit the torque in both directions:

1. Acts as generator converting the brake torque into electrical power during braking phase;
2. Acts as motor to increase the maximum power of the powertrain or to decrease the load of the ICE operating point as result of the EMS optimization.

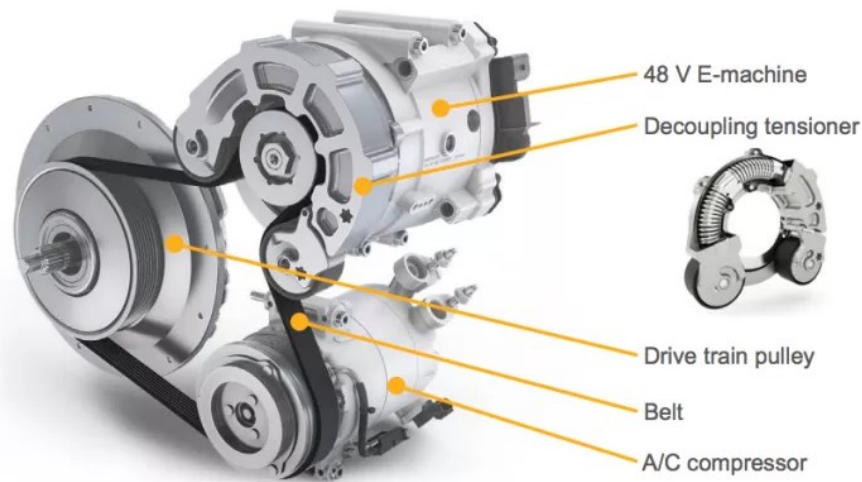


Figure 5.4 - 48 V Belt Starter Generator [33]

5.2 Electrified Vehicle Model Assessment

The vehicle has been modeled with GT-SUITE software, that is able to couple the 1-D CFD analysis of the engine and the longitudinal dynamics analysis of the vehicle. The vehicle model can be divided into four main parts: *Driveline, engine, electric network and controllers*.

Regarding the driveline, several 1-D inertia components (shaft, axles, brakes, tires, vehicle body) are present in the model connected with either rigid/kinematic connections (single degree of freedom) or slipping/compliant connections (two degrees of freedom).

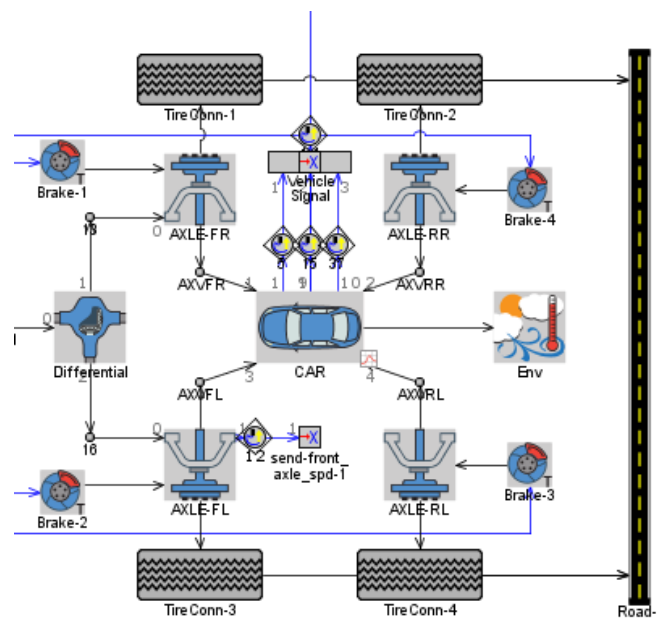


Figure 5.5 - GT-SUITE Vehicle Modelling

As far as engine model concerns, the above-mentioned description of GT-SUITE engine modelling for the steady-state analysis is valid also for the transient simulations. A FRM model was used also for driving cycles and transient maneuvers evaluation.

The controllers used in the engine model translate an input of engine power demand into a boost pressure target, an intake manifold pressure target and a combustion phasing (MFB50 and MFB10-90). Those values of pressures and combustion timing are obtained from the part load steady-state simulation complying with all the engine limitations (compressor surge, turbocharger speed, knock, T3).

The electric network was modeled in an adaptable way with a switchable sub-assembly, reproducing a conventional 12V electric network and a dual voltage 12 + 48V electric network.

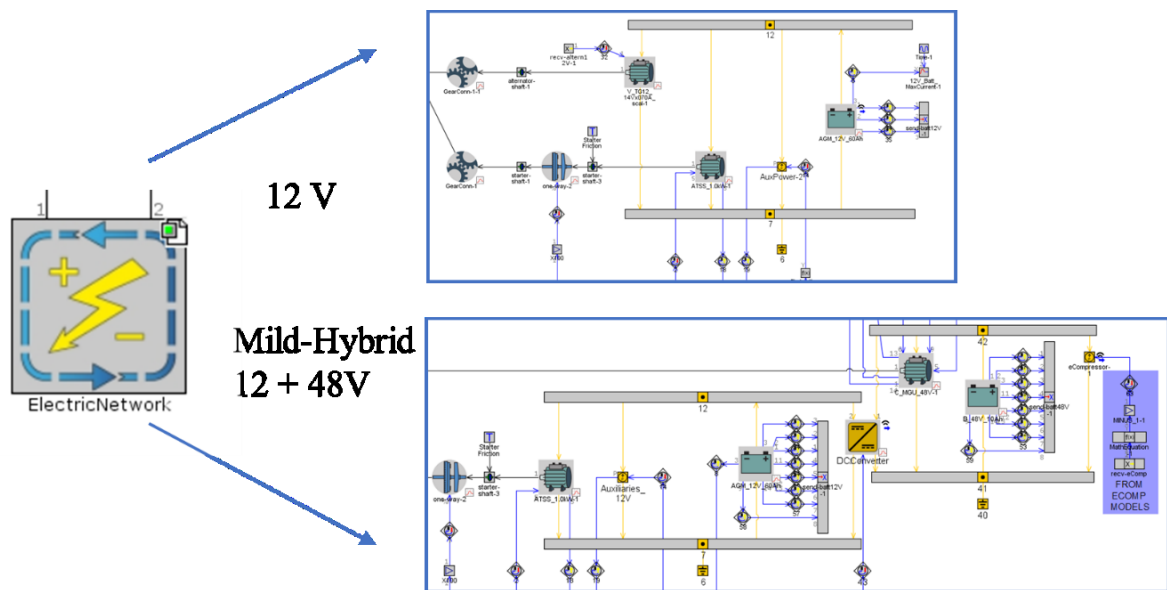


Figure 5.6 - GT-SUITE Electric Network modelling: 12 V and 12+48V systems

The main technical data of the electric devices (Electric Machine and Batteries) are reported in the Table 5.5.

| | | 12 V | 12+48V |
|-------------------|-----------------------|-------------|------------|
| Alternator | Mech. Power Motor | 0 kW | 5.5 kW |
| | Mech. Power Generator | 3.4 kW | 7.5 kW |
| | Elec. Power Generator | 14V x 140 A | 48V x 250A |
| Starter | Mech. Power | 1 kW | 1 kW |
| Battery | Capacity (12V) | 60 Ah | 60 Ah |
| | Capacity (48V) | NA | 10 Ah |

Table 5.5 - Electric Network Technical Data

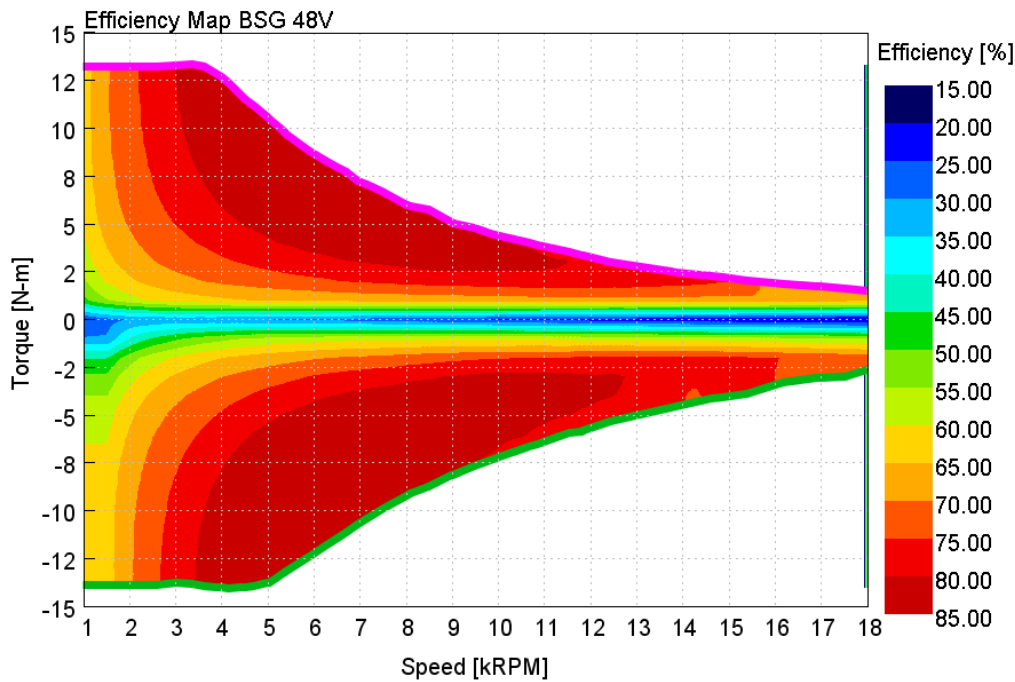
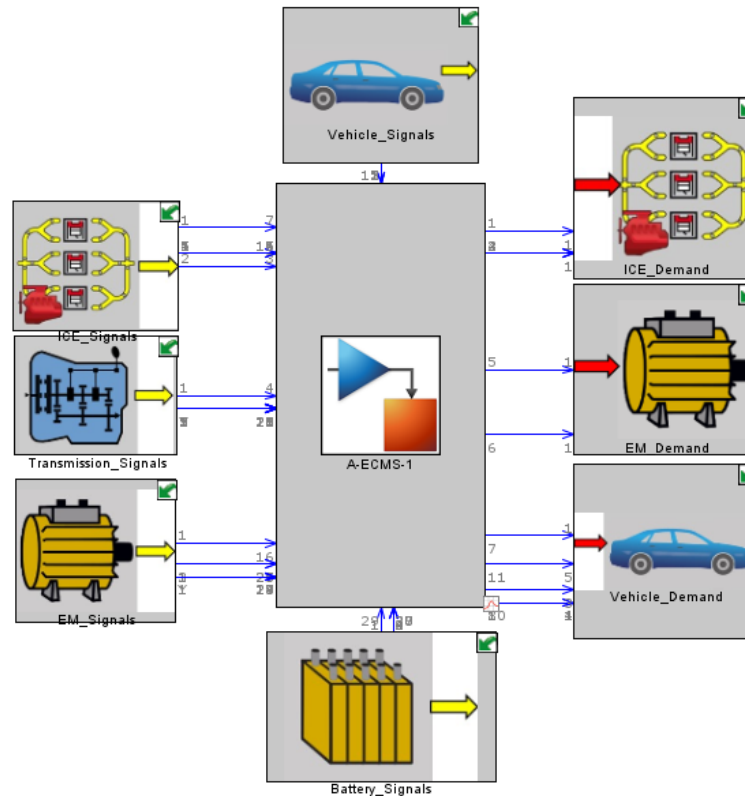


Figure 5.7 - Electric Machine efficiency map and maximum (pink) and minimum (green) torque curves

The driving operation is simulated in the model by means of a Driver Controller: the need to reproduce a specified target speed in case of driving cycles' simulation or to reproduce a tip-in maneuvers define a *driver power demand*. It is automatically converted into brake actuation and accelerator actuation. The requirement of using a fixed gear strategy corresponds to a gear and a clutch position during the shifting phase. In case of the conventional powertrain simulation – B-SUV (1) – these signals are used directly in the engine, transmission and clutch objects of the model. For the electrified powertrain analysis, the load of the engine and the brake actuation are input for the energy management strategy. Signals as engine and electric motor speeds, State of Charge (SoC) of the battery, driver power demand and engine and transmission status are required to the energy management controller in order to optimize the power split between ICE and EM. In the Figure 5.8 a GT user interface is reported for clarifying the idea of the EMS.



energy management strategy optimization. Actually, load point moving is actuated, and defined through the ECMS, when the driver power demand is positive; when it is negative (deceleration phase) the EM is actuated in order to recover a certain percentage of the requested braking power.

There are different regenerative braking strategies adopted in MHEV applications: recover a fixed percentage of the braking power demand or a certain percentage function for example of the brake pedal or the deceleration value. The adopted solution in the work was to recover a percentage of the maximum BSG mechanical power, always considering the mechanical limitation of the BSG and the electric limitations of the electric network.

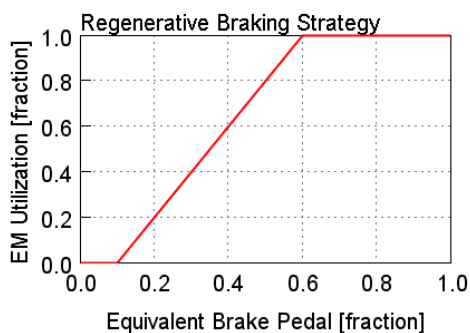


Figure 5.9 - Regenerative Braking Strategy defined through an equivalent brake pedal function

With a P0 hybrid architecture the engine braking effect (due to pumping power and friction power) limits the maximum recoverable energy during braking phase. A P2 architecture is more efficient because during regenerative braking phase an additional clutch is capable to uncouple the driveline to the engine thus leading to an increment of the recoverable energy.

The energy management strategy instead is the main core of the investigation and for this reason it will be explained in detail. The idea of the ECMS is to minimize a cost function; in this work the fuel consumption is the only variable of interest, but also pollutant formation (NO_x for diesel engine) or more than one cost function could be minimized [10],[12]. Different combinations of power split correspond to different equivalent fuel consumption, as defined in 2.1 equation. The idea is to find out the optimum power split, i.e. the one that minimize the equivalent fuel flow rate.

Based on this reasoning, a set of possible power split combination corresponds at each driving power demand value.

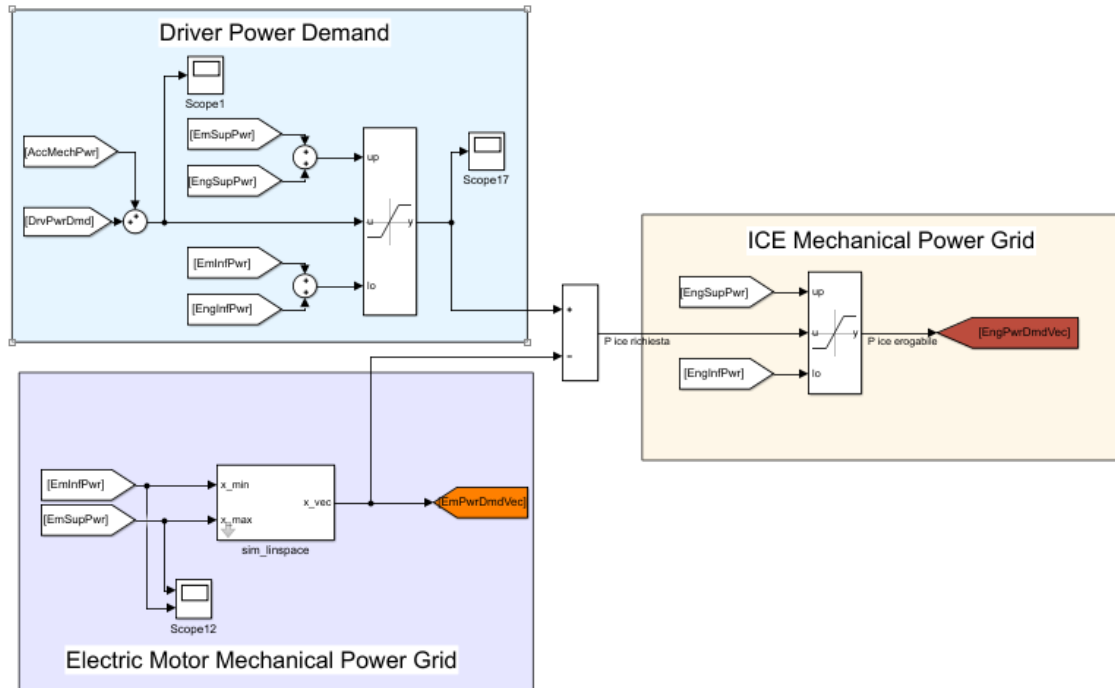


Figure 5.10 - Energy Management Strategy Modelling -1: set of power split combinations definition

Driver Power Demand is limited if necessary in order to comply with ICE and EM mechanical limit. In the model for this reason full load ICE curve, electric limit as voltage and current limitations are defined. For the evaluation of the fuel consumption a fuel map is used, defined through the steady-state simulations. Similarly, the Battery Power evaluation is performed with a static approach; it depends on the electric EM power demand and on the SoC of the battery. The equivalence factor has set constant and calibrated for each driving cycle in order to guarantee the charge sustaining condition.

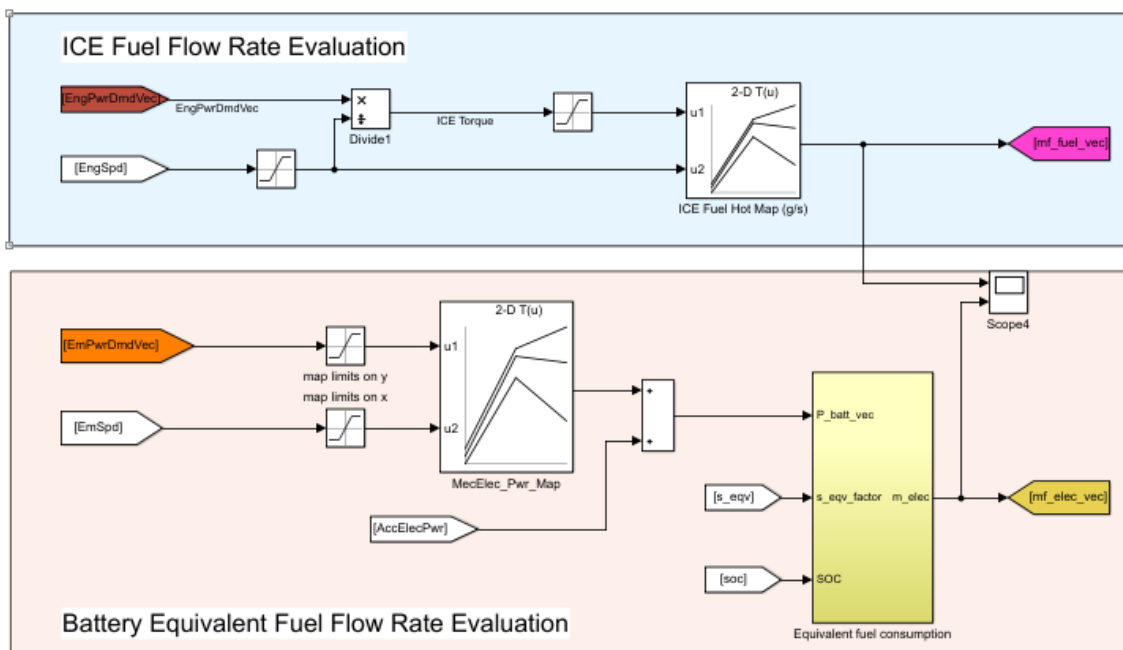


Figure 5.11 - Energy Management Strategy Modelling -2: ice fuel flow rate and battery equivalent fuel flow rate

Finally, the minimum value of the equivalent fuel flow rate will define the optimum power split. In the model there is already implemented, but not used, the possibility to consider also penalty factors for some combinations (for example for the cases in which the ICE power demand is very different with respect to the actual power of the engine and it could be not undesirable).

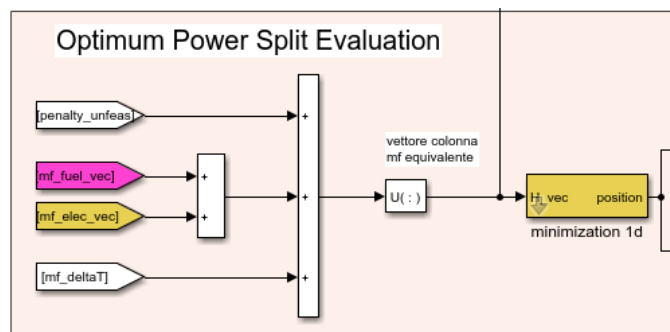


Figure 5.12 - Energy Management Strategy Modelling – 3: optimum power split definition

5.3 eSupercharger Control Strategy

The proposed energy management strategy handles the electric power of the ancillaries in a passive way, in the sense that it is not capable to provide actuation/deactivation of additional devices. The eSupercharger controlling is for sure a challenging application of an efficient management for electric auxiliaries. The eSupercharger controlling strategy adopted in the transient simulation is explained:

- A driver power demand (pedal accelerator) is converted through the engine controllers in a target boost pressure.

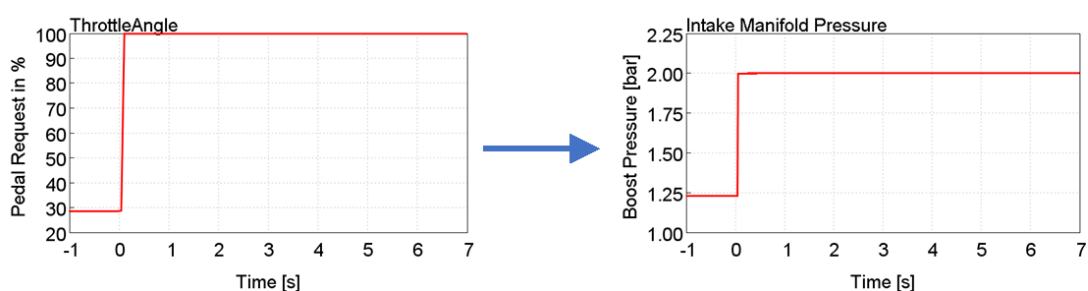


Figure 5.13 - eSC Activation Strategy - 1

- Because of mechanical and fluid-dynamical inertia of the system, a certain amount of time is required in a conventional engine (not supercharged electrically) before the actual pressure rises to the target one. A certain pressure ratio gap can be identified, and it will be the target pressure ratio for the eSupercharger.

5.3 eSupercharger Control Strategy

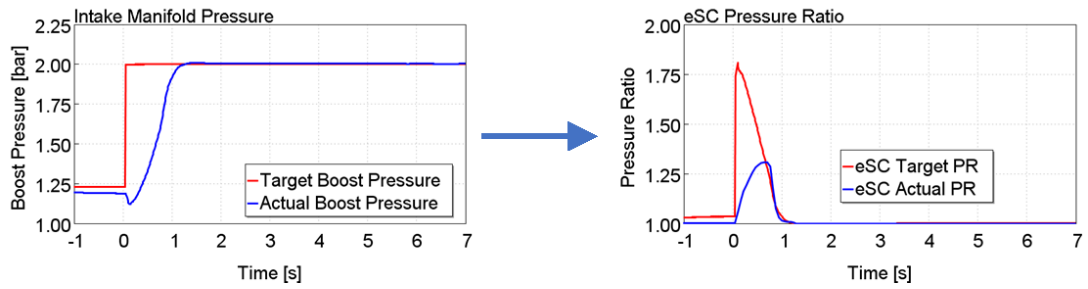


Figure 5.14 - eSC Activation Strategy - 2

- The eSC pressure ratio target together with the corrected mass flow rate through the compressor define an eSC speed target. A proportional integrative controller converts the error between the actual eSC speed and the target one into an electric power demand for the motor driving the eSC.

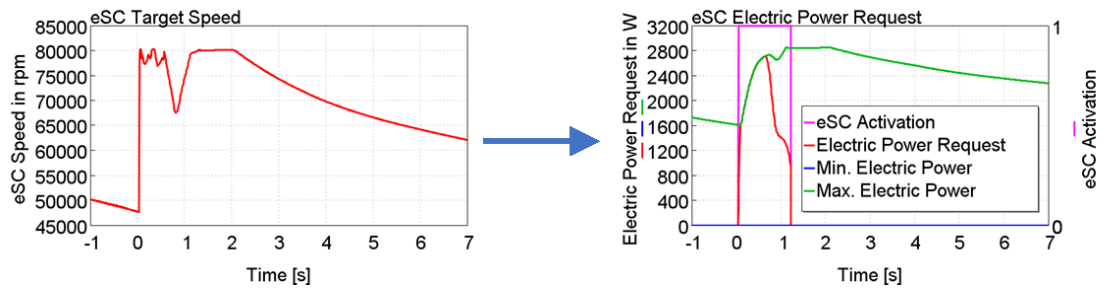


Figure 5.15 - eSC Activation Strategy - 3

Different aggressiveness of the PI controller has been adopted during the eSC operation. The aim is to speed up the eSC activation and then to regulate the compressor.

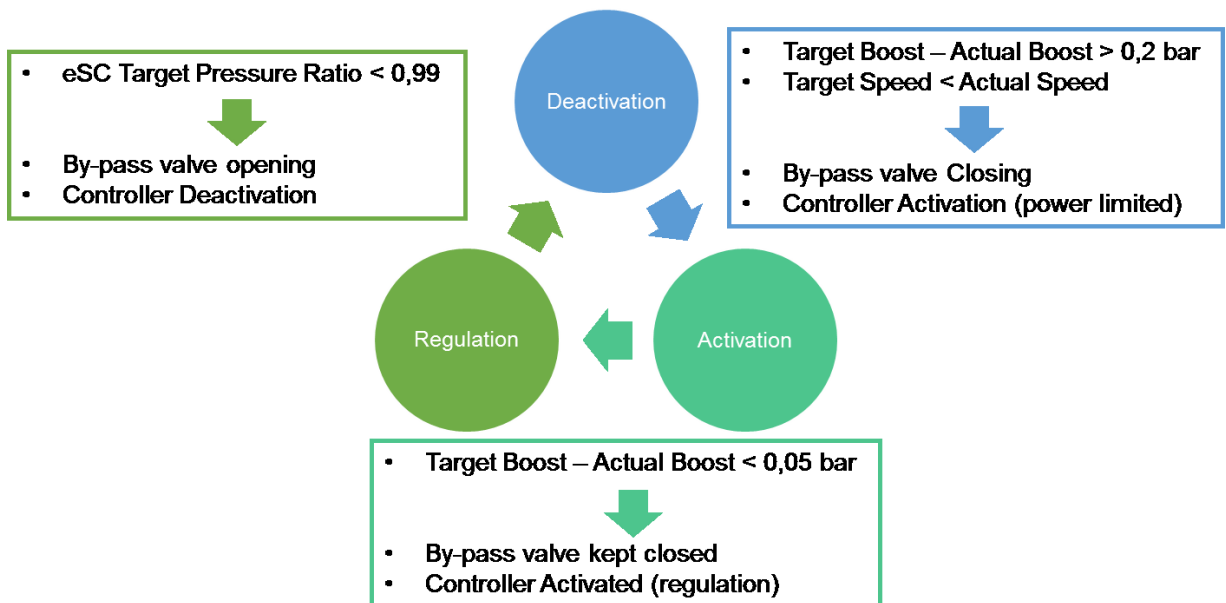


Figure 5.16 - Work Flow of eSC controlling

From an energetic view point, it is worth to highlight that the acceleration of the eSupercharger from the idle speed (5000 RPM) to the maximum speed (75000 RPM) in a time frame smaller than one second requires a not negligible amount of energy. It plays a key role, as it will be explained, in the management of the eSC operation with the ECMS. More in detail, during the eSC activation many power terms are present:

- Power transferred to fluid, so used for compressing it;
- Friction Power lost in the mechanical system;
- Inertia Power for eSupercharger acceleration;

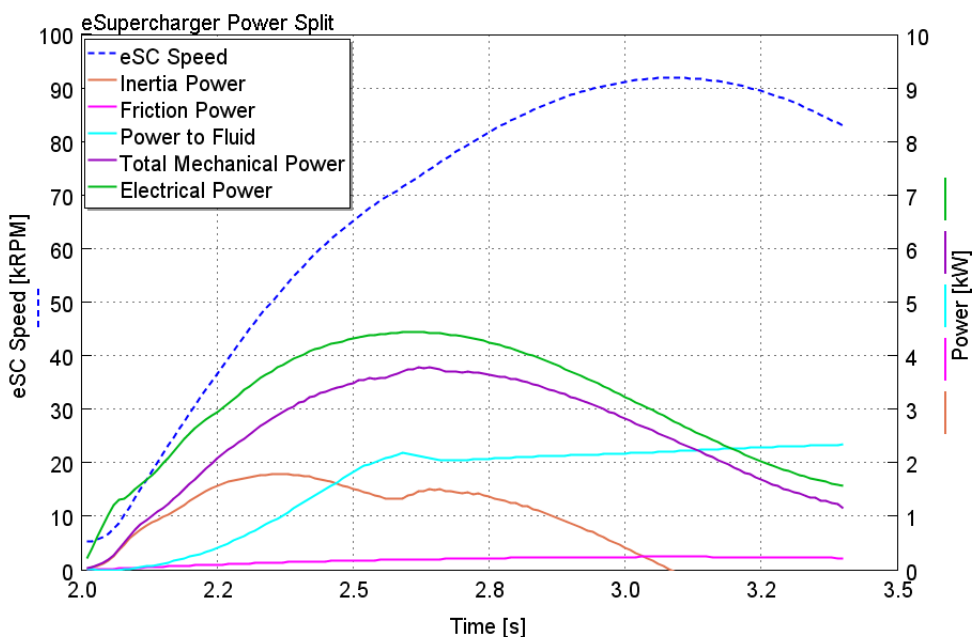


Figure 5.17 - eSC Power Split

From the Figure 5.17 it is possible to understand that the inertia power represents a relevant contribution in the first part of the eSC operation.

Two different eSC control techniques were implemented and investigated. They are based on the above-explained activation strategy.

5.3.1 GT-SUITE Integrated eSC Control

The control of the eSupercharger during transient maneuvers and driving cycles has been implemented in GT-SUITE. The model implements exactly the four steps described in 5.3. The actual ECMS is not able to evaluate the electric power consumption during the eSC operation; it should be considered during power split optimization through the

equivalent fuel minimization. However, this solution is easier to be implemented and monitored with respect to the ECMS integrated solution.

5.3.2 ECMS Integrated eSC Control

The integration of the eSupercharger controller in the ECMS aims to take into account all the energetic terms during the activation and to have a better match between what ECMS is predicting in terms of fuel consumption during the exploitation of one ICE operating point and what really happens in the model. The integration process was performed gradually, following the path reported in the scheme in Figure 5.18.

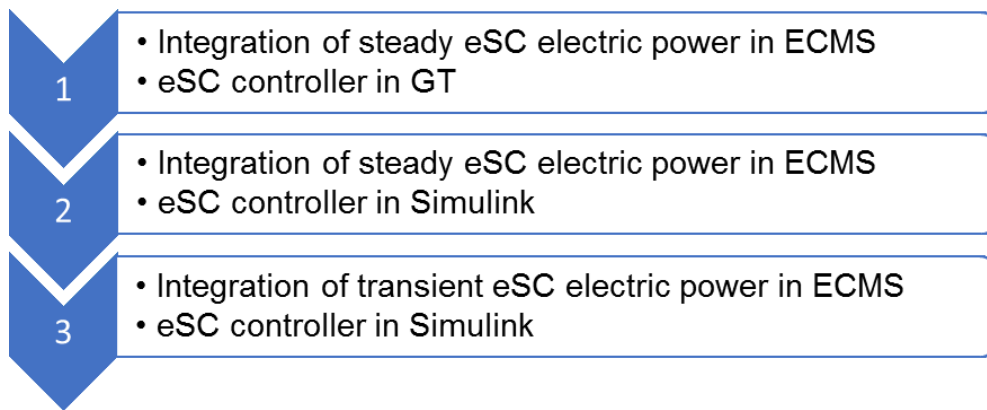


Figure 5.18 - Simulink integrated eSC Cotrolling Development

1. As first step, the eSC electric power consumption evaluated through the steady-state analysis was introduced in the ECMS model. In this way a steady-state electric power is considered during the power split optimization; the eSC controller however is GT integrated and this not guarantee an accurate match between the real eSC operation and the predicted one in the ECMS.
2. The controller of the eSC was imported in the ECMS model. The eSC activation and regulation criteria are the same used in the previous chapter. The main difference is that the eSC activation is evaluated for each combination of power split.
3. An additional inertia power contribution was included in the requested power for the eSC. It was computed in a simplified way:

$$P_{in} = k (eSC_{TgtSpd} - eSC_{ActSpd}) \quad (5.1)$$

In detail, for each possible operating point of the ICE, the corresponding Boost Pressure, eSC Pressure Ratio and eSC Target Speed are evaluated.

5 Vehicle Transient Analysis

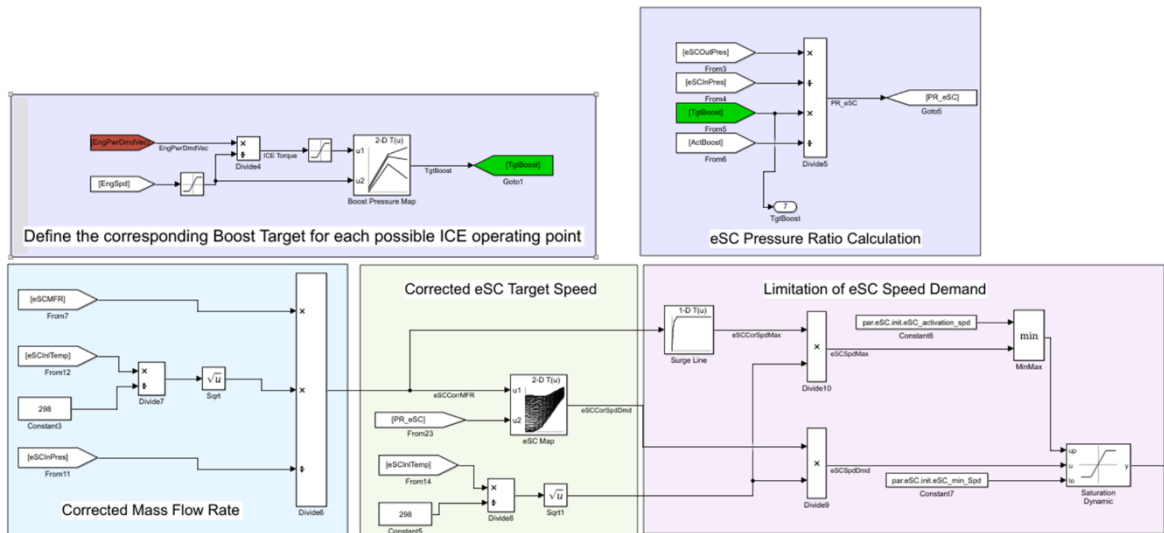


Figure 5.19 - Simulink integrated eSC controlling model – 1: eSC Speed demand and eSC target pressure ratio computation

A Matlab function determines, for each combination of inputs, the corresponding eSC Status (activation, controlling, deactivation) and the related input for the eSC actuation.

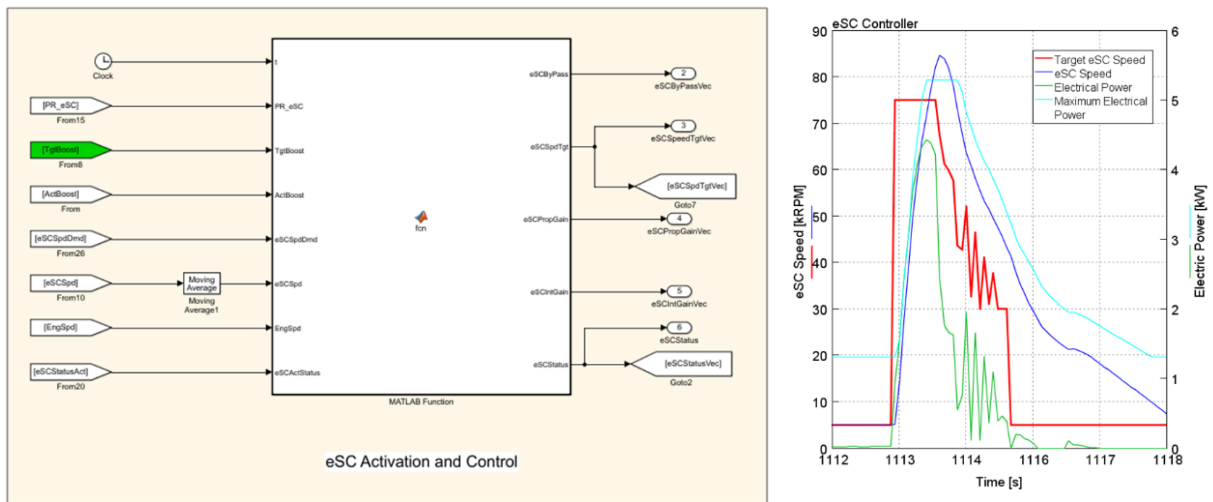


Figure 5.20 - Simulink integrated eSC controlling model – 2: eSC activation and controlling

The overall eSupercharger Electrical Power is evaluated for each power split combination, considering both a steady-state evaluated eSC electric power and a transient inertia power.

5.3 eSupercharger Control Strategy

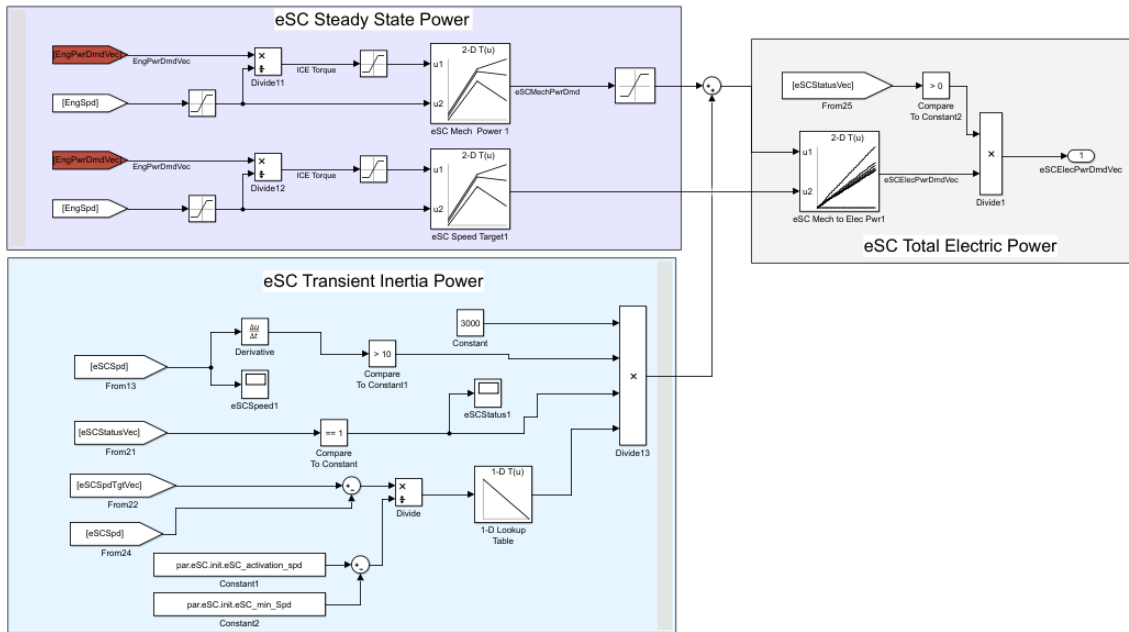


Figure 5.21 - Simulink integrated eSC controlling model - 3

6 Results

In this chapter, the results of the proposed electrified powertrains concept are presented, comparing them with the conventional vehicle. The attention is focused on the energy management strategy capabilities and its effectiveness both in terms of fuel consumption and performance.

Finally, two sensitivity analysis to the Electric Machine characteristics are reported, that aim to put in evidence the influence of the BSG on fuel consumption and also to fully prove the robustness of the EMS.

6.1 Hybrid Control Strategy Results

Firstly, the results of CO₂ emissions are reported for four different vehicle configurations:

| Legend | Engine | Hybrid Architecture | Electric Network | eSupercharger | EMS |
|---|-----------------|---|------------------|---|---|
| B-SUV (1)  | Stoic. Engine C |  | 12 V |  |  |
| B-SUV (2)  | Stoic. Engine C | P0 48 V | 12+48 V |  | ECMS |
| B-SUV (3)  | Stoic. Engine D | P0 48 V | 12+48 V |  | ECMS |
| B-SUV (3)  | Stoic. Engine D | P0 48 V | 12+48 V |  | ECMS - 3 |

Table 6.1 - Vehicle configurations analyzed

A comparison of B-SUV (1) and B-SUV (2) is presented, focusing on the power split operation effectiveness performed by means of the ECMS. Later, later, the focus is on the different control strategy provided by the ECMS and the ECMS-3, updated for eSC control and energy management improvement. For each value of CO₂ emission compute in a driving cycle simulation, the corresponding C-criterion value is reported, in order to ensure the charge sustained condition as explained in the chapter 1.1. Even the condition of charge sustaining is valid only for WLTC cycle; it has been adopted also for NEDC and RTS-95 in order to make a coherence comparison of the different results.

Regarding transient maneuvers results, also in this case the investigation is extended to the four vehicle configurations reported in Table 6.1. A Performance Index (PI) has been defined, in order to have a direct feedback of the improvement.

$$PI = \frac{3600}{v_{max}} + t_{0-100} + t_{60-100} + t_{80-120} \quad (6.1)$$

6 Results

- v_{max} = maximum vehicle speed [km/h];
- t_{0-100} = time for 0-100 km/h maneuver;
- t_{60-100} = time for 60-100 km/h in V gear maneuver;
- t_{80-120} = time for 0-100 km/h in VI gear maneuver;

6.1.1 CO₂ Emissions

The results of CO₂ emissions are reported in Figure 6.1. As it is possible to note from the bar plots on the left side of the Figure, all the values of emissions can be compared because the C-criterion factor is lower than the limit value of 0.5 %.

| Legend | Engine | Hybrid Architecture | Electric Network | eSupercharger | EMS |
|-----------|-----------------|---------------------|------------------|---------------|----------|
| B-SUV (1) | Stoic. Engine C | ✗ | 12 V | ✗ | ✗ |
| B-SUV (2) | Stoic. Engine C | PO 48 V | 12+48 V | ✗ | ECMS |
| B-SUV (3) | Stoic. Engine D | PO 48 V | 12+48 V | ✓ | ECMS |
| B-SUV (3) | Stoic. Engine D | PO 48 V | 12+48 V | ✓ | ECMS - 3 |

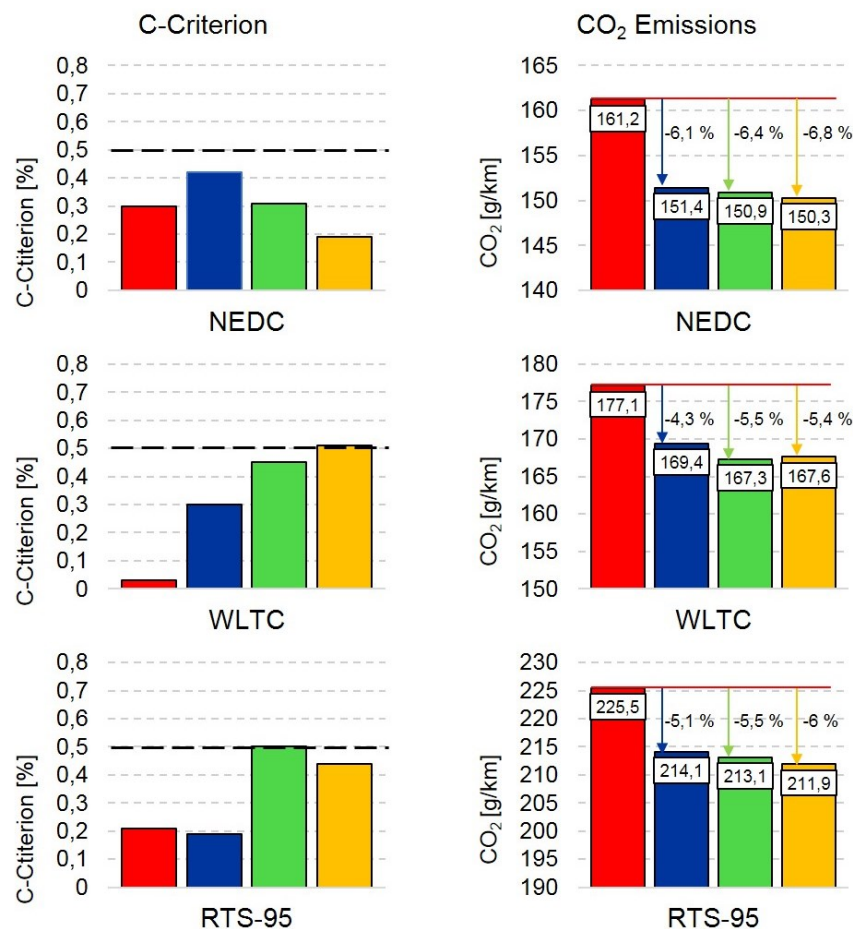


Figure 6.6.1 - CO₂ Emissions results for NEDC, WLTC and RTS-95 cycles

A reduction of about 5% in terms of CO₂ emissions is achieved for the electrified vehicle configuration (B-SUV (2)). An additional fuel consumption improvement of 0.4 % on the NEDC and RTS-95 and of 1.2% on WLTC can be noticed with the adoption of the Stoichiometric Engine D. As far as control strategy concerns, a further improvement of about 0.5 % is present on the NEDC and the RTS-95. On the WLTC the ECMS update does not lead to a significant benefit.

In Figures 6.2 and 6.3 a deeper investigation has been performed regarding the effectiveness of the power split operation on the NEDC cycle for the B-SUV (2) concept. In particular, in Figure 6.2 the optimum power split between ICE and EM defined by the ECMS is reported for the NEDC cycle.

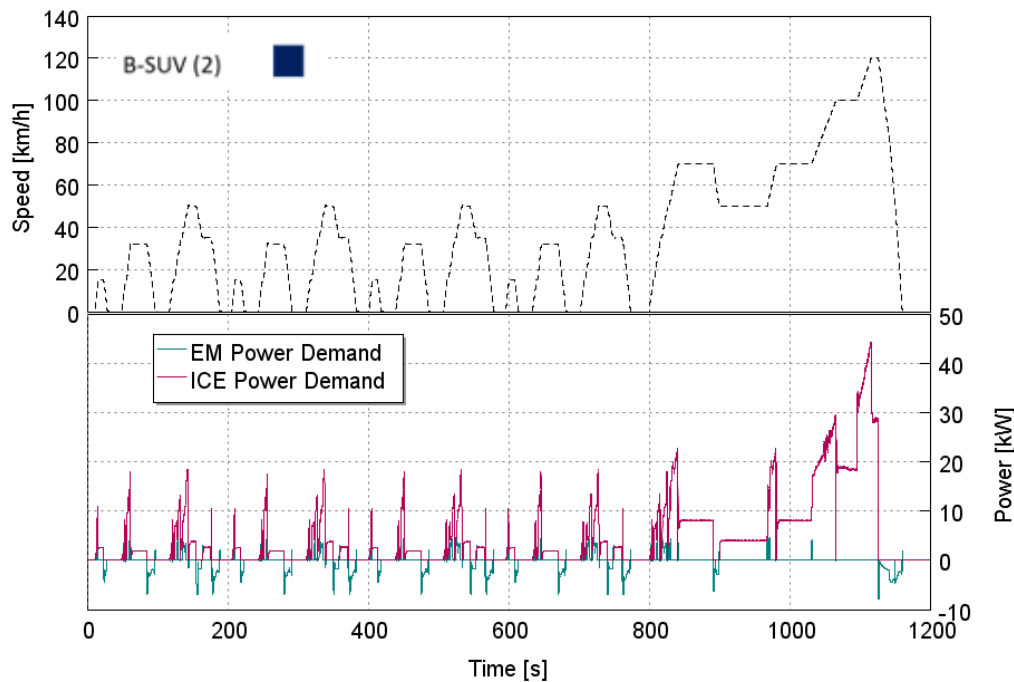


Figure 6.6.2 - ECMS Power Split for NEDC driving cycle for B-SUV (2) concept

The BSG power demand is negative in the deceleration phase of the driving cycle, thus storing energy from the braking phase. In the traction phase, the BSG power demand is positive mostly during the launch phases, in which, according to the ECMS, is convenient to decrease the ICE load and to take advantage of the e-boost functionality available with the BSG. Load Point Moving is never actuated in NEDC cycle, because the availability of electric power recovered with regenerative braking is sufficient for the traction phases ensuring the charge sustained conditions. In Figure 6.3 a deeper investigation of a reduced time frame of the NEDC is proposed; in the bottom part of the Figure the advantage of the power split is highlighted, comparing the instantaneous and the cumulated fuel consumption of the conventional and of the electrified vehicles (B-SUV(1) and B-SUV (2) respectively).

| Legend | Engine | Hybrid Architecture | Electric Network | eSupercharger | EMS |
|-----------|-----------------|---------------------|------------------|---------------|----------|
| B-SUV (1) | Stoic. Engine C | ✗ | 12 V | ✗ | ✗ |
| B-SUV (2) | Stoic. Engine C | P0 48 V | 12+48 V | ✗ | ECMS |
| B-SUV (3) | Stoic. Engine D | P0 48 V | 12+48 V | ✓ | ECMS |
| B-SUV (3) | Stoic. Engine D | P0 48 V | 12+48 V | ✓ | ECMS - 3 |

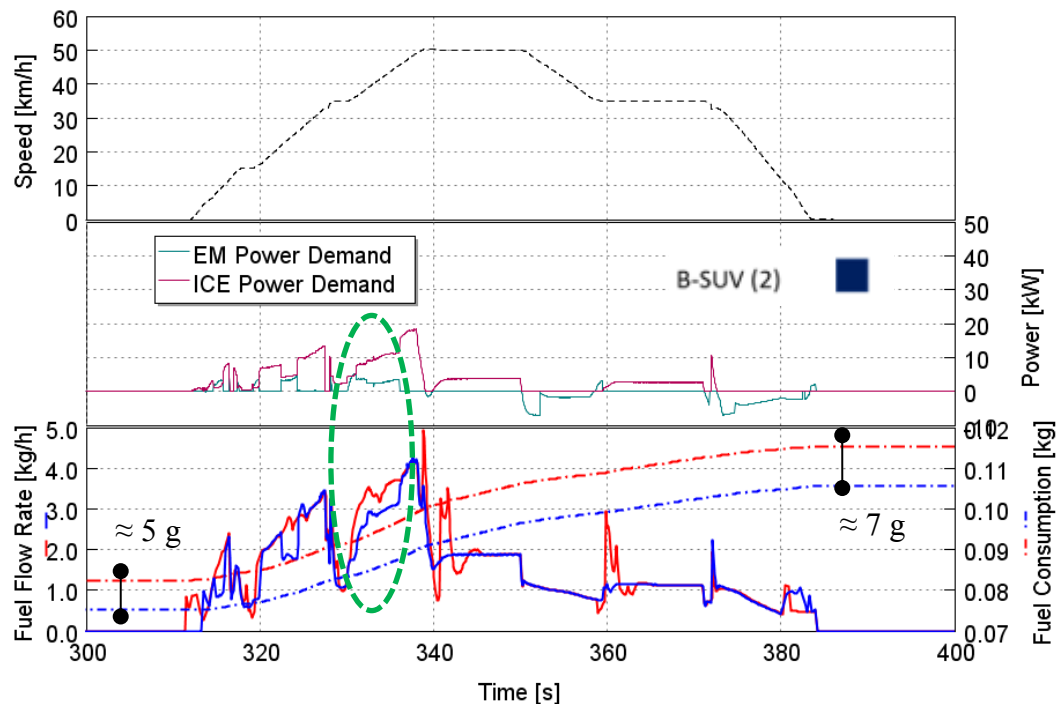


Figure 6.6.3 - B-SUV (1) and B-SUV (2) fuel consumption comparison: the optimum power split is reported for 300-400 s time frame

The eSupercharger adoption leads to a reduction of the BSG operation, as it can be noticed comparing the blue and green lines in the Figure 6.4, in which the energy used by the eSC and the BSG for propulsion is plotted. The reason is that the eSC operation cannot be controlled by the ECMS and it is a real electrical load. In order to respect the charge sustaining condition a reduction of BSG energy consumption must be obtained.

The updated ECMS (ECMS - 3) instead, considers the energy consumption resulting from an eSC operation, and it reduces the ICE load (reducing consequently the eSC power consumption) and increase the power demand to the BSG. This EMS is quite effective on the RTS-95 cycle (-1,2 g/km CO₂) and on the NEDC (-0,6 g/km CO₂). On the WLTC that strategy does not leads to appreciable results (+0,3 g/km CO₂). Further investigations are necessary in order to improve the eSC management strategy.

6.1 Hybrid Control Strategy Results

| Legend | Engine | Hybrid Architecture | Electric Network | eSupercharger | EMS |
|-----------|-----------------|---------------------|------------------|---------------|----------|
| B-SUV (1) | Stoic. Engine C | ✗ | 12 V | ✗ | ✗ |
| B-SUV (2) | Stoic. Engine C | P0 48 V | 12+48 V | ✗ | ECMS |
| B-SUV (3) | Stoic. Engine D | P0 48 V | 12+48 V | ✓ | ECMS |
| B-SUV (3) | Stoic. Engine D | P0 48 V | 12+48 V | ✓ | ECMS - 3 |

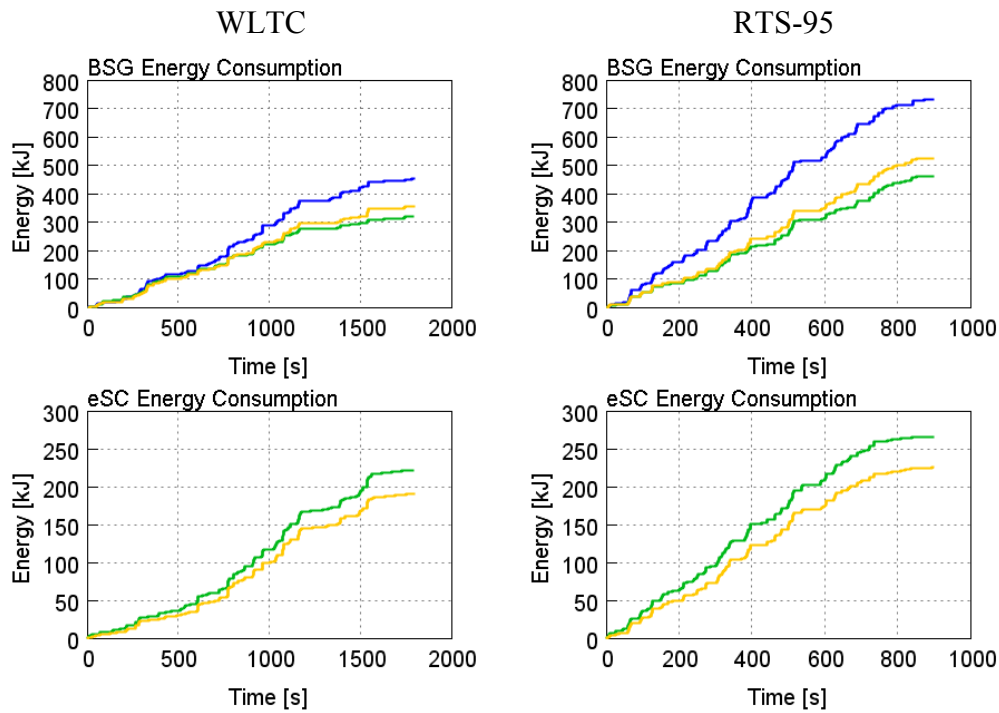


Figure 6.4 – Energy consumption comparison for eSC and BSG

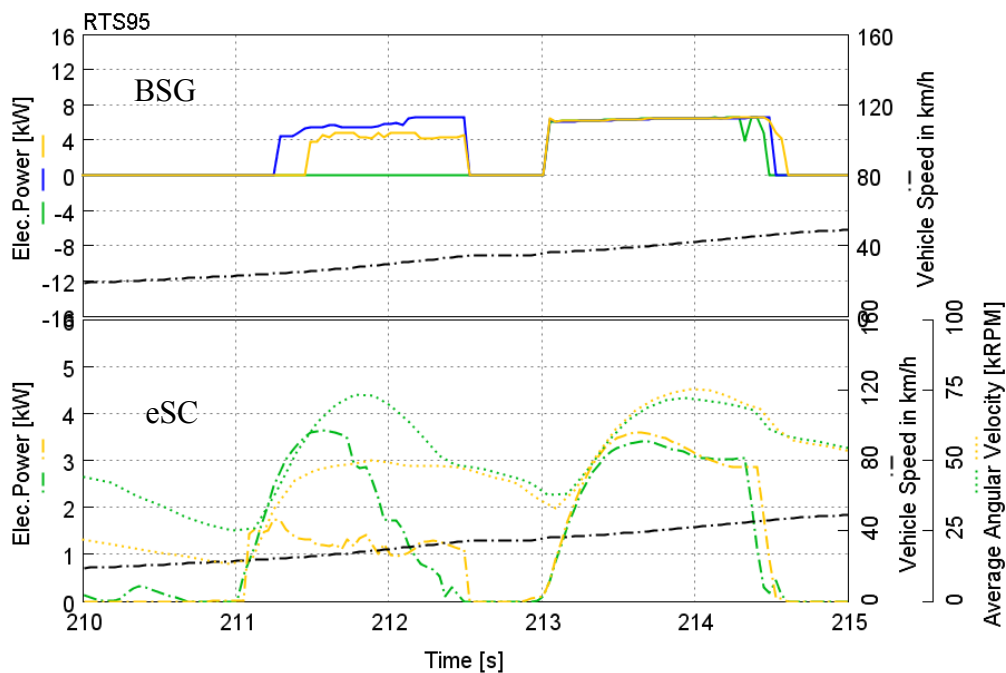


Figure 6.5 - eSC activation and BSG comparison

6.1.2 Transient Maneuvers

Shifting to Transient Manoeuvres analysis, no limitations in time have been considered for the BSG operation. It delivers the maximum mechanical power complying with current, voltage and battery limitations, in addition to the maximum mechanical power limit.

The results are reported in Figure 6.6. An improvement of 2.5 s on average of time reduction for all the maneuvers considered. The Stoichiometric Engine D, taking advantage of the higher brake torque achievable with the Miller cycle and the eSC adoption, is able to reduce the time of an additional 0.5 s on average. The battery power availability and the operating current and voltage limits allows the simultaneous operation of the BSG and the eSupercharger.

| Legend | Engine | Hybrid Architecture | Electric Network | eSupercharger | EMS |
|-----------|-----------------|---------------------|------------------|---------------|----------|
| B-SUV (1) | Stoic. Engine C | ✗ | 12 V | ✗ | ✗ |
| B-SUV (2) | Stoic. Engine C | P0 48 V | 12+48 V | ✗ | ECMS |
| B-SUV (3) | Stoic. Engine D | P0 48 V | 12+48 V | ✓ | ECMS |
| B-SUV (3) | Stoic. Engine D | P0 48 V | 12+48 V | ✓ | ECMS - 3 |

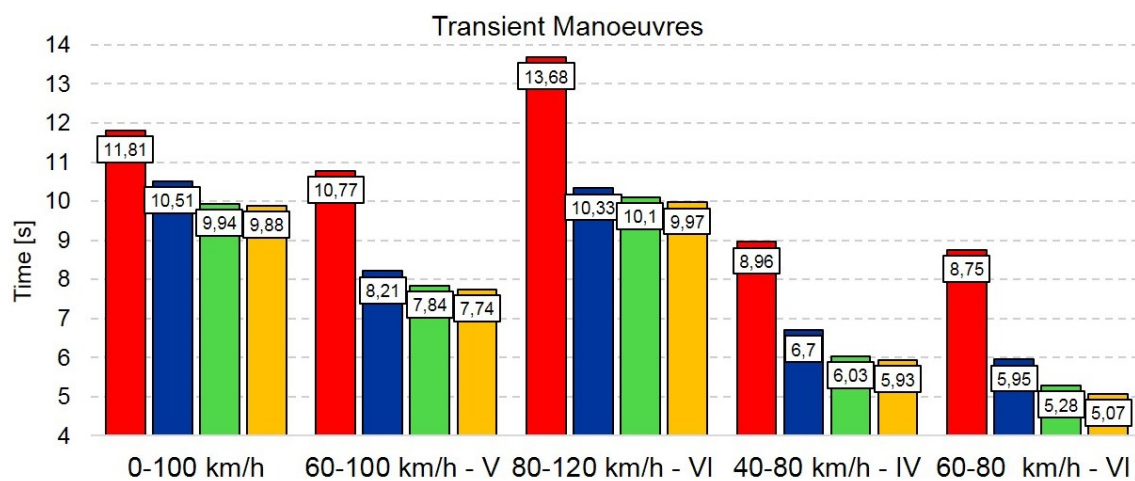


Figure 6.6 - Transient Manoeuvres results

In Figure 6.7 a deeper investigation of the 40-80 km/h in IV gear is proposed.

It can be seen how the torque of the engine increases much more quickly in the case of electrified vehicles, with the same full load curve. The reason consists of a greater acceleration of the engine with the assistance of the BSG, reaching more quickly the engine speeds in which the maximum torque is higher. It can also be noted that the torque achievable with the eSC and with the Miller cycle is higher than the conventional engine.

6.1 Hybrid Control Strategy Results

The electric power required by the eSC is higher than that identified in the steady-state analysis, reported in Figure 4.20.

| Legend | Engine | Hybrid Architecture | Electric Network | eSupercharger | EMS |
|-----------|-----------------|---------------------|------------------|---------------|----------|
| B-SUV (1) | Stoic. Engine C | ✗ | 12 V | ✗ | ✗ |
| B-SUV (2) | Stoic. Engine C | P0 48 V | 12+48 V | ✗ | ECMS |
| B-SUV (3) | Stoic. Engine D | P0 48 V | 12+48 V | ✓ | ECMS |
| B-SUV (3) | Stoic. Engine D | P0 48 V | 12+48 V | ✓ | ECMS - 3 |

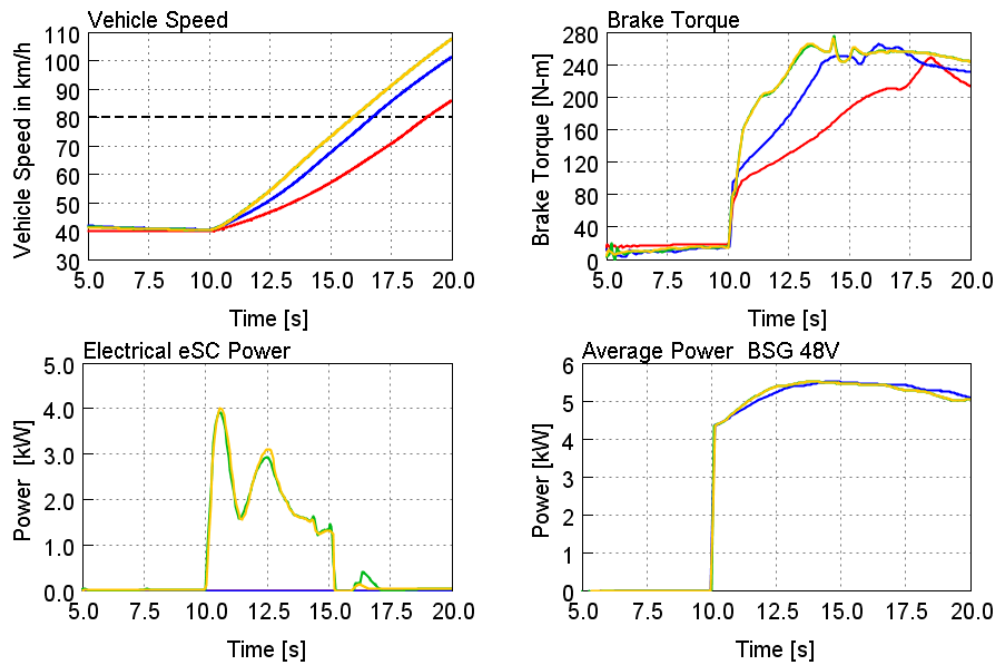


Figure 6.7 - 40-80 km/h -IV Gear

The PI, according to the equation 6.1, is reported in Table 6.2.

| | B-SUV (1) | B-SUV (2) | B-SUV (3) | B-SUV (3) - ECMS 3 |
|-----------------------|-----------|-----------|-----------|--------------------|
| v_{max} [km/h] | 200 | 200 | 200 | 200 |
| $t_{0-100 km/h}$ [s] | 11.81 | 10.51 | 9.94 | 9.88 |
| $t_{60-100 km/h}$ [s] | 10.77 | 8.21 | 7.84 | 7.74 |
| $t_{80-120 km/h}$ [s] | 13.68 | 10.33 | 10.1 | 9.97 |
| PI [s] | 82.74 | 67.91 | 65.03 | 64.33 |

Table 6.2 - Performance Index for four different vehicle configurations

In this chapter two sensitivity analysis are reported:

6 Results

1. Sensitivity analysis to the transmission ratio;
2. Sensitivity analysis to the BSG size.

The reason of these two activities is to assess the influence of the characteristics of the electrical machine on the effectiveness and robustness of the control strategy.

6.2 Sensitivity Analysis Transmission Ratio

A first investigation regarding the transmission ratio of the coupling between ICE and EM has been considered. The aim of this sensitivity analysis is to evaluate the influence of the above-mentioned parameter in terms of fuel consumption. The values chosen for the analysis are reported in Table 6.3.

| Transmission Ratio | |
|------------------------|------------|
| $\tau = 2, 1$ (design) | $\tau = 3$ |

Table 6.3 – Transmission Ratio Values

In Figure 6.8 the EM operating points are reported during the WLTC cycle. Considering the angular velocity, the EM map is not fully exploited.

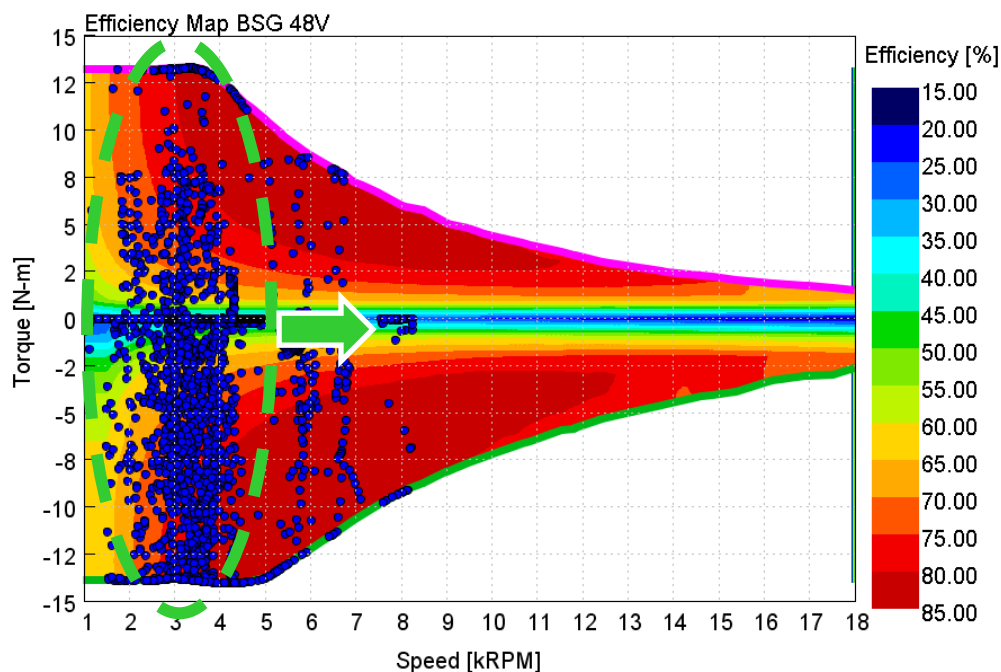


Figure 6.8 - EM operating points during WLTC driving cycle

Shifting the operating points at higher rotating speeds, the effects will be:

- Higher available mechanical power: the operating points are concentrated in a region below the Base Speed of the electric motor.
- Lower available brake torque for load point moving functionality.
- Increase of the average electromechanical efficiency of the BSG.

6.2 Sensitivity Analysis Transmission Ratio

| Legend | Engine | Hybrid Architecture | Electric Network | eSC | EMS | τ |
|-------------|-----------------|---------------------|------------------|-----|---------|--------|
| B-SUV (1) | Stoic. Engine C | ✗ | 12 V | ✗ | ✗ | ✗ |
| B-SUV (2-1) | Stoic. Engine C | P0 48 V | 12+48 V | ✗ | ECMS | 2,1 |
| B-SUV (3-1) | Stoic. Engine D | P0 48 V | 12+48 V | ✓ | ECMS -3 | 2,1 |
| B-SUV (2-2) | Stoic. Engine C | P0 48 V | 12+48 V | ✗ | ECMS | 3 |
| B-SUV (3-2) | Stoic. Engine D | P0 48 V | 12+48 V | ✓ | ECMS -3 | 3 |

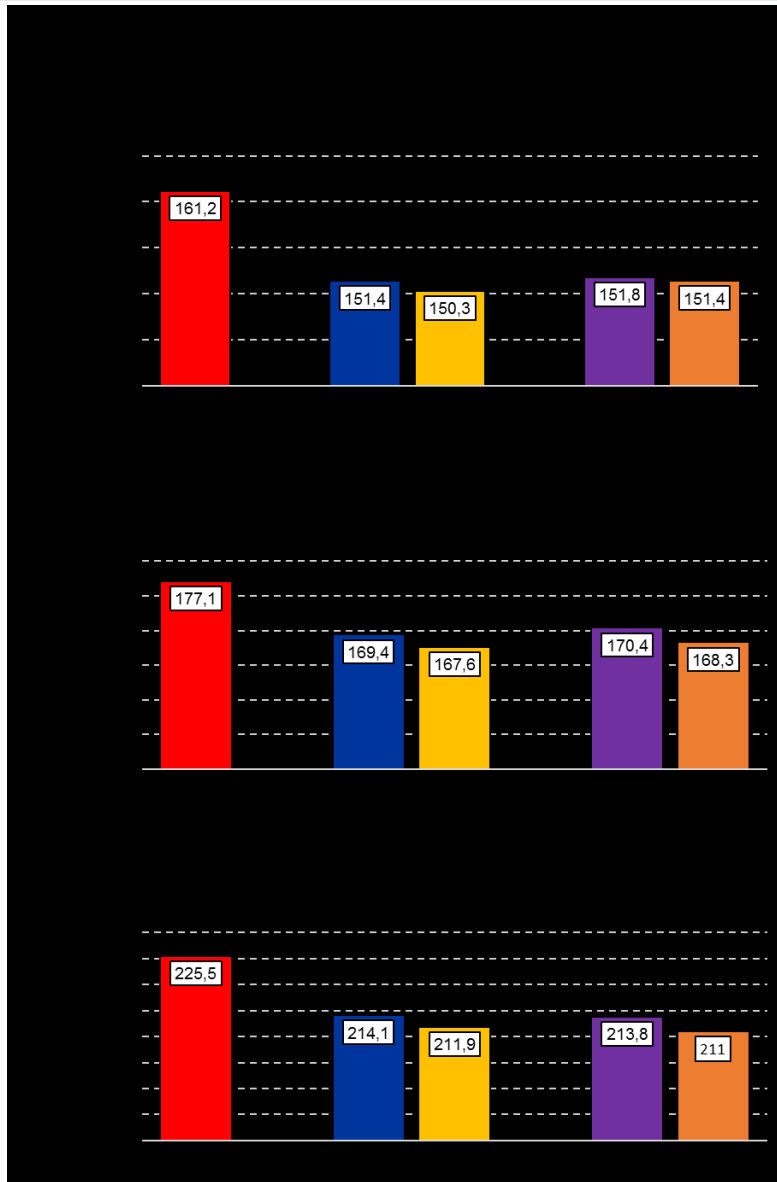


Figure 6.9 - CO₂ Emissions results Tau sensitivity

In Figure 6.9 the results of the sensitivity analysis are reported. Both in NEDC and WLTC the adoption of a higher transmission ratio worsen the fuel consumption reduction. In RTS-95 instead, a further reduction of CO₂ emission of around 0.8 g/km is achieved. The reason why different results are obtained can be explained considering the decrease of available BSG torque (Figure 6.10) for load point moving operation, whose negative

6 Results

effect is balanced in the RTS-95 cycle by the increased recovered energy during deceleration phase and is not balanced for NEDC and WLTC.

| Legend | Engine | Hybrid Architecture | Electric Network | eSC | EMS | τ |
|-------------|-----------------|---------------------|------------------|-----|---------|--------|
| B-SUV (1) | Stoic. Engine C | ✗ | 12 V | ✗ | ✗ | ✗ |
| B-SUV (2-1) | Stoic. Engine C | PO 48 V | 12+48 V | ✗ | ECMS | 2,1 |
| B-SUV (3-1) | Stoic. Engine D | PO 48 V | 12+48 V | ✓ | ECMS -3 | 2,1 |
| B-SUV (2-2) | Stoic. Engine C | PO 48 V | 12+48 V | ✗ | ECMS | 3 |
| B-SUV (3-2) | Stoic. Engine D | PO 48 V | 12+48 V | ✓ | ECMS -3 | 3 |

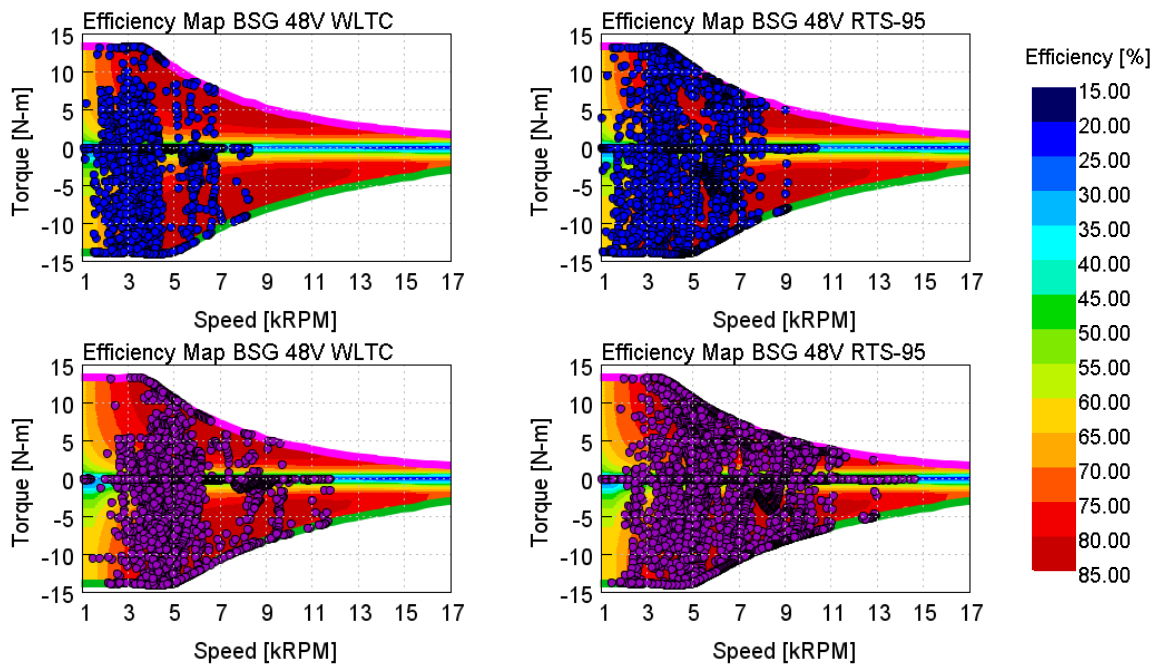


Figure 6.10 - EM operating points for different transmission ratio

As it is possible to note from the Figure 6.10 for WLTC the available maximum torque of the BSG decreases while on average the EM efficiency increase to a minor extent; for the RTS-95 cycle the EM operating points are characterized by a higher efficiency that balances the limitation of maximum brake torque.

In the Table 6.4 the amount of energy recovered during the driving cycle through regenerative braking is reported for each configuration of vehicle described up to now.

| Energy recovered with Regenerative Braking | | | | |
|--|-----------|--------------|-------------|-----------|
| | | $\tau = 2,1$ | $\tau = 3$ | Δ |
| NEDC | B-SUV (2) | 5,83 Wh/km | 8,07 Wh/km | + 38,52 % |
| | B-SUV (3) | 5,80 Wh/km | 8,23 Wh/km | + 41,69 % |
| WLTC | B-SUV (2) | 4,69 Wh/km | 6,13 Wh/km | + 30,73 % |
| | B-SUV (3) | 4,98 Wh/km | 6,95 Wh/km | + 39,75 % |
| RTS-95 | B-SUV (2) | 9,76 Wh/km | 12,66 Wh/km | + 26,63 % |
| | B-SUV (3) | 10,31 Wh/km | 13,38 Wh/km | + 29,68 % |

Table 6.4 - Recovered Energy with Regenerative Braking

6.3 Sensitivity Analysis EM Size

A last analysis was performed regarding the BSG size (i.e. maximum and minimum mechanical power). The battery has been consequently scaled in order to avoid limitation in electric power. The aim of this sensitivity analysis is the evaluation of the influence of the EM size in the effectiveness of the energy management strategy for fuel consumption minimization. As it is possible to note from the Figure 6.11, during dynamic cycle as RTS-95, a great number of operating points on the EM map are located in the maximum and minimum torque curves.

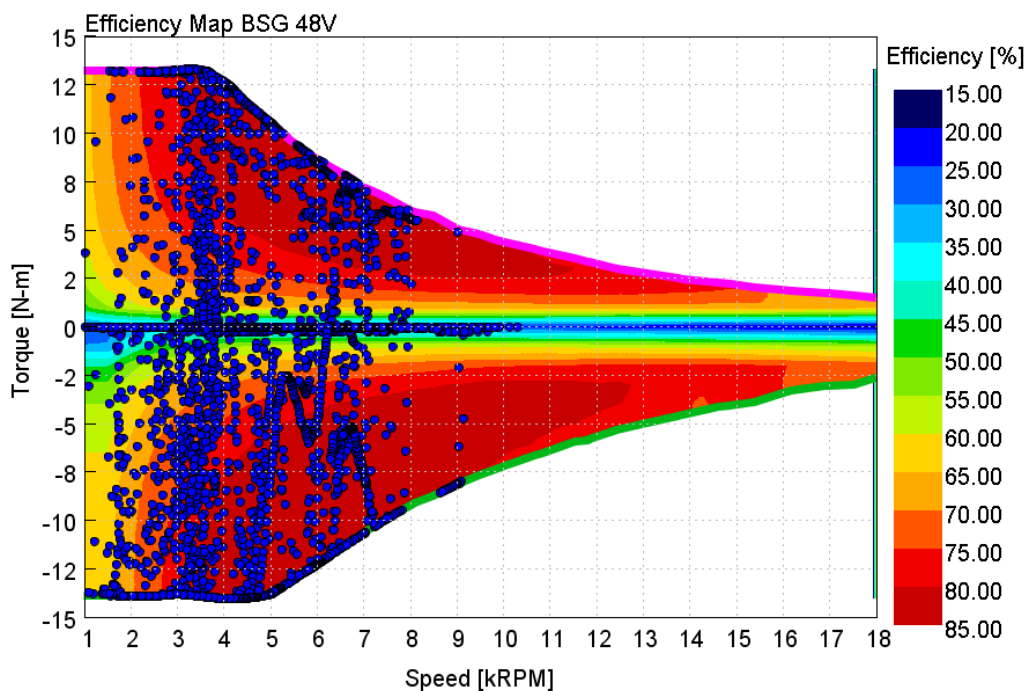


Figure 6.11 - EM operating points during RTS-95 driving cycle

6 Results

Hence, from one side, the energy recovered through regenerative braking is limited by the BSG size, from the other side, the optimum power split corresponds to the maximum BSG mechanical power and also in this case, the size of the BSG could limit the optimization.

For this activity, three different electric network setups have been considered. In Table 6.5 the main technical data are reported.

| | | BSG A | BSG B | BSG C |
|--------------------|-----------------------|--------------|--------------|--------------|
| BSG | Mech. Power Motor | 5.5 kW | 12 kW | 23 kW |
| | Mech. Power Generator | 7.5 kW | 16 kW | 23 kW |
| | Elec. Power Generator | 48V x 250 A | 48V x 500 A | 48V x 750 A |
| Battery 48V | Capacity | 10 Ah | 20 Ah | 30 Ah |

Table 6.5 - BSG Technical Data

The Electric machine efficiency maps are shown in Figure 6.12.

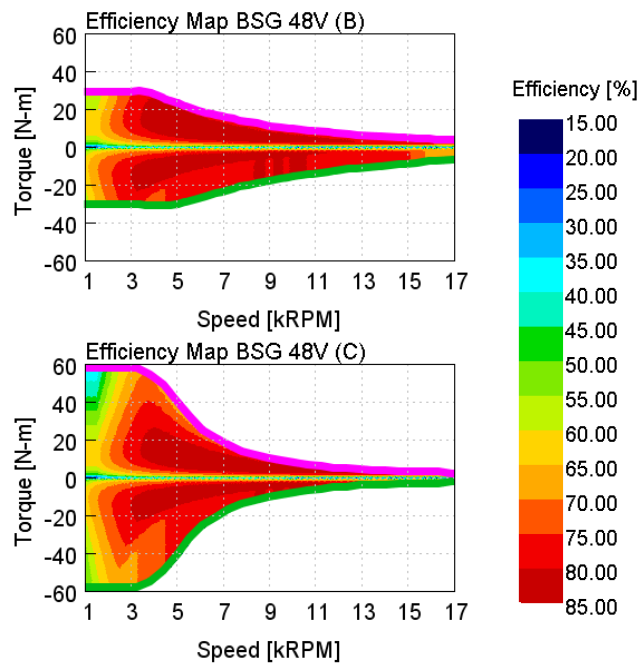


Figure 6.12 – Electric Machines efficiency maps

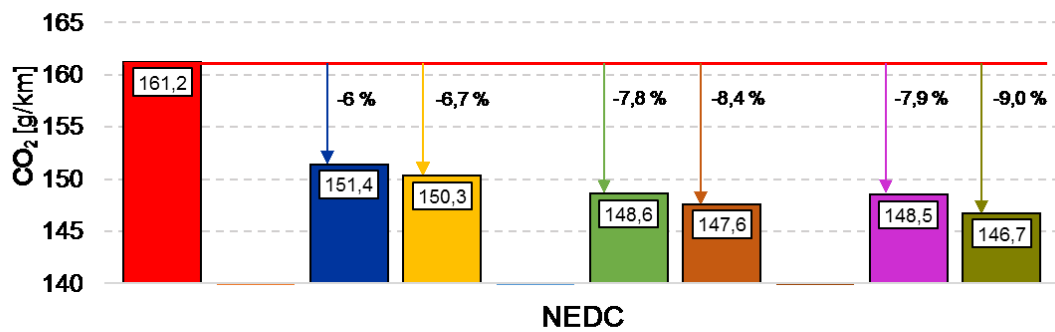
The sensitivity analysis concerns the fuel consumption only. The benefits in terms of transient manoeuvres are proportionally to the mechanical power deliverable by the BSG. Instead, it is more useful to focus on the effect of a larger machine on fuel consumption, so that it is not possible to predict the trend on the various driving cycles. The results are reported in Figure 6.13.

6.3 Sensitivity Analysis EM Size

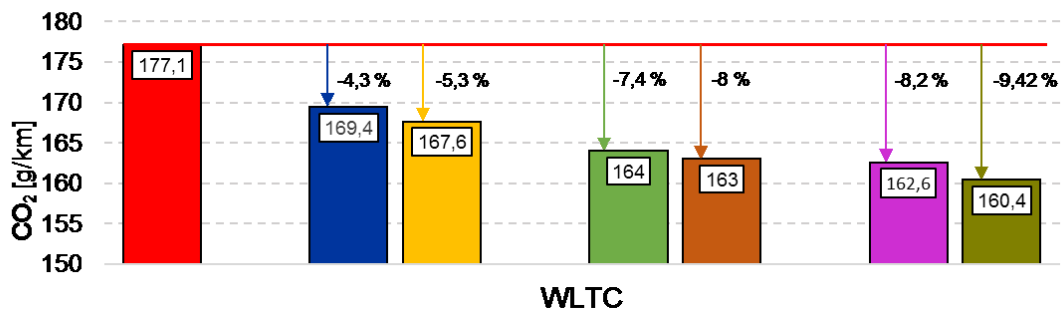
| Legend | Engine | Hybrid Architecture | Electric Network | eSC | EMS | BSG [kW] |
|-------------|-----------------|---------------------|------------------|-----|---------|----------|
| B-SUV (1) | Stoic. Engine C | ✗ | 12 V | ✗ | ✗ | ✗ |
| B-SUV (2-A) | Stoic. Engine C | P0 48 V | 12+48 V | ✗ | ECMS | 7,5 |
| B-SUV (3-A) | Stoic. Engine D | P0 48 V | 12+48 V | ✓ | ECMS -3 | 7,5 |
| B-SUV (2-B) | Stoic. Engine C | P0 48 V | 12+48 V | ✗ | ECMS | 16 |
| B-SUV (3-B) | Stoic. Engine D | P0 48 V | 12+48 V | ✓ | ECMS -3 | 16 |
| B-SUV (2-C) | Stoic. Engine C | P0 48 V | 12+48 V | ✗ | ECMS | 23 |
| B-SUV (3-C) | Stoic. Engine D | P0 48 V | 12+48 V | ✓ | ECMS -3 | 23 |

CO₂ Emissions

| C-Criterion [%] | 0,3% | 0,42% | 0,20% | 0,54% | 0 % | 0,20% | 0,13% |
|-----------------|------|-------|-------|-------|-----|-------|-------|
|-----------------|------|-------|-------|-------|-----|-------|-------|



| C-Criterion [%] | 0,03% | 0,31% | 0,50% | 0,35% | 0,38% | 0,28% | 0,36% |
|-----------------|-------|-------|-------|-------|-------|-------|-------|
|-----------------|-------|-------|-------|-------|-------|-------|-------|



| C-Criterion [%] | 0,21% | 0,19% | 0,42% | 0,25% | 0,61% | 0,31% | 0,40% |
|-----------------|-------|-------|-------|-------|-------|-------|-------|
|-----------------|-------|-------|-------|-------|-------|-------|-------|

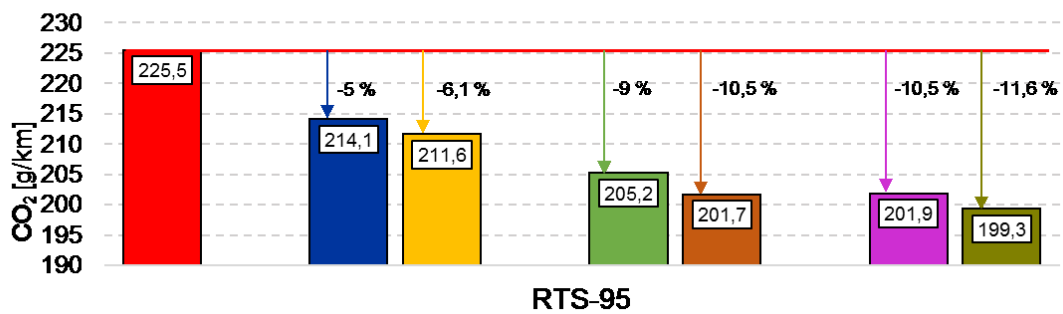


Figure 6.13 - BSG size sensitivity results

6 Results

The size of the electric machine has an influence on fuel consumption, as shown in Figure 6.13.

Focusing on the NEDC, it is possible to obtain a 2.8 g CO₂ emission reduction using BSG B and this improvement remains almost constant also increasing the electrical power further. The advantage of the stoichiometric engine D and of the eSupercharger remains almost constant for the different BSG coupling; it is mainly due to the increased compression ratio. As it is possible to evaluate from the Figure 6.14 in which operating points of B-SUV (3-C) are reported in EM and ICE maps, the BSG C map is not completely exploited; the BSG results oversized for this driving cycle. In the ICE map, the operating points are kept at low load, because of the electrical energy availability resulting from the regenerative braking phases, which can be used during traction operation.

| Legend | Engine | Hybrid Architecture | Electric Network | eSC | EMS | BSG [kW] |
|-------------|-----------------|---------------------|------------------|-----|---------|----------|
| B-SUV (1) | Stoic. Engine C | ✗ | 12 V | ✗ | ✗ | ✗ |
| B-SUV (2-A) | Stoic. Engine C | P0 48 V | 12+48 V | ✗ | ECMS | 7,5 |
| B-SUV (3-A) | Stoic. Engine D | P0 48 V | 12+48 V | ✓ | ECMS -3 | 7,5 |
| B-SUV (2-B) | Stoic. Engine C | P0 48 V | 12+48 V | ✗ | ECMS | 16 |
| B-SUV (3-B) | Stoic. Engine D | P0 48 V | 12+48 V | ✓ | ECMS -3 | 16 |
| B-SUV (2-C) | Stoic. Engine C | P0 48 V | 12+48 V | ✗ | ECMS | 23 |
| B-SUV (3-C) | Stoic. Engine D | P0 48 V | 12+48 V | ✓ | ECMS -3 | 23 |

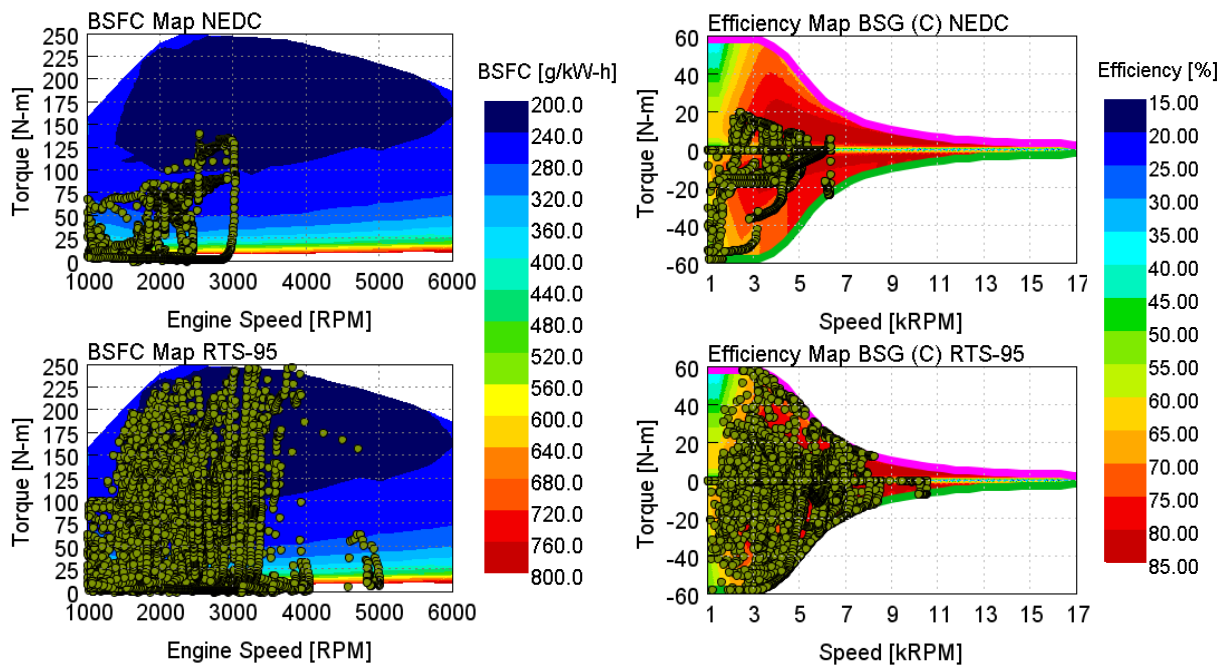


Figure 6.14 - Operating Points ICE and EM

Moving instead to the RTS-95 cycle, the considerations proposed for the NEDC cycle are no longer valid. The operating points are distributed over the electric machine map, both for the regenerative braking operation and for the power split between EM and ICE. The BSG A is effectively undersized for this very dynamic cycle. By adopting the BSG B, a reduction of about 9 g/km of CO₂ is obtained and increasing the size of the electric machine an additional benefit of about 3 g/km is present. Also in this case the difference in emissions between the C and D stoichiometric engines remains almost constant for all the electrical machine configurations.

It is possible to note the ECMS-3 control strategy of reducing the operating points of the ICE in the area in which the eSupercharger operation is expected, as it had already been highlighted in chapter 6.1.1 with the BSG-A. Being able to exploit also in this case the energy coming from the regenerative braking it is preferred to avoid operating points of the engine characterized by an absorption of electric power to overcome the inertia power due to the activation of the eSC.

Finally, in Figure 6.15 the normalized values of fuel consumption are shown for the three cycles taken into consideration and for the three electric machines adopted.

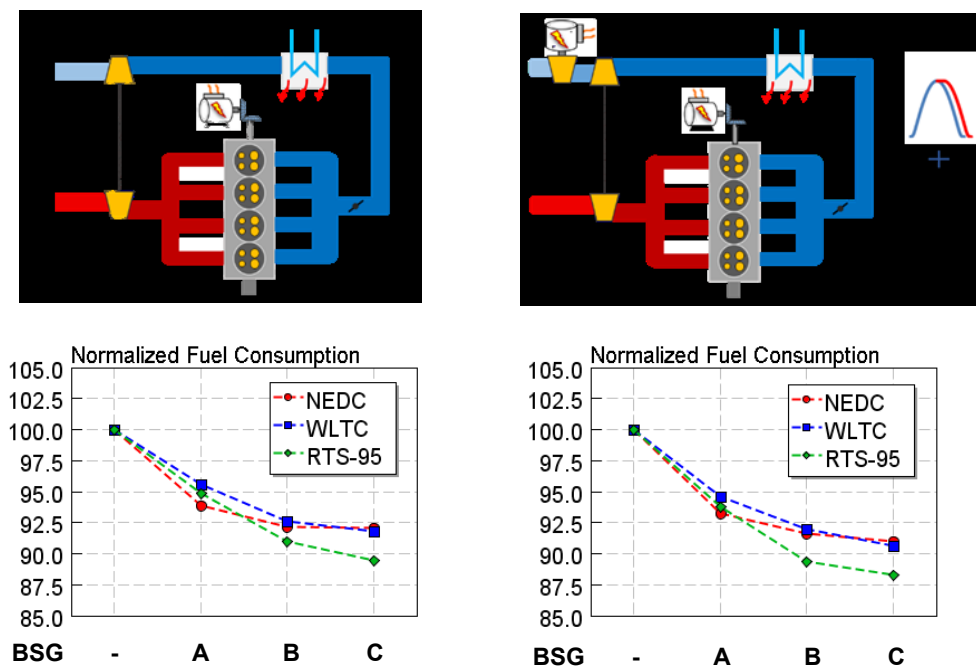


Figure 6.15 - Normalized Fuel Consumption adopting three different BSG evaluated on different driving cycles

- For NEDC it is evident that a sort of asymptote is achieved already with the BSG B. The adoption the BSG C electric machine, even if it were relatively usable for this application, would certainly not be justified by the results obtained. It can also be noted that on NEDC with electric machine A the highest percentage reduction of all three driving cycles is obtained (for B-SUV(2-A) the reduction is 6% and 6,7 % for B-SUV (3-A)).

6 Results

- As regards the WLTC, the adoption of the BSG B leads to almost double the reduction in fuel consumption, while the BSG C also this case does not lead to significant improvements (a few percent). As for the NEDC it is possible to achieve a reduction of more than 8% with the 16 kW BSG and a battery suitable for this electric machine.
- The RTS-95 driving cycle is the cycle in which the fuel consumption dependence on the size of the electric machine is the clearest: even in this case the CO₂ emissions show an almost linear dependence up to BSG B. with the adoption of the largest electric machine a further improvement of fuel consumption (about 3g/km) is achieved.

In all the driving cycles and for all the electric networks investigated, the advantage of a Miller cycle, the eSupercharger and the increased CR remains almost constant to the one analyzed in the chapter 6.1.1.

7 Conclusions

An innovative energy management strategy for a mild-hybrid 48V powertrains has been developed and its effectiveness has been tested among different driving cycles. The novel energy management strategy takes into account the electric power of engine ancillaries not devoted directly to traction. In this analysis an electrical boosting system has been chosen as electrical ancillaries to be included in the system and to be investigated. It represents a possible electrical device that a 48V vehicle with an increase of the onboard electric power is capable to integrate achieving important improvement in “fun to drive”. As far as steady-state analysis is concerned, with the current regulations the need of review the widely adopted technologies like mixture enrichment and scavenging has arisen; in this context Miller cycle appears to be a very promising solution. In this analysis the engine with the Miller option is able to recover the peak power at high engine speed while enhancing the low-end torque performance. At partial load the higher compression ratio leads to a benefit of 3% on average in terms of engine efficiency. This engine concept was therefore evaluated on a B-SUV vehicle using the well-known ECMS hybrid control strategy. The reduction of CO₂ emissions achievable with the electrified powertrain is around 5% and an additional 1% of benefits has been obtained with the adoption of the eSupercharger, the Miller cycle and the CR 12. At this point the base ECMS was modified including the electric power of the eSC. This electric power is composed by a steady-state eSC requirement (at low engine speed and high load) and a transient power due to the inertia contribution needed to activate the eSC. For the WLTC the update of the ECMS does not lead to benefits in terms of fuel consumption; for the RTS-95 cycle on the other hand it a further reduction of 1,5 g/km CO₂ is obtained; for the NEDC the update ECMS technique improve the fuel consumption controlling in a more efficient way the eSupercharger. Finally, a sensitivity analysis to the BSG size has been performed: three different values of maximum electric power have been considered (7,5 kW, 15 kW and 23 kW). The increase of the BSG and battery sizes leads to a reduction of the CO₂ emissions, but the improvement depends on the driving cycle considered: the advantage of a larger EM power availability is evident for dynamic cycles as RTS-95; for NEDC a large operating map of the EM is not fully exploited because there is not the need to shift significantly the load of the ICE.

An innovative energy management strategy that takes into account also the electrical ancillaries has been developed. The results are promising for what concern low cycles and aggressive cycles. This EMS can be validated on different case study, as for example the adoption of the eSC upstream of the TurboCharger. Additional ancillaries can be included in the system like for example an eCatalyst and to extend the assessment also for a cold-start driving cycle.

Bibliography

- [1] Nic Lutsey: “Transition to A Global Zero-Emission Vehicle Fleet: A Collaborative Agenda for Governments”. ICCT White Paper (2015).
- [2] <http://magazine.fev.com/en/fev-study-examines-drivetrain-topologies-in-2030-2> (accessed on October 2018).
- [3] Blanco-Rodriguez, David. “2025 Passenger Car and Light Commercial Vehicle Powertrain Technology Analysis”. FEV – Project-No. P33597/ Issue v03/ Report-No. 1/ ICCT (2015).
- [4] <https://eur-lex.europa.eu/legal-content/EN/TXT/HTML/?uri=CELEX:32009R0443&from=EN> (accessed on September 2018)
- [5] <https://eur-lex.europa.eu/legal-content/EN/TXT/HTML/?uri=CELEX:32017R1151&from=EN>(accessed on September 2018)
- [6] <https://eur-lex.europa.eu/legal-content/EN/TXT/HTML/?uri=CELEX:32014R0333&from=EN> (accessed on September 2018)
- [7] https://www.theicct.org/sites/default/files/publications/2017-Global-LDV-Standards-Update_ICCT-Report_23062017_vF.pdf (accessed on September 2018)
- [8] Bianchi D., Rolando, L. et al: “Layered control strategies for hybrid electric vehicles based on optimal control”, Int. J. Electric and Hybrid Vehicles, Vol. 3, No. 2, 2011, pp 191-216.
- [9] Ehsani M., Gao Y, Gay S. Emadi A.: “Modern electric, hybrid electric, and fuel cell vehicles: fundamentals, theory, and design”, CRC Press; II edition (2009).
- [10] Rolando L. “An innovative methodology for the development of HEVs energy management systems”. PhD Thesis, Politecnico di Torino (Torino, Italy). 2012.
- [11] Brian McKay: “48V Architectures for Enabling High Efficiency” Powertrain Technology & Innovation-Continental AG (https://www.theicct.org/sites/default/files/Panel%2020-%20Brian%20McKay_48V.pdf)
- [12] E. Erich; ADD Solution; “Voltage Classes & 48 Volt Application For Mild Hybrid Vehicles And High Power Loads”; February 2017; BIS Group, Automotive 48 Volt Power Supply and Electrification Systems Forum
- [13] Gerald Teuschl: “Evaluating different architectural options for hybridizing passenger vehicles and light trucks”. AVL GmbH -The battery Show, Europe – 2017

0 Bibliography

- [14] AVL UK Expo 2014 / Ulf Stenzel: “48V Mild Hybrid Systems Market Needs and Technical Solutions”. AVL Engineering and Technology (https://gansystems.com/wp-content/uploads/2016/07/AVL_UK_Expo_48V_Mild_Hybrid_Systems.pdf).
- [15] J. Dalby – Ricardo UK Ltd, “Transient EGR control with 48V E-boost simulation using integrated model based development” , CO2 Reduction for Transportation systems conference , Torino 2018.
- [16] Coppin O.: “From 12+12V to 48V: a new road map for hybridization”. Engine Expo - Stuttgart 2016
- [17] <https://www.borgwarner.com/technologies/electric-boosting-technologies> (accessed September 2018)
- [18] Simona Onori, Lorenzo Serrao, Giorgio Rizzoni auth. “Hybrid Electric Vehicles Energy Management Strategies”
- [19] Barbero L.: “Ottimizzazione della strategia di controllo e valutazione delle potenzialità di un sistema di propulsione ibrido a 48 volt per autovetture”. Master Thesis, Politecnico di Torino (Torino, Italy). 2017.
- [20] S. Onori, L. Serrao, G. Rizzoni:” Adaptive equivalent consumption minimization strategy for hybrid electric vehicles”. Proceedings of the 2010 ASME Dynamic Systems and Control Conference (2010).
- [21] C. Musardo, B. Staccia, S. Bittanti, Y. Guezennec, L. Guzzella, G. Rizzoni: “An adaptive algorithm for hybrid electric vehicles energy management”. Proceedings of the Fisita World Automotive Congress (2004).
- [22] Rolando L.:” Hybrid Electric Powertrain Design of Energy Management System”.
- [23] GT-SUITE example of SI engine model.
- [24] A. Ruggiero, I. Montalto, P. Poletto, E. Pautasso, K. Mustafaj, E. Servetto: “Development and assessment of a Fully-physical 0D Fast Running Model of an E6 passenger car Diesel engine for ECU testing on a Hardware-in-the-loop system”, SIA 2014
- [25] Millo, F., Di Lorenzo, G., Servetto, E., Capra, A. et al., "Analysis of the Performance of a Turbocharged S.I. Engine under Transient Operating Conditions by Means of Fast Running Models," SAE Int. J. Engines 6(2):2013, doi:10.4271/2013-01-1115.
- [26] Zanelli A. “Investigation of electrified powertrains using engine process simulation”, Master Thesis, Politecnico di Torino (Torino, Italy). 2014.
- [27] Isenstadt, A., German, J., Dorobantu, M., Boggs, D., & Watson, T. (2016). Downsized, boosted gasoline engines. Retrieved from <http://www.theicct.org/downsized-boostedgasoline-engines>.

- [28] Millo, F., Rolando, L., Pautasso, E., and Servetto, E., "A Methodology to Mimic Cycle to Cycle Variations and to Predict Knock Occurrence through Numerical Simulation," SAE Technical Paper 2014-01-1070, 2014, doi:10.4271/2014-01-1070.
- [29] Heywood, John B: "Internal Combustion Engine Fundamentals". New York: McGraw-Hill, 1988.
- [30] Millo F.: Slides from "Propulsori Termici" lectures (2018).
- [31] Luisi, S., Doria, V., Stroppiana, A., Millo, F. et al., "Experimental Investigation on Early and Late Intake Valve Closures for Knock Mitigation through Miller Cycle in a Downsized Turbocharged Engine," SAE Technical Paper 2015-01-0760, 2015, doi:10.4271/2015-01-0760.
- [32] <https://www.adandp.media/articles/continental-engineering-the-future> (accessed on October 2018)
- [33] <https://jalopnik.com/everything-you-need-to-know-about-the-upcoming-48-volt-1790364465> (accessed on October 2018)